AN INTELLIGENT ENERGY MANAGEMENT SYSTEM FOR MICROGRIDS

BY

SHEHAB EBRAHIM MOHAMMED AL-SAKKAF

A Thesis Presented to the
DEANSHIP OF GRADUATE STUDIES

KING FAHD UNIVERSITY OF PETROLEUM & MINERALS

DHAHRAN, SAUDI ARABIA

In Partial Fulfillment of the
Requirements for the Degree of

MASTER OF SCIENCE

In

ELECTRICAL ENGINEERING

May 2018

KING FAHD UNIVERSITY OF PETROLEUM & MINERALS

DHAHRAN- 31261, SAUDI ARABIA

DEANSHIP OF GRADUATE STUDIES

This thesis, written by **SHEHAB EBRAHIM MOHAMMED AL-SAKKAF** under the direction his thesis advisor and approved by his thesis committee, has been presented and accepted by the Dean of Graduate Studies, in partial fulfillment of the requirements for the degree of **MASTER OF SCIENCE IN ELECTRICAL ENGINEERING.**

Dr. Mahmoud Kassas
(Advisor)

Dr. Ali Ahmed Al-Shaikhi
Department Chairman

Dr. Mohammad Ali Abido
(Member)

Dr. Salam A. Zummo
Dean of Graduate Studies

Dr. Muhammad Khalid
(Member)

20/12/17

Date

Dedication

I dedicate this work to the persons who believed in me with endless love and support, to my father and my mother, to my brothers, sisters, aunts, my fiancée and all my family members and friends

ACKNOWLEDGMENTS

In the name of Allah, all praise be to him, the most Merciful and most Gracious. The one who has power overall. Blessings and peace be upon the most noble of Messengers, the Prophet Mohammad and upon his family and companions.

First, I would like to express my deep and great gratitude to my advisor Dr. Mahmoud Kassas for his endless support, his successful guidance during the past two years and his inspiration to me in hard times. I appreciate each single moment from his valuable time he spent with me to guide me or teach me new thing, such a great person cannot forget for the rest of my life.

I would like to give my great thankfulness to my committee members; Dr. Mohammad Abido who never hesitated to help me and give me from his great knowledge and experience. It is a great honor for me to work with. Dr. Muhammad Khalid for his sincere technical assistance and his help in publishing my work.

I would like to acknowledge the support that has been provided by King Fahd University of Petroleum and Minerals (KFUPM) especially electrical engineering department for using their resources and facilities. I would like also to acknowledge the support provided by Hadhramaut Foundation for Human Development (HFHD) for giving me the opportunity to complete the master's degree.

Finally, I would like to thank every person who stood by me, encouraged me and helped me through weakness times. Great thanks from the bottom of my heart to my family members and best friends.

TABLE OF CONTENTS

LIST OF TABLES

LIST OF FIGURES

LIST OF ABBREVIATIONS

ABC	:	Artificial Bee Colony
AUC	:	Area Under a Curve
BESS	:	Battery Energy Storage System
BSA	:	Battery Sizing Algorithm
CESS	:	Centralized Energy Management System
CHP	:	Combined Heat Power
DEMS	:	Decentralized Energy Management System
DER	:	Distributed Energy Resources
DG	:	Diesel Generator
ED	:	Economic Dispatch
EMS	:	Energy Management System
FC	:	Fuel Cell
FLC	:	Fuzzy Logic Controller
FLPID	:	Fuzzy Logic based Proportional Integral derivative
GA	:	Genetic Algorithm

MPPT	:	Maximum Power Point Tracker
PEMFC	:	Proton-Exchange Membrane Fuel Cell
PMSG	:	Permanent Magnetic Synchronous Generator
PSO	:	Particle Swarm Optimization
PV	:	Photovoltaic
REG	:	Renewable Energy Generation
SOC	:	State of Charge
WT	:	Wind Turbine

ABSTRACT

Full Name : Shehab Ebrahim Mohammed Al-Sakkaf

Thesis Title : An Intelligent Energy Management System for Microgrids

Major Field : Electrical Engineering

Date of Degree : May, 2018

In recent years, research and development for power systems depending on renewable energy resources has become a hot topic due to the climate change and growing global interest in the issue of global warming. Many world countries are moving toward cleaner energy sources and encouraging citizens to use them within their own electrical grids. One of the most interesting concepts of utilizing renewable energy is microgrids. Microgrid is a system that integrates more than one renewable resource in addition to one or more conventional power source to produce clean, sustainable, stable and reliable power. These advantages cannot achieve fully without a proper energy management system (EMS) within the microgrid. Intelligent control techniques such as fuzzy logic was used for EMS to form what is known as fuzzy logic energy management system (FLEMS). Cost reduction and energy saving while maintaining high performance are the most challenges that faces the growth of microgrids.

This work aims to model, integrate and simulate different renewable energy systems such as solar and wind with the help of backup systems in order to form a complete standalone DC microgrid. FLEMS of low complexity with minimum possible fuzzy rules is designed for the microgrid. The control system enables the microgrid to supply the load demand while giving the priority to renewable energy resources. The performance of the proposed

FLEMS is optimized using an efficient intelligent optimization technique that is the artificial bee colony algorithm (ABC). Furthermore, a new proposed method depending on economic dispatch is used in the FLEMS of the microgrid to enhance the system efficiency and to minimize the total generation cost. Comparison between conventional economic dispatch method and proposed one is presented.

Particularly, the effect of some environmental parameters on the microgrid components such as ambient temperature on the solar system is studied and the potential for using small-scale renewables for residential house usage is investigated for different year seasons. The overall system is simulated using real climate data and real load consumption of a house collected from Dhahran city in Kingdom of Saudi Arabia in 2016.

Keywords: Renewable Energy, Microgrid, Energy Management System, Power Dispatch, Intelligent Control, Fuzzy Logic Control, Artificial Bee Colony

ملخص الرسالة

الاسم الكامل: شهاب إبراهيم محمد السقاف

عنوان الرسالة: نظام تحكم ذكي للطاقة الكهربائية المولدة من شبكة طاقة نظيفة مصغرة

التخصص: هندسة كهربائية

تاريخ الدرجة العلمية: مايو ٢٠١٨

في الآونة الأخيرة، أصبحَ مجال إنتاج الطاقة المتجددة مصبُّ اهتمام عدد كبير من الأبحاث والدراسات الأكاديمية بسبب التغيّر المناخي والاهتمام المتزايد بقضية الاحتباس الحراري حيث تتجه العديد من دول العالم نحو توليد الطاقة باستخدام مصادر الطاقة المتجددة وتشجيع مواطنيها على إدخال مصادر الطاقة النظيفة ضمن شبكات الكهرباء الخاصة بهم مما جعلها مرغوبة بشكل أكبر على نطاق واسع. تعتبر (شبكة الطاقة النظيفة المصغّرة) واحدة من أكثر المفاهيم بروزاً في الآونة الأخيرة في مجال الطاقة النظيفة لما لها من مميزات عدّة ويمكن تعريفها على أنها شبكة كهرباء مصغّرة تحتوي على أكثر من مصدر للطاقة المتجددة بالإضافة إلى مصدر أو أكثر من مصادر الطاقة التقليدية، وتمتلك هذه الشبكة المصغّرة عدد من الخصائص تجعلها في مقدمة أبحاث مجال الطاقة المتجددة، حيث تمتلك القدرة على إنتاج طاقة نظيفة، مستدامة، مستقرة وموثوق بها، ولا يمكن تحقيق تلك المميزات ما لم يكن هناك نظام إدارة طاقة مناسب ضمن الشبكة. يتم استخدام نظم التحكم الذكية مثل (التحكم المنطقي الضبابي) في نظم الطاقة تلك لقدرتها على إدارة نظم الطاقة بكفاءة، لكن يظل خفض التكلفة وحفظ الطاقة من أكبر التحديات التي تواجه نمو شبكات الطاقة النظيفة المصغّرة.

تهدف هذه الدراسة إلى تصميم عدد من نماذج أنظمة الطاقة المتجددة مثل نظام الطاقة الشمسية، نظام طاقة الرياح بالإضافة إلى أنظمة الطاقة الاحتياطية ودمجها في نموذج واحد من أجل تكوين شبكة طاقة نظيفة مصغّرة مستقلّة. حيث تم تطوير نظام إدارة طاقة ذكي قليل التعقيد بالاعتماد على التحكم باستخدام المنطق الضبابي إذ يقوم هذا النظام بتمكين الشبكة المصغّرة من توفير الطاقة لطلب الاستهلاك مع إعطاء الأولوية لمصادر الطاقة المتجددة. كما تم أيضاً تحسين أداء كفاءة نظام إدارة الطاقة من خلال استخدام تقنية تحسين ذكية تعرف بخوارزمية (مملكة النحل). وأخيراً وليس آخراً تم استحداث طريقة تعتمد على مبدأ (التقسيم الاقتصادي للطاقة) ما من شأنها تحسين كفاءة نظام الطاقة وتقليص كلفة

التوليد على حدٍ سواء، وتعرض هذه الدراسة مقارنة بين الطرق التقليدية للتقسيم الاقتصادي للطاقة والطريقة المستحدثة في هذا العمل.

إضافة إلى ما سبق، تحتوي هذه الرسالة على دراستان منفصلتان عن تأثير العوامل المناخية على أداء بعض مكونات الشبكة المصغرة مثل تأثير درجة الحرارة على نظام الطاقة الشمسية وأيضاً دراسة إمكانية تركيب مصادر طاقة متجددة صغيرة للاستخدام المنزلي في مختلف ظروف فصول السنة. تمت محاكاة النظام في هذه العمل بالاعتماد على بيانات مناخية حقيقية وبيانات استهلاك سكني حقيقية تم رصدها وتسجيلها في مدينة الظهران بالمملكة العربية السعودية في العام ٢٠١٦.

CHAPTER 1

INTRODUCTION

Renewable energy resources have been used for many centuries before our time and due to the low price of petroleum, they were derelict. In recent years, awareness of climate changes and concerns to reduce the fossil energy consumption and carbon dioxide emission has been raised. Therefore, reverting back to renewable energy resources is one of the most important solutions [1].

Renewable energy can offer enormous advantages making it the best choice for future. It is inexhaustible, clean and has decentralization advantage making it usable at the same place where it exists. Renewable energy also has complementary feature enables it to integrate more than one type. For example, solar panels can supply power on sunny days in the presence of low wind, whereas wind turbine can supply more power in windy and cloudy days [2].

A microgrid is a term used for a local, small-scale power system that has its own resources; usually renewable resources such as micro wind turbines (WT), photovoltaic system (PV), fuel cell (FC) or diesel generator (DG), etc., integrated together with storage system devices such as battery energy storage system (BESS), flywheel and finally integrated with loads. microgrids usually operate in two modes; the first mode interconnected to the main power grid called (grid-connected) and the other one is isolated mode which called (standalone) [3], [4].

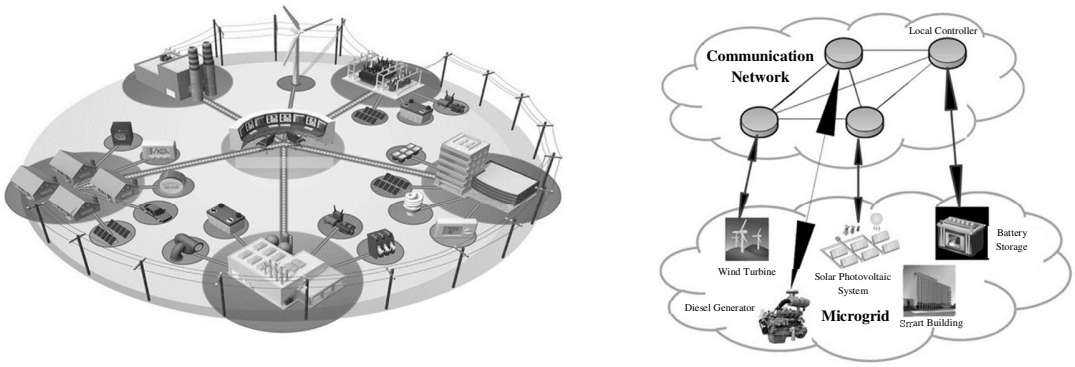

(a) (b)

Figure 1.1: (a) Centralized Microgrid EMS (b) Decentralized Microgrid EMS

Energy management system (EMS) for a microgrid is control software that can optimally decide which unit of the distribution generation units should be used. From general point of view EMS can manage the power among microgrid sources and loads. There are two main approaches for EMS: the first one is centralized EMS (CEMS), and the other one is decentralized EMS (DEMS) as illustrated Figure 1.1 [5].

1.1 Renewables Energy Status in 2016

The past three years has recorded the most significant growth of renewable energy around the world. Renewable energy is estimated to produce about 23.7% of the world electricity according to the renewable energy policy network for the 21 century in its final report. This means quarter of the world electricity is generated from renewable resources whereas 77% of the new renewable installation was in favor to PV and WT systems.

The peak demand of power in Kingdom of Saudi Arabia is around 60 GW in 2013. Saudi Arabia is targeting to produce around 54 GW from Renewable energy by 2040; with 41 GW form solar energy and 13 GW from other combined resources such as wind power, waste-to-energy and geothermal. The kingdom also targeting to reduce CO_2 emissions by 130 million tons by 2030 [6]–[9]. Figure 1.2 shows the annual growth rate of renewable power compared with biofuels power production.

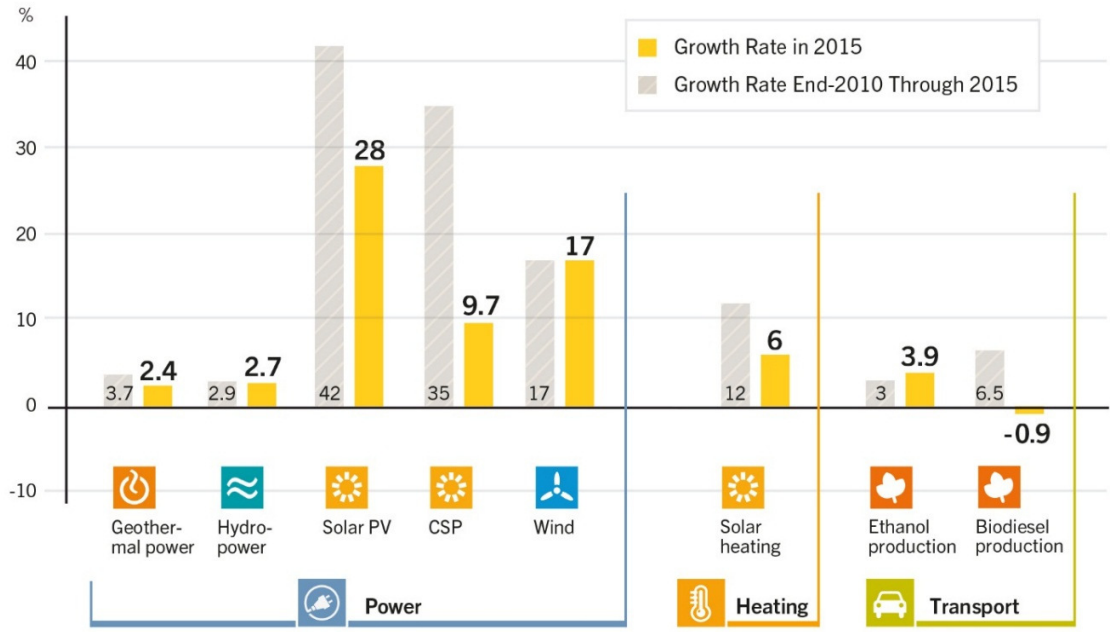

Figure 1.2: Average Annual Growth Rates of Renewable Energy Capacity and Biofuels Production

1.2 Problem Description

Intermittency in nature of renewable resources makes it a challenging task to control the operation of microgrids. Balancing between power consumed and power generated is a necessary task in any power grid. Renewable resources such as wind or solar is fluctuated in their nature and do not have constant production of energy. Due to this challenge, EMS should govern the operation of the microgrid all the time. For example, when the power generated from solar system is reduced due to weather changes such as in rainy or cloudy days, the wind turbine should compensate the reduction with the help of other backup sources in the microgrid such as FC, micro DG or storage systems. A reverse process takes place in days with low wind speed.

Operation cost is another challenge faces microgrids growth and considered as one of the most important challenges. Intelligent techniques such as fuzzy logic (FL) are playing a key role in enhancing and optimizing EMS of microgrids and reducing generation cost of backup systems. Number of researches have been conducted recently on optimizing microgrids EMS using intelligent technique such as fuzzy logic controller (FLC). However, very limited researches focus on lowering the complexity of the FLC by minimizing number of fuzzy rules, also very few studies in the literature optimized the performance of the FLC by modern intelligent optimization techniques such as artificial bee colony algorithm.

In this work, the mentioned challenges will be addressed by developing an economic energy dispatch for the proposed microgrid using fuzzy logic energy management system (FLEMS) with low complex FLC of only 25 base rules, Enhancing the performance of the

FLC using artificial bee colony optimization technique. Economic energy dispatch will be achieved by controlling the power provided from the microgrid to meet load demand with least possible cost while giving the priority to renewable resources depending on intelligent technique algorithms such as particle swarm optimization (PSO) and genetic algorithm (GA). Additionally, controlling the state of charge (SOC) of the BESS must be taken in account for energy dispatch. This will lead toward smoother operation and lower cost operation.

The increase of ambient temperature is considered as a major issue that effect the solar system efficiency. Another part of this work has been allocated for studying the effect of ambient temperature on PV system. The ambient temperature plays a key role in PV modules operation and affects their power production. The best operating temperature for 5kW PV system will be explored based on ambient temperature variations during different year seasons in Dhahran City in Saudi Arabia in order to improve the performance of solar PV model. In addition, investigating the potential for installing small-scale renewables for residential house usage in Dhahran city during different year seasons will also be conducted.

1.3 Thesis Aims and Objectives

This thesis aims to survey the state-of-art for microgrid energy management system, build models for each component of the microgrid using MATLAB/SIMULINK and integrate them together in order to form the proposed microgrid for the study. PV system of the microgrid will be studied extensively and the effect of ambient temperature on the

PV modules will be investigated. Next stage will be the design of an optimized energy dispatch based on intelligent techniques such as Fuzzy logic for controlling the operation of the microgrid.

The list of objectives may be summarized as follows:

- To survey state-of-the-art for microgrid energy management system (EMS).
- To model solar, wind and energy storage in order to form a microgrid based on the given power load demand.
- In particular, the effect of ambient temperature on the designed solar PV system will be extensively investigated.
- To develop microgrid an optimized energy dispatch system using one of the advanced intelligent control techniques such as Fuzzy logic, Neural network and/or Neuro-Fuzzy.
- Finally, a comparison with existing techniques of energy management system is presented.

1.4 Thesis Structure

The thesis is comprised of five chapters. A brief summary of each chapter is illustrated here.

- **Chapter 1** presents a background overview of basic idea of this work and states the statistical data and the growth of renewable energy in last years. Additionally, the

basic objectives and the scope of the study have briefly discussed along with the thesis outline.

- **Chapter 2** gives the literature review from previous research studies about energy management systems for microgrids.
- **Chapter 3** addresses the microgrid configuration, define the renewable energy models and other components specifications. Discusses the microgrid energy dispatch in details and the control technique that used in the system, covers the mathematical model development for all components also the simulation approach is discussed in this chapter. It also gives a comprehensive explanation of the proposed FLEMS and the control the operation of the microgrid. The proposed method for using economic dispatch within FLEMS is also explained.
- **Chapter 4** discusses and compares simulation results of the microgrid with the proposed FLEMS. In addition, results of the study that allocated for investigating the effect of environmental parameter on microgrid renewables that stated previously is also presented.
- **Chapter 5** illustrates the significant outcomes of this thesis and conclude by offering several recommendations for further work.

CHAPTER 2

LITERATURE REVIEW

Renewable energy field has become one of the major and hottest areas in research field. Governments all over the world are encouraging their nations through specific policies and regulations to employ renewable energy technologies. Recently, a great attention is being conducted on research of hybrid renewable resources systems or what is known as (microgrids). Energy management system (EMS) is usually associated with microgrid due to the need for control system to manage the operation of microgrid resources. The following subsections provide state of art for development of microgrids and their controlling strategies.

2.1 Development of Microgrid

Microgrid distributed generators were transited from laboratory to markets by the beginning of 2000s. One of the basic characteristics of distributed generators is that they can installed at distribution sites rather than installed in transmission lines. PV systems, FC, WT systems and combined heat power CHP are examples of distributed energy resources (DER). Two or more of these resources may interconnected together with the help of storage system such as BESS, flywheels or other possible types of storage systems.

The integration of DER must has control system in order to control the power generation along with the load demand [10]. The power systems and future electricity were on the threshold of new era depending on the integration of DERs as introduced in [11], in the work, a new approach for integrating DER in sites near the distribution networks was introduced.

With the development of the microgrid concept, it is important to examine its ability to use in industrial environment applications. DER were reported in [12] as a plant included with induction machines that located near industrial location. As presented in [13], a microgrid system is defined as integration of loads and renewable resources such as micro WT, FC, and other alternating power resources. EMS was also introduced and proposed for making decisions to choose the best source for electrical power generation. These decisions depend on several considerations: local equipment, heat requirement, climate conditions, electrical power cost, fuel cost and many other considerations. The EMS provides necessary information about controlling parameters to the operator.

The integration of DER encounters technical issues such as constraints of short circuit current, power stability, active and reactive power control, voltage profile and control, protection aspects, ability of DG to endure during disturbances, islanded operation and safety issues for the system as reviewed in [14]. With the continuous evolution of DER integration, the United State Department of Energy has developed and planned a new plan (by the year 2020) to control the spread of implementing DERs as reported in [15]. The work studied the factors involve in forming the optimal microgrid architecture such as cost and savings. The work also simulated the microgrid in a six-bus system in an optimized way and programmed nonlinearly. In [16], analysis of microgrid characteristics is done

from two points of view technically and politically. The work proposed and designed a control strategy that rolling an independent decentralized system.

The general architecture of a microgrid (EMS) based on multi-agent system technologies proposed in [17]. Authors emphasized on describing the implementation of a secondary control system based on the microgrid EMS architecture developed and tested on actual microgrid in order to assess its performance and capability. EMS of a microgrid operation was overviewed in [18]. Authors showed the important components and factors involving the design of EMS. Overview of the primary, secondary, and tertiary proposed control levels were described. Challenges and opportunities were explored in the paper. EMS for a standalone droop controlled microgrid ensuring stable operation and minimizing fuel consumption were presented in [19]. They optimized the generator outputs through adjustments to droop characteristics. Experimental results were illustrated to demonstrate its proposed mechanism. The work in [20] presented a microgrid controlled by EMS using novel double-layer coordinated approach. The approach consists of two main layers: dispatch layer and schedule layer. The approach provided stable, safe and economic operation by utilizing the market prices and DG bids to maximize the revenues in a grid-connected mode. Moreover, utilized the best renewable source based on forecasted data to minimize the operation cost in a standalone mode. In addition, optimized power flow and voltage regulation were achieved in the dispatched layer. EMS of a microgrid with DER was investigated in [21]. The operation of standalone microgrid, a grid-connected microgrid, and a network of microgrids were simulated using multi-agent infrastructure based on weighting factors and dynamic electricity price. They showed some significant

effects of service quality and presented the overall performance indexes between different types of microgrid systems.

A microgrid consisted of advanced PV system, gas micro turbine and embedded energy storage system with a determinist EMS was studied in [22]. The study presented the procedure for aggregation and implementation of the proposed deterministic energy management methods. The EMS consisted of two parts: customer side and microgrid side. Optimized EMS models for microgrid associated with economic analysis had been conducted in [23] considering Taiwan as a case of study. The study determined the optimal strategies for microgrid operation with maximum revenues. A detailed analysis for increasing the size of BESS compared with the growth of load demand was done and the results showed that the optimal capacity for storage system can be achieved by considering the storage efficiency and power supply.

A cost investigation for renewable generation potential in various location in USA was conducted in [24]. The study analyzed the potential for installing PV, WT and biomass as renewable resources and investigated the performance of two microgrid modes: grid-connected and standalone. The results showed that the grid-connected mode was much cost effective when compared with standalone mode due to the absence of batteries, hence the cost reduced drastically. A novel approach was presented in [25] for secondary control of droop-controlled standalone microgrid. The distributed networked control approach did not restore the voltage and frequency only but shared the reactive power also. The new methodology was validated by experimental part of the study. A distributed EMS of a microgrid was proposed in [26]. The proposed method considered constrains of underlying power for the distribution network. The EMS was formulated as an optimal power problem.

The approach had been applied to an existing microgrid in Guangdong in China and it showed effective operation in both grid-connected and standalone modes. The proposed approach had a fast converge and inclusive analysis had been conducted.

The increase of natural disaster around the world brings the need for a resilient power grid system to restore the critical loads after an urgent outage. The work [27] proposed an approach for a microgrid that was suitable for restoring the maximum number of critical loads during natural disaster power outage while satisfying the ability and the important requirements of the microgrid. A mixed-integer linear program problem was formulated to achieve the novel approach and the system was tested experimentally to validate the effectiveness. A laboratory scale microgrid was developed and tested experimentally for the purpose of research in [28]. The microgrid consisted of two renewable resources that were PV and WT in addition to a BESS controlled by EMS that managed the power generation and provide stable power to the load demand. The EMS of the microgrid in the study was open source to enable modification and addition or replacement of components or apply new control strategies for further enhancement.

2.2 Effect of Ambient Temperature on PV Modules

Solar energy is considered as one of the most important renewable resources. Each day the earth is provided by 1.4×10^5 TW of energy from sun; 3.6×10^4 TW can be used while the worldwide demand is only 1.7 TW, this means that the solar energy can cover the whole planet demand of power [29].

Electricity can be generated from sunlight in several ways; it can be converted into electricity by using solar thermal power solutions such as steam engines that use the solar heat, It also can be converted into electricity by photovoltaic cells [30]. PV cells technology was born by the space age in 1950s for satellites and spacecraft. It was emerged in other earthly application by 1970s [31]. PV cells are fundamentally semiconductors diodes. Their p-n junction must face the sunlight to produce electrical current. Polycrystalline, silicon, monocrystalline are the most materials used in manufacturing PV cells. When sunlight hits the surface of PV cells, it charges the carriers and electrical current generated [32].

The ambient temperature plays a key role in the power output generated from PV system. The efficiency of PV cells is mounted around (9-12) % and the PV cells use only 20% of the sun irradiation while the other energy converts to heat that affects the power output. The power output decreases by (0.4-0.5) % for each one-Kelvin increase in temperature of PV [33]. Therefore, the ambient temperature has a great effect the power output of PV systems. In [34], three PV models were tested in two tropical countries (Singapore and Indonesia) to investigate the effect of high temperature on the PV performance and to notice whether the wind speed plays a role in cooling process or not. The variations among the three models were low due to the low wind speed. Hence, the three models results were equally like with RMSE of 1.5 – 3.8 °C and the power output differentiated by 0.3 - 1.6 %, respectively. The authors concluded that ambient temperature has a direct impact on the module temperature despite of the presence of wind. The work [35] differentiated between the ambient temperature and module temperature and it showed that the module temperature has higher effect on PV modules with 10-20% than ambient temperature.

The authors in work [36] presented two PV models that were tested to investigate the effect of ambient temperature on power output. One of them was placed indoor with an ambient temperature of 25 °C while the other one placed outdoor with high temperature and high irradiation. Due to the low irradiation amount for indoor model, it gave only 27% of its maximum efficiency while the power output of the outdoor model gave 78% of its maximum efficiency. The work showed that the ambient temperature affects the power output, but it is not the only factor, irradiation amount is also playing a major role in the performance. In [37], 50W mono-crystalline solar panel model was simulated using MATLAB/SIMULINK to investigate the effect of ambient temperature on the voltage output. Different temperature values ranged between 25 °C to 60 °C were applied to the model and the irradiation was fixed to 458.2 w/m². The authors found that the ambient temperature has a great effect on the voltage output, which affects the power output consequently. Works done in [38], [39] showed that the power output decreases with the increase of ambient temperature. The system in [38] was tested during sunny days of February 2016 at KIIT, India while the system in [39] tested during different season of 2013 in Nigeria.

Dhahran city in eastern region of Saudi Arabia exposes high amount of sun irradiation daily, however high temperature degrees at this region near the earth equator plays a key role in the power production efficiency of the solar PV system. Therefore, a part of this work is allocated for studying the effect of ambient temperature of Dhahran during different year seasons on a small-scale PV system that will be used in the microgrid the work.

2.3 Energy Management System for Microgrid Based on Intelligent Techniques

Recently, many researches were conducted on controlling microgrids through EMS based on intelligent techniques, such as differential revolution, genetic algorithm, fuzzy logic, neural network and fuzzy-neuro. In this work, we are interested in EMS based on fuzzy logic technique. The following subsections present a brief overview on fuzzy logic controller (FLC) and review several published papers that have proposed similar methodologies for EMS based on this controller.

2.3.1 Fuzzy Logic Controller

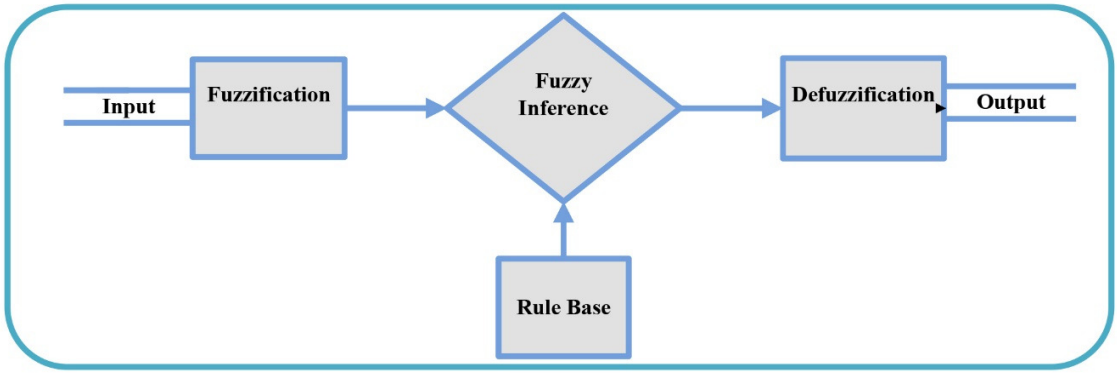

Figure 2.1: Main Parts of Fuzzy Expert System

Fuzzy logic consists of three basic processes. Figure 2.1 illustrates the main parts of fuzzy logic system. The first process is fuzzification which defined as a process of mapping crisp numbers in the input data matrix to the fuzzy sets. Then there will be membership functions which play the major role during this process by mapping each input value to a degree of membership between 1 and 0. Membership functions are such as gaussian

distribution, triangular, trapezoidal, sigmoidal functions and bell functions. Second process is fuzzy inference system which maps a fuzzy set into a several fuzzy sets using logical operations and fuzzy rules. Furthermore, fuzzy rules are just like IF-THEN statements and they can be obtained by professionals or generated from available numerical data using computing techniques (software) or evolutionary algorithms. Fuzzy inference systems have two principle types: Sugeno fuzzy inference and Mamdani fuzzy inference. Mamdani type is mostly accepted and more used while Sugeno type is especially used for dynamic non-linear systems.

Defuzzification process produced the aggregate linguistic, which the output value that can be derived from the former processes input of defuzzification. The main point is to have a single crisp value at the output that we are getting from the final process [40].

2.3.2 Fuzzy Logic Energy Management System

Recently, several studies have been adopted FLC to employ EMS on microgrids. Fuzzy logic shows an efficient management for microgrid especially when multi-functions is performed on the microgrid. FLC can deal with different tasks simultaneously. It can predict the wind velocity, sun radiation and load consumption or even the status of the grid. It is an efficient tool for dealing with different tasks instead of having a precise model dealing with each task individually.

FLEMS for DC microgrid was designed and implemented in [41]. The work presented modeling, analyzing and controlling process of PV, WT and BESS models that were

conducted using MATLAB/Simulink and the monitoring process was done using LabVIEW. The work focused on controlling SOC of the BESS using FLC in order to increase their lifetime. In [42], authors proposed a FLEMS for microgrid that consisted of PV, WT and FC of the type Proton-Exchange Membrane PEMFC. The inputs of the controller were the frequency of the microgrid, the batteries SOC and the level of the water inside the water desalination tank. The control process is achieved by frequency control of the main inverter. Efficiency in operation and reduction in size of the microgrid was achieved by the proposed FLEMS. An integrated FLEMS was proposed in [43] for a microgrid that had a combined heat and power (CHP) system in order to optimize the heat production and energy dispatch. The optimal selection of the system components was obtained by the proposed FLEMS.

FLEMS was proposed for regulating the power flow and maintaining the system batteries SOC of a microgrid in [44]. The microgrid consisted of PV, WT, FC, and BESS. The inputs of the FLC was the difference between load demand and power generated by the microgrid in addition to the SOC of the batteries. Load shedding and reduction of energy utilization cost as well as CO^2 emissions were the main aims of the work done in [45]. The microgrid in the work composed of PV model and BESS controlled by FLEMS.

Authors in [46] explored FLEMS for a microgrid to achieve gratification of load demand and maintaining the batteries SOC in order to increase their lifetime while keeping the hydrogen storage tank within its maximum limits. A cuckoo search algorithm associated with FLC was used in [47] to control battery SOC and power flow of a microgrid components that consisted of PV model, DG and BESS. A standalone AC/DC microgrid controlled by FLEMS was conducted in [48] in order to operate the renewable resources

efficiently, maintain battery SOC and manage the exchange power between the two AC/DC microgrids. Maximizing hydrogen production, optimizing and managing the power flow and generation of the microgrid was the main objectives in [49]. The microgrid in the work composed of PV, FC and BESS controlled by FLEMS. Smoothing the grid power profile while maintaining the SOC of the BESS were the main objectives of FLEMS of the microgrid in [50]. The authors claimed that they reached the lowest possible fuzzy logic rules (25 rules); hence, the system response was enhanced. The study conducted in simulation part and experimental part.

Research on FLEMS of microgrid is continued to gain more popularity. The work in [51], proposed an efficient way to manage a microgrid that consisted of PV system and BESS using FLEMS under different values of irradiation by controlling the duty cycle of the maximum power point tracker (MPPT). An efficient approach to manage the energy for electro-thermal grid-connected microgrid using FLEMS based on rate of change was presented in [52]. The work showed that the usage of thermal part in the microgrid contributes in decreasing the grid power consumption by 50% and smoothing the overall grid power profile. The required power for electrical water heater was reduced due to the existence of thermal photovoltaic that used for heating the water deposit tank for domestic usage.

Limited researches conducted on optimizing the FLEMS using ABC intelligent technique. In [53], a standalone microgrid that consisted of WT and DG used fuzzy logic based proportional integral derivative (FLPID) controller to control the diesel governor and the pitch angle of the WT. The work used ABC optimization technique to optimize 49 fuzzy rules as well as scaling factors. The authors in [54] also used ABC to optimize the

parameters of FLPID controller of a microgrid that has 49 fuzzy rules. The microgrid in the work consisted of PV system, WT, DG and FC. The FLPID controlled the operation of the FC depending on active and reactive power fluctuations of the renewable generation.

Previous works used the FLEMS for different types and topologies of microgrids. Various purposes were achieved, however lowering the complexity and optimizing of the FLC while maintaining the lowest possible cost were not took in consideration. I this work, a standalone DC microgrid is controlled by FLEMS with lowest possible fuzzy rules (25-base rules) and has been optimized using an efficient intelligent control technique that is ABC. In addition, a new approach is also introduced to minimize the operation cost of the backup sources (FC and DG) by using Economic dispatch along with the proposed and optimized FLEMS.

CHAPTER 3

MICROGRID MODELING and CONTROL METHODOLOGY

This work aims to come up with a real time intelligent energy management system for standalone DC microgrid that consists of PV model, wind turbine, fuel cell, diesel generator and battery energy storage systems connected to a residential load. Dealing with renewable energy systems needs to take into consideration the fluctuation in system inputs such as weather changes that affect amount of solar radiation and wind speed. Other natural factors also affect the operation of renewable energy systems passively such as the effect of ambient temperature on the PV system. Therefore, dealing with these factors efficiently along with insuring stable energy supply to the load represent the most important challenges that face the proposed system. Aggregation of the system components models with loads and development of energy management system using an intelligent technique (Fuzzy logic controller) for comprehensive simulation are presented in this chapter. Low complexity fuzzy logic controller that contains only 25 rules to control the microgrid is exhibited in detail. Furthermore, optimization problem of the controller will be developed using one of the most effective optimization techniques that is the artificial bee colony to increase the microgrid efficiency will be explained. Moreover, a new method for using economic dispatch optimization along with the optimized FLEMS to lower the generation cost of the microgrid. In addition to that, the methodologies used for the investigation studies will be presented.

3.1 Microgrid Components

As mentioned previously, the proposed microgrid consists of several components. Part of them are the renewable energy systems such as PV solar system and WT system. The other part contains the backup components such as BESS, FC and DG. The following subsections contain the mathematical models for these parts.

3.1.1 Photovoltaic Solar Model

PV cells are the fundamental unit of the PV system. These cells aggregated in a series manner to form a module, and modules could be connected in series, parallel or even both to form what is known as an array.

The ideal photovoltaic cell is represented mathematically by the following equation:

$$I = I_{pv} - I_0 \left[\exp\left(\frac{V + R_s I}{V_t a}\right) - 1\right] - \frac{V + R_s I}{R_p} \quad (1)$$

where I_{pv} and I_0 are the photovoltaic and saturation currents of the array. V_t is the thermal voltage of the array and equals to $(NskT/q)$ where N_s is the cells connected in series; greater output voltage obtained if cells connected in series while greater current obtained if cell connected in parallel. R_s is the equivalent series resistance of the array and R_P is the equivalent parallel resistance.

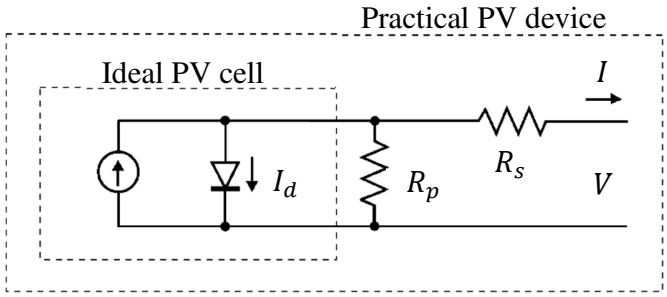

Figure 3.1: Equivalent Circuit of a Single Diode PV Cell

Formula in (1) is used for modeling single panel or module that its output power is usually low. To increase the output power to a certain value, the system should be modeled as number of arrays composes several modules that are connected even in series, parallel or both. The light generated current of the PV cell depends linearly on the solar irradiation and affected by the temperature given as:

$$I = \left(I_{pv,n} + K_I \Delta_T\right) \frac{G}{G_n} \tag{2}$$

where $I_{pv,n}$ is the light-generated current at the nominal condition (usually 25° C and 1000W/m2) given in Ampere. Δ_T = T – T_n (being T and T_n the actual and nominal temperatures) given in Kelvin. *G* is the irradiation on the device surface, and G_n is the nominal irradiation given in [W/m2].

I_0 is the diode saturation current and it is directly depending on the temperature and it can be calculated as follows:

$$I_0 = I_{0,n} \left(\frac{T_n}{T}\right)^3 exp\left[\frac{qE_g}{ak}\right]\left(\frac{1}{T_n} - \frac{1}{T}\right) \tag{3}$$

where E_g is the semiconductor band gap energy and equals to $E_g \approx 1.12$ eV for the polycrystalline Silicon at temperature of 25° C. $I_{0,n}$ represents the nominal saturation current given by:

$$I_{0,n} = \frac{I_{sc,n}}{\exp\left(\frac{V_{0c,n}}{aV_{t,n}}\right) - 1} \tag{4}$$

where $V_{t,n}$ being the thermal voltage of Ns cells connected series at the nominal temperature T_n , $V = V_{0c,n}$, I=0, and $I_{pv} \approx I_{sc,n}$

For modeling an array that gives higher amount of power, several models with different ways of connection are existed. The first way of connection shown in Figure 3.2, there will be no change in current while the voltage will increase. In second way of connection shown in Figure 3.3 the current will increase while the voltage will remain unchanged. In third way of connection as illustrated in Figure 3.4, the current and voltage will both increase, and for this approach, formula in (1) became as given in (5).

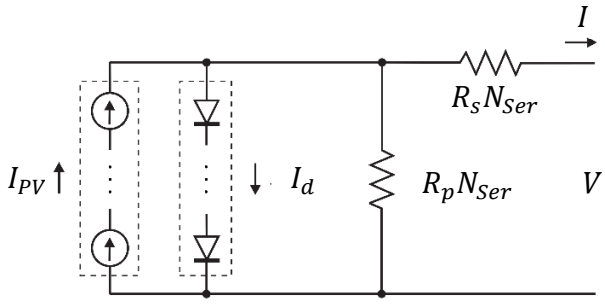

Figure 3.2: Equivalent Circuit of an Array Consists of Modules Connected in Series

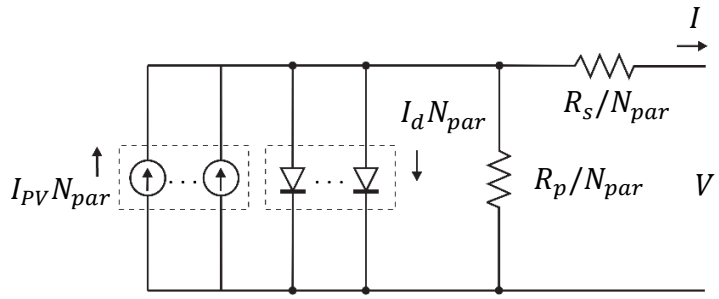

Figure 3.3: Equivalent Circuit of an Array Consists of Modules Connected in Parallel

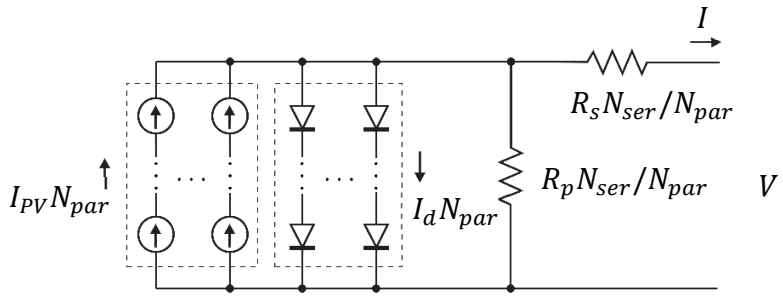

Figure 3.4: Equivalent Circuit of an Array Consists of Modules Connected in Parallel and Series

$$I = I_{pv} N_{par} - I_0 N_{par} \left[\exp\left(\frac{V + R_s \left(\frac{N_{Ser}}{N_{par}} \right) I}{V_t a N_{Ser}} \right) - 1 \right] - \frac{V + R_s \left(\frac{N_{Ser}}{N_{par}} \right) I}{R_p \left(\frac{N_{Ser}}{N_{par}} \right)} \quad (5)$$

where N_{Ser} and N_{par} are the number of series and parallel modules in an array and N_S is the number series cells in each individual module [32], [55].

3.1.2 Wind Turbine Model

Wind energy; one of most abundant resources, is the second fastest growing renewable energy technology worldwide. The wind turbine generators are evolving rapidly in two directions; technically and industrially.

WT system consists of three main parts forming the system that converts the wind energy into electricity. The first part is the rotor and it has three fiberglass blades. They are included within a hub that has a hydraulic motor, which has the ability to change the blades directions in order to operate efficiently with variable wind speeds. The nacelle behind the turbine contains the shaft and gearbox that increases the speed. In addition, it contains the transformer and the generator. The third part is the tower that supports the previous two parts.

WT integrated with permanent magnet synchronous generator (PMSG) became more popular due to its efficiency when experiencing low wind speed. Several studies in the literature included the model of wind turbine using PMSG [56]–[58].

The power generated by the wind turbine is given by:

$$P_w = 0.5\rho A V^3 C_P(\lambda, \theta) \tag{6}$$

where P_w is the power comes from WT, A is the cross-section area of the blades of the WT given in m², ρ is gas density available in the atmosphere, C_P is the WT energy conversion coefficient, and V is the wind velocity given in (m/sec).

The energy conversion coefficient C_P and the gas density ρ are given as:

$$\rho = 0.5A\left(\frac{353.05}{T}\right) exp^{-0.034\left(\frac{Z}{T}\right)} \quad (7)$$

$$C_P(\lambda,\theta) = \left(\frac{116}{\lambda_i} - 0.4 * \theta - 5\right).0.5\, exp^{\frac{-16.5}{\lambda_i}} \quad (8)$$

where Z is the altitude, T is the ambient temperature, λ_i is the tip speed ratio. Θ represents angle of the blades tilt. Formula in (9) expresses the tip speed ratio and (10) expresses the initial tip speed:

$$\lambda_i = \frac{1}{1/(\lambda + 0.089\theta) - 0.035/(\theta^3 + 1)} \quad (9)$$

$$\lambda = r\frac{\omega R}{V} \quad (10)$$

where ω is the rotor rotational speed in radians/second, R is the rotor radius in meters, and V is the wind speed specified in meters/second.

3.1.3 Fuel Cell Model

Fuel cell considered as electrochemical system that has the ability to convert the chemical energy into electrical energy and produces heat and water as secondary products. It composes of a pair of electrolytes and electrode. Its structure seems like a battery with a difference that it can delivers power as long as it supplied by fuel. There are five types of fuel cells depending on the material used in electrolyte: Polymer Electrolyte Membrane

Fuel Cell (PEMFC), Phosphoric Acid Fuel Cell (PAFC), Solid Oxide Fuel Cell (SOFC), Alkaline Fuel Cell (AFC) and Molten Carbonate Fuel Cell (MCFC). Among these five types, PEMFC considered as the best due to its rapidly development, simple structure, low operating temperature, quick start and high efficiency. It has two electrodes in each side with electrolyte layer in the middle. Fuel; hydrogen and oxygen, is fed to the anode and cathode electrode respectively [59]. The output voltage of the fuel cell is given by:

$$E = E_n - (-V_{act} + V_{ohm} + V_{con}) \tag{11}$$

where E_n is the Nernst voltage, V_{act}, V_{ohm} and V_{con} are the activation, ohmic and concentration voltages respectively. Each one of these losses is calculated as in (12- 15).

$$V_{act} = -[\xi_1 + \xi_2.T + \xi_3.T.\ln(C_{O_2}) + \xi_4.T.\ln(i_f)] \tag{12}$$

$$V_{ohm=} i_f.R_M \tag{13}$$

$$R_M = \frac{181.6[1 + 0.03(i_f/A_f) + 0.062(T/303)^2(i_f/A_f)^{2.5}}{[\lambda_1 - 0.634 - 3(i_f/A_f)] - exp[4.18((T-303)/T]} .\frac{l_1}{A_f} \tag{14}$$

$$V_{con} = -B_0.\ln(1 - \frac{J}{J_{max}}) \tag{15}$$

where T is the absolute operating temperature, C_{O_2} represents the concentration of oxygen, i_f represents the fuel cell output current, A_f represents the effective area, $l_1$is the effective thickness of membrane, $\xi_1, \xi_2, \xi_3, \xi_4$ are the reference coefficients, B_0 represents the operating constant. J and J_{max} are the current and maximum current density respectively.

3.1.4 Battery Energy Storage System Model

batteries are one of the most efficacious storage devices. They can store energy in electrochemical form. They can store energy from both DC and AC sources for future usage. Batteries are needed as a basic part of the microgrid. They discharge their energy to supply the loads whenever the microgrid resources are unable to meet the load demand or whenever one of the resources or more goes out of service. On the other hand, they charge with energy when the microgrid generation overcomes the load demand.

Lithium-ion and lead-acid batteries are widely used for small electrical systems due to its special characteristics such as superior usable capacity, extended life cycle, small size, weight and climate resistances among other types. The discharging and charging expressions for BESS are given in (16) and (17) respectively:

$$f_1(it\ i^*i) = E_0 - K.\frac{Q}{Q-it}.i^* - K.\frac{Q}{Q-it}.it + A.\exp(-B.it) \qquad (16)$$

$$f_2(it\ i^*i) = E_0 - K.\frac{Q}{it+0.1.Q}.i^* - K.\frac{Q}{Q-it}.it + A.\exp(-B.it) \qquad (17)$$

where E_0 represents the initial voltage, A is the exponential voltage given in (Volt), i represents the battery current, i^*represents the low frequency dynamic current given in (Ampere), K represents the polarization resistance, Q related to the maximum capacity of the battery, it is the extraction capacity of the battery given in (Ah) and B represents the exponential capacity given in $(\mathrm{Ah})^{-1}$.

One of the most important parameters of BESS is the state-of-charge and its calculated as given in (18):

$$SOC = 100\left(1 - \frac{\int_0^t idt}{Q}\right) \tag{18}$$

Battery Sizing:

To determine the suitable and optimal size capacity of the battery storage system, one of the recent and effective algorithms for calculating the optimal size of BESS named battery sizing algorithm (BSA) is used in this work [60]. The idea behind this algorithm is to find a optimal size for the BESS of the microgrid depending on the difference between the renewable systems generation and load demand. The total generation of the renewable systems calculated according to:

$$PG_{Renewable,t} = PG_{solar,t} + PG_{wind,t} \tag{19}$$

where $PG_{solar,t}$ is the power generated from PV solar system and $PG_{wind,t}$ is the power generated from WT system at time *t* respectively. The difference between the generation and the load demand is calculated as:

$$P_{Differnce,t} = PG_{Renewable,t} - \ PL_{demand,t} \tag{20}$$

First stage is to find the maximum storage size according to the excess power from the difference between generation and load demand:

$$BESS_{max} = Max(\sum_{t=1}^{T} P_{Differnce,t}) \quad (21)$$

where $BESS_{max}$ is the maximum capacity size of the BESS. Second stage is to find the required capacity of the battery which should not to be the maximum all the time. The required capacity of BESS is found according to:

$$BESS_{Cap} = \begin{cases} BESS_{max}, & x = 1 \\ CBS \quad , & x = 0 \end{cases} \quad (22)$$

where $BESS_{Cap}$ is the required capacity of the BESS during all time and CBS is the corrected battery size. The condition $x = 1$ denotes that the BESS is fully discharged after charging and the condition $x = 0$ denotes that the BESS in not fully discharged after charging process and the battery capacity is oversized. Region reduction iterative algorithm is used to calculate the corrected BESS size (CBS).

The third stage of the algorithm is to find the optimal capacity size of the BESS and calculated according to the given formula in (23):

$$BESS_{opt} = \begin{cases} BESS_{cap} & , BESS_{DV} \geq BESS_{lim} \\ BCS & , otherwise \end{cases} \quad (23)$$

where $BESS_{opt}$ is the optimal capacity size of the BESS, $BESS_{DV}$ is the battery decision variable and calculated as stated in the literature [60]. BCS is the BESS corrected size for the third stage and calculated using region reduction iterative algorithm.

In order to find the optimal size of the battery storage system for the microgrid in this work, average generation from PV system and WT system for one year used in the BSA depending on real data such as irradiation, ambient temperature and wind speed. In

addition, a real load demand recorded from residential house inside KFUPM campus in the same year is also used in the algorithm.

3.1.5 Diesel Generator Model

In general, Diesel generator consists of a diesel engine compiled with generator. The output power of DG can be controlled by the speed governor. DG usually used as a backup source when integrated in a microgrid system [61]. The energy generated by the DG with rated power output is given by:

$$E_{DG} = P_{DG} \times \eta_{DG} \times t \tag{24}$$

where η_{DG} represents the efficiency of the DG. The cost operation is presented in section 3.5 where the optimization problem for economic dispatch is developed.

3.2 Investigating and Analyzing Data of the Renewable Systems

The work is divided into several stages. In first stage, modeling, analyzing, studying and investigating the RES of the microgrid are conducted. For analysis purpose, real environmental data is applied to the RES as shown in the methodologies in next subsections. Components of the microgrid are modeled using MATLAB/Simulink program. All these components are integrated together using power electronics devices.

3.2.1 Studying the Effect of Ambient Temperature on 5kw PV System

PV system model is created using MATLAB/SIMULINK based on the KC200GT array module that gives 200W as rated power output at ideal condition (ambient temperature at 25°C and irradiation at 1000 W/m^2) [62]. Parameters of this module is exhibited in Table 3.1. The size of the PV solar system is chosen to be 5kw. Therefore, to increase the output power up to 5kw, special way of connection must be chosen to achieve this purpose. number of modules must be connected in series, parallel or series/parallel manner as stated in 3.1.1, Hence, three models are built. Each one of them has a different way of connection, Different temperature values applied with a fixed irradiation to the three models in order to investigate which model can handle temperature variation effectively.

Irradiation and ambient temperature data of Dhahran city at in Eastern region of Saudi Arabia for different seasons in 2016 are applied to the models. The most effective model among three ones depending on the simulation results is analyzed to study the influence of ambient temperature on the power output of the PV system. According to the power output, the best-operating ambient temperature for each month is obtained. It is known that the ideal ambient temperature for PV models which is 25°C. However, existed cooling technologies cannot achieve this value in PV system in hot areas such as Dhahran city. Therefore, a determination of a set point for ambient temperature in each month will help in proper operation for the PV system and gives acceptable amount of power output compared to its rated power and will help in the cooling process of the PV [63].

Table 3.1 Parameters of KC200GT PV Module at 25 C° and 1000W/m²

PARAMETERS	VALUES
$\boldsymbol{I_{mp}}$	22.5 A
V_{mp}	28.74 V
$P_{max,e}$	200.143
I_{sc}	8.21 A
V_{oc}	32.9 V
K_V	-0.1230 V/K
K_I	0.0032 A/K
N_s	54
A	1.3
R_p	415.405 Ω
R_s	0.221 Ω

3.2.2 Investigation Renewable Energy Potential in Dhahran City

In this stage, a small-scale hybrid renewable energy system (HRES) consists of PV solar system and WT system connected and operated together to supply a house load demand. Real environmental data is used to obtain average annual generation from the RES in this location and compared with the annual load demand for residential house at the same place of the study. In addition, three days from different seasons of Dhahran city are simulated and compared with the house demand in these days. Energy analysis are conducted to investigate the system ability to meet the load demand during different weather condition.

Figure 3.5 shows both PV and WT systems integrated with the help of power electronics to form the proposed HRES for investigation study.

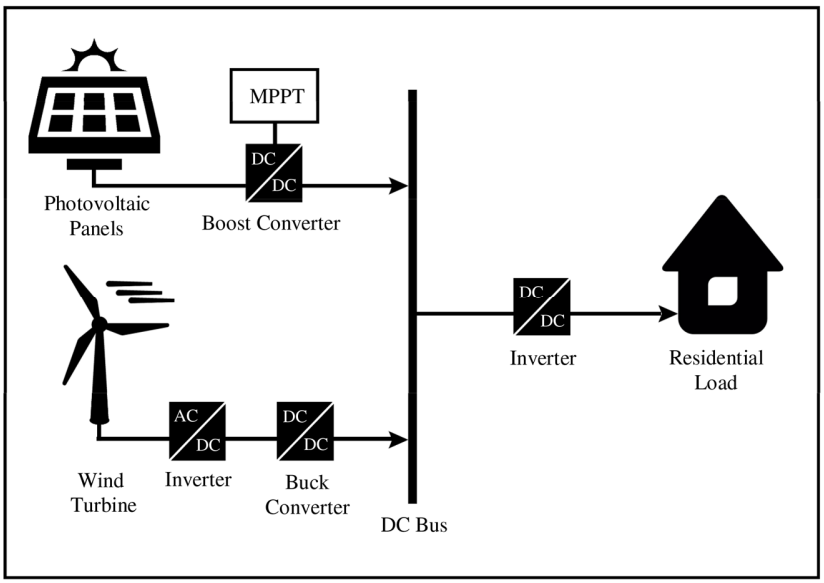

Figure 3.5: Hybrid Reneable Energy System Used In Investigation Study

The solar PV system is the same that used in previous study in 3.2.1 with same parameters and rated power of 5kW. The WT system is modeled according to the mathematical model presented in subsection 3.1.1 previously. as stated, WT integrated with PMSG will provide enhanced model that can work with low wind speed. All parameters of PMSG is considered as existed in [57]. The rated power of the WT system is 5kW. This part of the work aims to investigate the feasibility for installing small scale renewables for residential usage in Dhahran.

3.3 Fuzzy Logic Energy Management System of the Microgrid

The components of the microgrid in this work are integrated using power electronics devices and modeled using MATLAB/Simulink environment. Energy management system of the proposed microgrid as shown in Figure 3.6 is designed using FLC. In this work, FLEMS is designed with possible minimum fuzzy rules to reduce the complexity and enhance the fast controlling response for the proposed standalone DC microgrid.

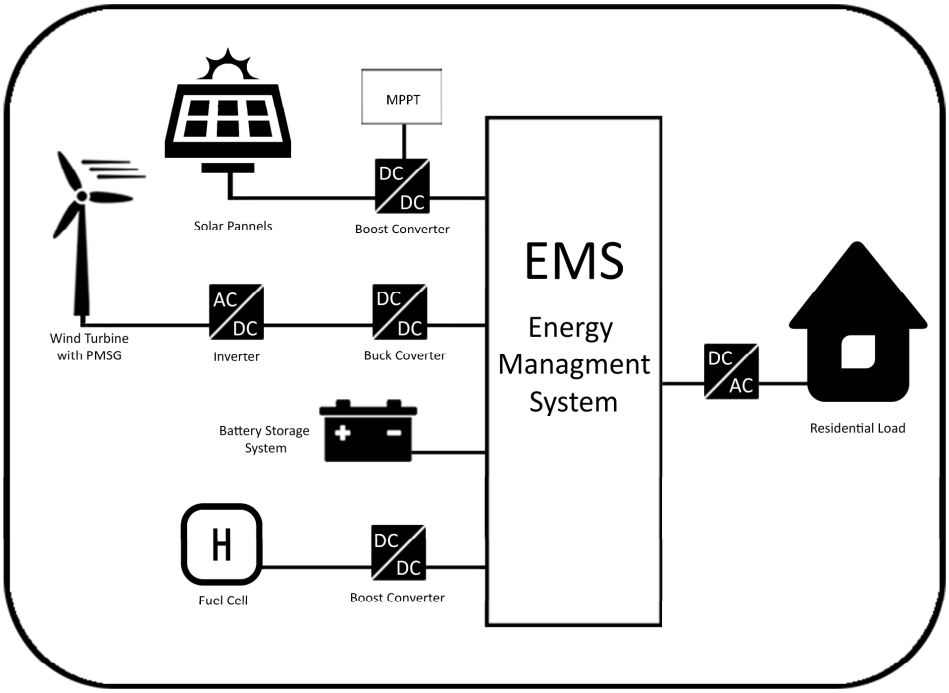

Figure 3.6: Basic structure of the standalone microgrid

3.3.1 Microgrid Specification

The following points summarizes the specification of the proposed system:

- Photovoltaic solar system of 5kw is connected to power electronics such as DC/DC boost converter to meet the microgrid requirement. More details on the model used

and explained extensively in subsection 3.3.1. Maximum power point tracker is integrated with the converter to enable the PV system harvesting maximum power regardless to the variations of temperature and irradiation.

- Wind turbine system of 5kw is connected to power electronics such as AC/DC inverter to invert the AC output of the wind turbine to DC. Also, DC/DC buck converter used to step down the voltage and meet DC bus requirements of the microgrid. Parameters of the PMSG are the same as used in the investigation study in Section 3.2.2.
- Fuel cell of the type Proton exchange membrane (PEMFC) (5KW-45V) connected to DC/DC converter to meet the DC bus requirements of the microgrid.
- Battery energy storage system of 20 kWh capacity of the type Lead Acid. The size of the battery is obtained based on BSA that explained in detail in subsection 3.1.4.
- House load demand modeled based on real data recorded from real house inside KFUPM campus. (House NO. 3307 based HVAC VFD system).
- 110-volt DC bus collects the power from generation and backup sources according the control actions of the FLEMS and supplies the load demand.

The main objective of the FLEMS is to guarantee that the house load is supplied by enough power to meet the variable load demand with the maximum use of renewable energy sources. EMS stores the surplus energy harvested from renewables in BESS and uses it when renewables cannot generate enough power. When renewable generation and the BESS are unable to meet the load demand, EMS controls the operation of the fuel cell to compensate the absence of PV, WT and BESS.

FLC is used to control the operation of the fuel cell with the help of control switches in order to compensate the absence of renewables generation and the battery energy storage system. FLC used the system is explained in detail in next subsection. The control system also maintains the SOC of the BESS that should operate between 20% to 95% to increase its lifetime.

3.3.2 Fuzzy Logic Controller

The fuzzy logic controller has two inputs which are the SOC of the BESS and the net power. Net power is the difference between power generated from renewables and the load demand power calculated as:

$$P_{net} = P_{Renewable} - P_{load} \tag{25}$$

P_{net} represents the net power, $P_{Renewables}$ represents the power generated from RES and P_{Load} represents the load demand power. $P_{Renewable}$ is given by the sum of power generated from renewables in the microgrid as:

$$P_{Renewable} = P_{Solar} + P_{Wind} \tag{26}$$

P_{Solar} and P_{Wind} are the power generated from PV and WT systems respectively. By using (25), the fuzzy rules decreased from 125 rules (if three inputs used) to only 25 rules (using two inputs only), hence, enhancing the system response and lowering the complexity. Figures (3.7, 3.8, and 3.9) illustrate the un-optimized membership functions for inputs and output of the FLC. Table 3.2 illustrates FLC base rules.

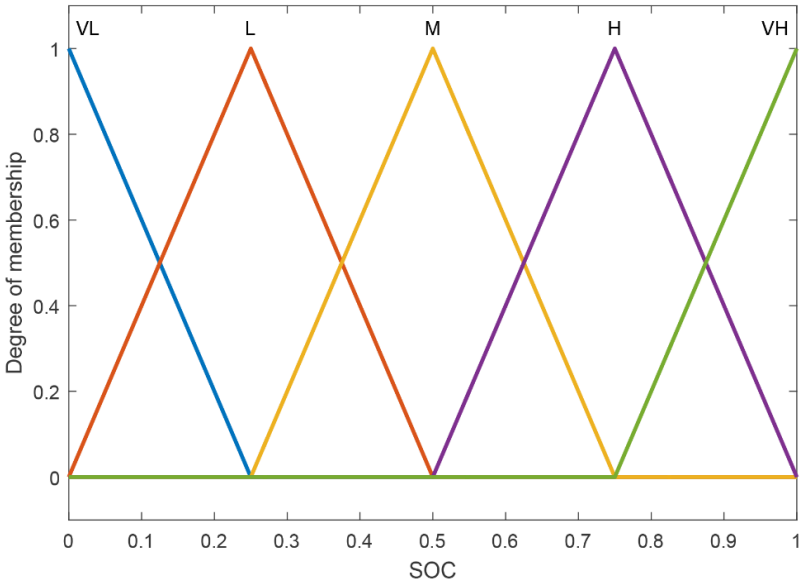

Figure 3.7: First Input Membership Functions of FLC

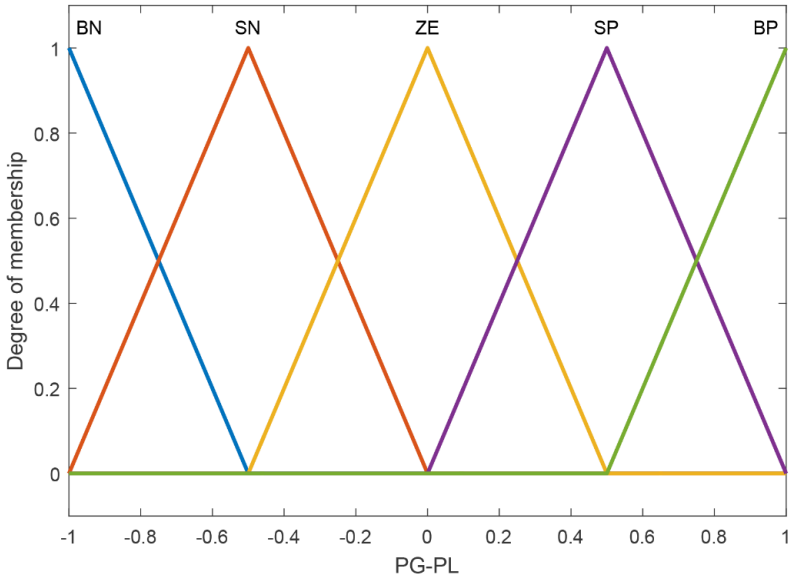

Figure 3.8: Second Input Membership Functions of FLC

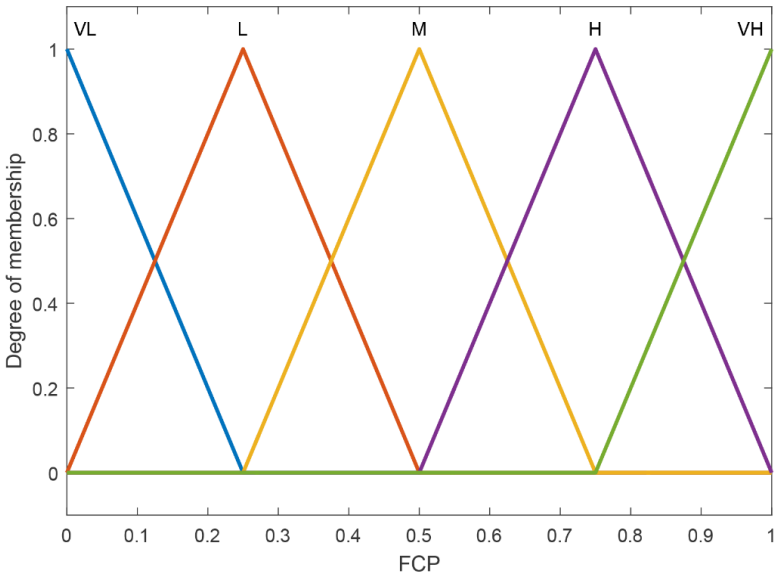

Figure 3.9: Output Membership Functions of FLC

Table 3.2: Fuzzy Rules of the Microgrid EMS FLC

Backup Power		Net Power ($P_{net} = P_{Renewable} - P_{load}$)				
		BN	SN	ZE	SP	BP
SOC	VL	VH	H	L	L	VL
	L	H	M	VL	VL	VL
	M	VL	VL	VL	VL	VL
	H	VL	VL	VL	VL	VL
	VH	VL	VL	VL	VL	VL

The abbreviations VL, L, M, H, VH stand for: very low, low, medium, high and very high respectively and the abbreviations BN, SN, ZE, SP, BP stand for: big negative, small negative, zero, small positive and big positive respectively.

3.4 Optimization of FLEMS Using Artificial Bee Colony

FLC can be optimized using intelligent optimization techniques. The optimization is done to enhance the output of the FLC to reach the desired action with good performance and high efficiency. In this work, FLC controls the operation of the backup systems in the microgrid such as the fuel cell or the diesel generator during the insufficient or absence of renewable generation and storage system. However, making theses backup systems following the varying load demand by minimum fuzzy rules is difficult process. Therefore, optimizing the FLC using intelligent technique can make a difference in controlling process.

One of the recent and effective intelligent optimization techniques is the artificial bee colony (ABC). It is considered as one of the evolutionary algorithms. This technique simulates the foraging behavior of honey bees and has been used successfully in many applications. It was first proposed by Karaboaga in 2005.

3.4.1 Natural Honeybee Swarm Behavior

To understand the concept of the ABC algorithm, first, an overview on the behavior of natural honeybees that inspired the proposed optimization technique is given below. In general, The honeybees behavior for seeking the food sources divided into three parts [64]:

- Food Sources: the worth of the food source depends on many factors such as its nearness from the beehive and the nutritional value of the food, in other words, the amount of energy that can be extracted from that source. The food source

represents the probable solution and the quality of the food source represents the fitness of the solution for the optimization problem.

- Employed bees: They go to utilize the food source and come back to the hive in a manner called (waggle dance). The employed bees share the information of their food sources such as the distance and direction from the beehive with onlooker bees. The number of employed bees equals the number of the used food sources. When such food source is left, the associated employed bee become scout bee and searches for another food source. The number of employed bees represents the number of solutions.
- Unemployed bees: they are divided into two types. Scout bees who their food sources vanished, and they search for another food source. The other type is onlooker bees which are continually at a look and wait to the (waggle dance) to establish food source exploiting.

3.4.2 Artificial Bee Colony Algorithm

ABC algorithm divided into two halves represent the two stages of the honeybee's behavior. The first half allocated for the behavior of the employed bees and unemployed bees. The second half contains two types of bees: the scout bees and the onlooker bees. Figure 3.10 illustrates the algorithm flowchart and shows the steps of ABC optimization.

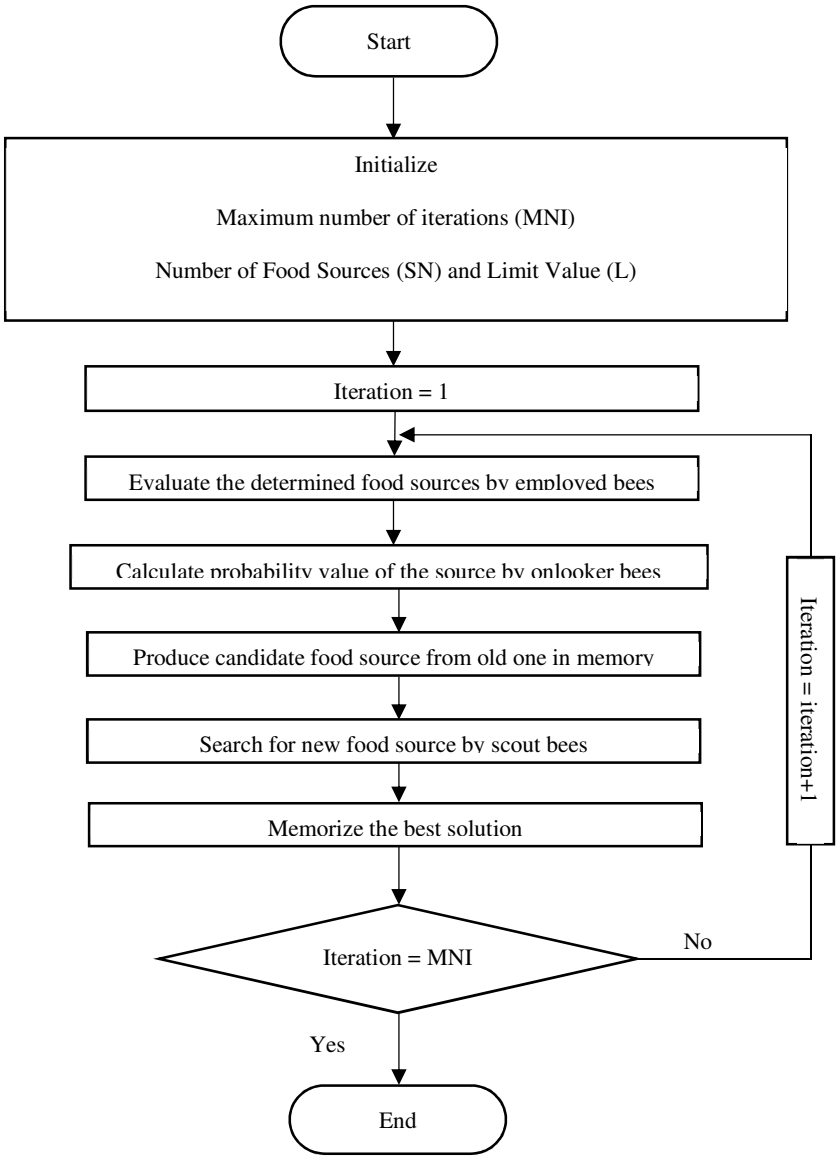

Figure 3.10: ABC Algorithm

The first stage of the algorithm initializes the initial solutions S_i (food sources) in a random distributed manner in N-dimensional vectors ($i = 1,2,3 \ldots . FN$) where N is the number of optimized parameters and FN is the food sources number. After that, these

solutions subjected to number of iterations of the complete search procedure. The employed bees start exploiting these sources, evaluate its quality according to the fitness function, and then share the information with the onlooker bees.

Depending on the probability value of the food source, the onlooker bee chooses a source food. The onlooker bee calculates the probability value as:

$$P_n = \frac{S_{fitness,n}}{\sum_{i=1}^{FN} S_{fitness,i}} \tag{27}$$

where P_n is the probability value of the desired source, $S_{fitness,n}$ is the current fitness source. After that, ABC produces a candidate food source from old one in memory as:

$$V_{i,j} = x_{i,j} + \phi_{i,j}(x_{i,j} - x_{k,j}) \tag{28}$$

where $k = 1,2,3, \ldots . FN$, $j = 1,2,3, \ldots \ldots, N$ and $i = 1,2,3, \ldots \ldots, N$ are random indexes, k must be different from i value and $\phi_{i,j}$ is a random constant between [-1,1]. If the position source cannot be improved, the source is abandoned, and the employed bee become a scout bee and searches for new food source. The operation is defined as:

$$x_i^j = x_{min}^j + rand(0,1)(x_{max}^j - x_{min}^j) \tag{29}$$

where $x_i$is the abandoned sources and $j \in \{1,2,3, \ldots, N\}$. The procedure repeated according to the iteration number until the best solution obtained [65].

3.4.3 Optimizing Microgrid FLC using ABC

Depending on ABC intelligent optimization algorithm, the FLC is optimized by finding the optimal values for inputs and output scaling factors as well the optimal values of the membership functions base values. The ABC algorithm searches for the optimal values according to the developed fitness function. Figure 3.11 illustrates the optimization process for FLC.

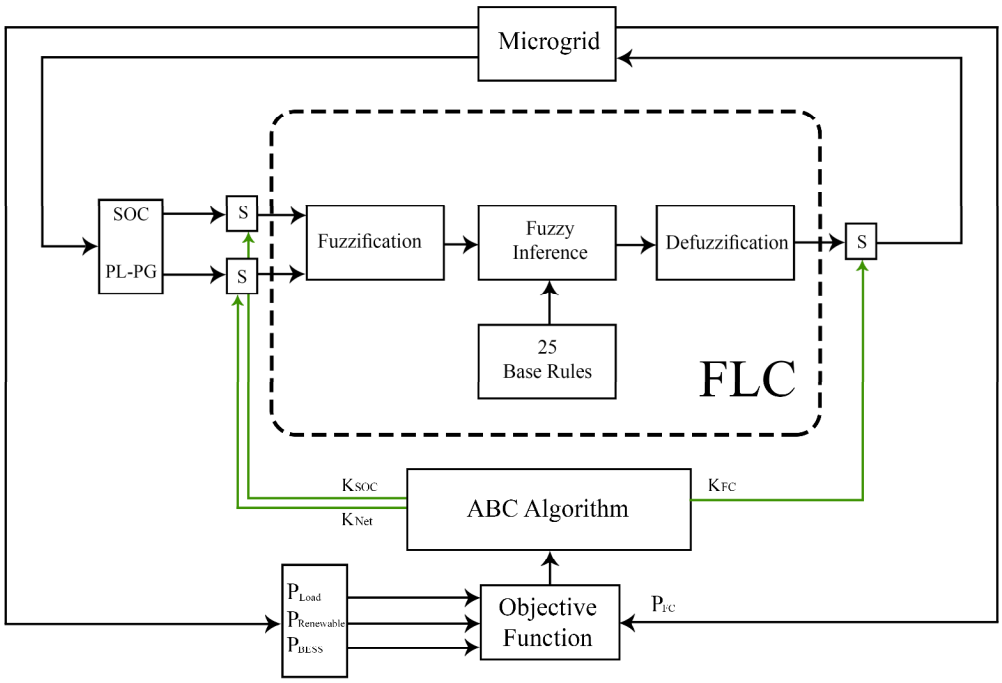

Figure 3.11: Optimization of Fuzzy Logic Controller Using ABC Algorithm

The Objective Function:

The aim of the optimization process in this stage is to enhance the operation of the FLC. In other words, it should minimize the error between the current operation of the fuel cell and the actual power needed from it. The fitness function in this stage can be written as:

$$f = \int_0^T |\Delta P|^2 dt \tag{30}$$

where T is the simulation time which is 24 hours (86400 seconds) and ΔP is the difference between the generated power from fuel cell and the reference power. ΔP calculated as:

$$\Delta P = P_{Ref} - P_{FC} \tag{31}$$

where P_{FC} is the fuel cell power and P_{Ref} represents the reference power (actual needed power) and given as:

$$P_{Ref} = \begin{cases} P_{Load} - P_{Renewable} - P_{BESS}, & P_{Load} \geq P_{Renewable} \\ 0, & otherwisw \end{cases} \tag{32}$$

where P_{Load}, $P_{Renewable}$, P_{BESS}, are load power, power generated from the renewables systems, and power discharged from the battery storage system respectively. Hence ΔP can be written as:

$$\Delta P = \begin{cases} P_{Load} - P_{Renewable} - P_{BESS} - P_{FC}, & P_{Load} \geq P_{Renewable} \\ 0, & otherwisw \end{cases} \tag{33}$$

The objective function constrains given as:

$$K_{Soc}^{min} \leq K_{SOC} \leq K_{Soc}^{max} \tag{34}$$

$$K_{NetPower}^{min} \leq K_{NetPower} \leq K_{NetPower}^{max} \tag{35}$$

$$K_{FCPower}^{min} \leq K_{FCPower} \leq K_{FCPower}^{max} \tag{36}$$

$$N_{MF\ Point}^{min} \leq N_{MFpoint} \leq N_{MF\ Point}^{max} \tag{37}$$

were K_{SOC}, $K_{NetPower}$ and $K_{FCPower}$ are the scaling factors of the two inputs and output of the FLC. $N_{MFpoint}$ is the value of each base of each membership function, thus each input and output of the FLC in this work has 10 base values. The minimum and maximum boundaries of these constants are initially determined by trial and error method.

3.5 Economic Dispatch for the Microgrid

Due to low wind speed in Dhahran city which is the location of current study, the generation of small-scale WT for residential use will be less efficient. In addition to that, the installation cost of the WT is more expensive. Hence, from economic point of view, it will be better if the WT system replaced by another source such as a diesel generator.

Unlike WTs, DGs are a dispatchable sources since their rated power can be controlled according to the load demand. In this work, the microgrid has already a dispatchable source which is fuel cell. Hence, to reduce the generation cost for these sources, economic dispatch problem is solved and will be integrated with the FLEMS. Figure 3.12 illustrates the microgrid configuration in this stage.

Economic dispatch is an expression using for describing the optimal generation of several generators in an electrical system to meet the load demand while maintaining the lower possible cost of generation subjected to several constrains [66]. The economic dispatch problem usually solved using special software program. Recently, optimization techniques are used, and they are gaining wide popularity.

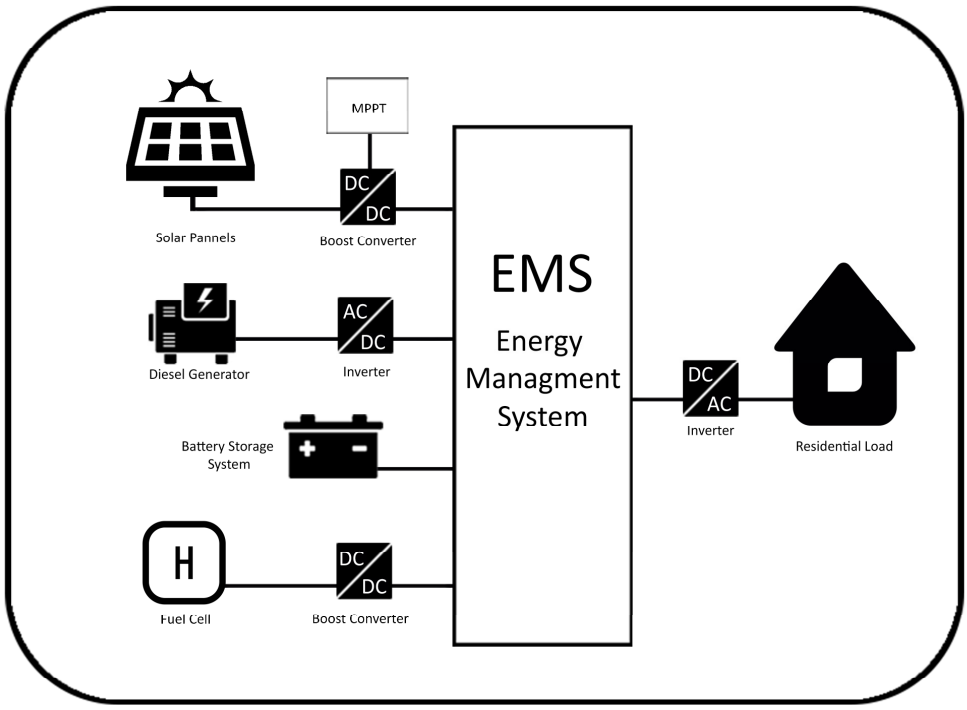

Figure 3.12: Structure of the Microgrid in Economic Dispatch Stage

The specification of the modified version of the microgrid in this stage can be summarized as follows:

- Dispatchable back up sources of the microgrid in this stage are fuel cell and diesel generator.

- The size of the diesel generator is 1KW and the size of fuel cell is 3KW, together they can deliver up to 4KW during operation.

3.5.1 Objective Function of Microgrid for Economic Dispatch

The aim of applying the economic dispatch within the FLEMS of the microgrid is to minimize the total generation cost. In order to develop the microgrid cost function, the cost function of each dispatchable source must be determined. The cost function of DG is assumed as a second order polynomial function as:

$$F_t(P_{DG,t}) = a_{DG} + b_{DG}P_{DG,t} + c_{DG}{P_{DG,t}}^2 \quad (38)$$

where F_t is the cost function of the diesel generator at time t. $(P_{DG,t})$ is the output power of the diesel generator at the same time. a_{DG}, b_{DG} and c_{DG} are the cost coefficient of the DG. The cost function of the fuel cell is also assumed as a second order polynomial function as:

$$F_t(P_{FC,t}) = a_{FC} + b_{FC}P_{FC,t} + c_{FC}{P_{FC,t}}^2 \quad (39)$$

where F_t is the cost function of the FC at time t. $(P_{FC,t})$ is the output power of the fuel cell at the same time. a_{FC}, b_{FC} and c_{FC} are the cost coefficient of the FC. Hence, the objective function can be written as follows:

$$Min. \quad C = \sum_{t=1}^{T} [F_t(P_{DG}) + F_t(P_{FC})] \quad (40)$$

where C is Total generation cost, $F_t(P_{DG})$ is cost function of the diesel generator at time t and $F_t(P_{FC})$ is cost function of the fuel cell at time *t*. the constrains are stated as follows; (41) represents the equality constrain while (42) and (43) represent the inequality constrains.

$$P_{DG,t} + P_{FC,t} = P_{Load,t} - P_{renewable,t} - P_{BESS,t} \quad (41)$$

$$P_{DG}{}^{min} \leq P_{DG} \leq P_{DG}{}^{max} \quad (42)$$

$$P_{FC}{}^{min} \leq P_{FC} \leq P_{FC}{}^{max} \quad (43)$$

Parameter of the Cost Function

The maximum and minimum boundaries of the inequality constrains are set depending on the rated power of DG and FC as:

$$0 \leq P_{DG} \leq 1KW \quad (44)$$

$$0 \leq P_{FC} \leq 3KW \quad (45)$$

The cost coefficient of the FC and the DG are set according to the literature [67], [68] as shown in Table 3.3.

Table 3.3: Cost Coefficient of the dispatchable sources of the microgrid

Coefficient	Fuel Cell	Diesel Generator
a	19.36	10
b	4.94	200
c	0.77	100

3.5.2 Intelligent Techniques for Solving Economic Dispatch Problem

To lower the cost of operation by economic dispatch, three intelligent optimization techniques conducted to solve the problem. One of them is the artificial bee colony (ABC) which was explained previously for optimizing the FLC. The other techniques are particle swarm optimization (PSO) and genetic algorithm (GA) techniques.

Particle Swarm Optimization

PSO is an intelligent technique used for optimizing formulated problem inspired by the natural behavior of the fish and birds swarm. It was first proposed by Kennedy and Eberhart 1n 1995 [69] and modified later by Shi and Eberhart [70]. The concept of this algorithm is that each particle in the search space has its own co-ordinates and represents a probable solution for the problem. These particles update their position and velocity in each iteration according to their best-known solution. Finally, all particles contribute in obtaining the best global solution.

Let vectors $Y_i = [Y_{i1}, Y_{i2}, Y_{i3}, \ldots., Y_{in}\ ]$ and $S_i = [S_{i1}, S_{i2}, S_{i3}, \ldots., S_{in}]$ represent the position and velocity of the PSO algorithm. Vectors $L_{besti} = [Y_{i1Lbest}, Y_{i2Lbest}, Y_{i3Lbest}, \ldots., Y_{inLbest}]$ and $G_{best} = [Y_{1Gbest}, Y_{2Gbest}, Y_{3Gbest}, \ldots\ , \ Y_{nGbest}]$ represent the best position of the particle and the best position of particle neighbors respectively which is the global best solution. When a particle finds its best values, its position and velocity updated as follows:

$$S_i^{k+1} = S_i^k * \omega + C_1 * rand(0,1) * \left(L_{besti} - Y_i^k\right) + C_2 * rand(1,0) * (G_{best} - Y_i^k) \tag{46}$$

$$Y_i^{k+1} = Y_i^k + S_i^{k+1} \tag{47}$$

where S_i^k and Y_i^k are the particle velocity and position at iteration k respectively. C_1 and C_2 are the acceleration factors. ω is inertia weight and calculated as:

$$\omega = \omega_{max} - \left[\frac{\omega_{max} - \omega_{min}}{K_{max}}\right] K \tag{48}$$

where ω_{min} and ω_{max} are the initial and final inertia weight respectively while K and K_{max} are the current and the final number of iteration respectively [71], [72].

The objective function of the economic dispatch problem used in this stage is defined in 3.5.3. Figure 3.13 illustrates the flow chart of PSO algorithm for solving ED problem.

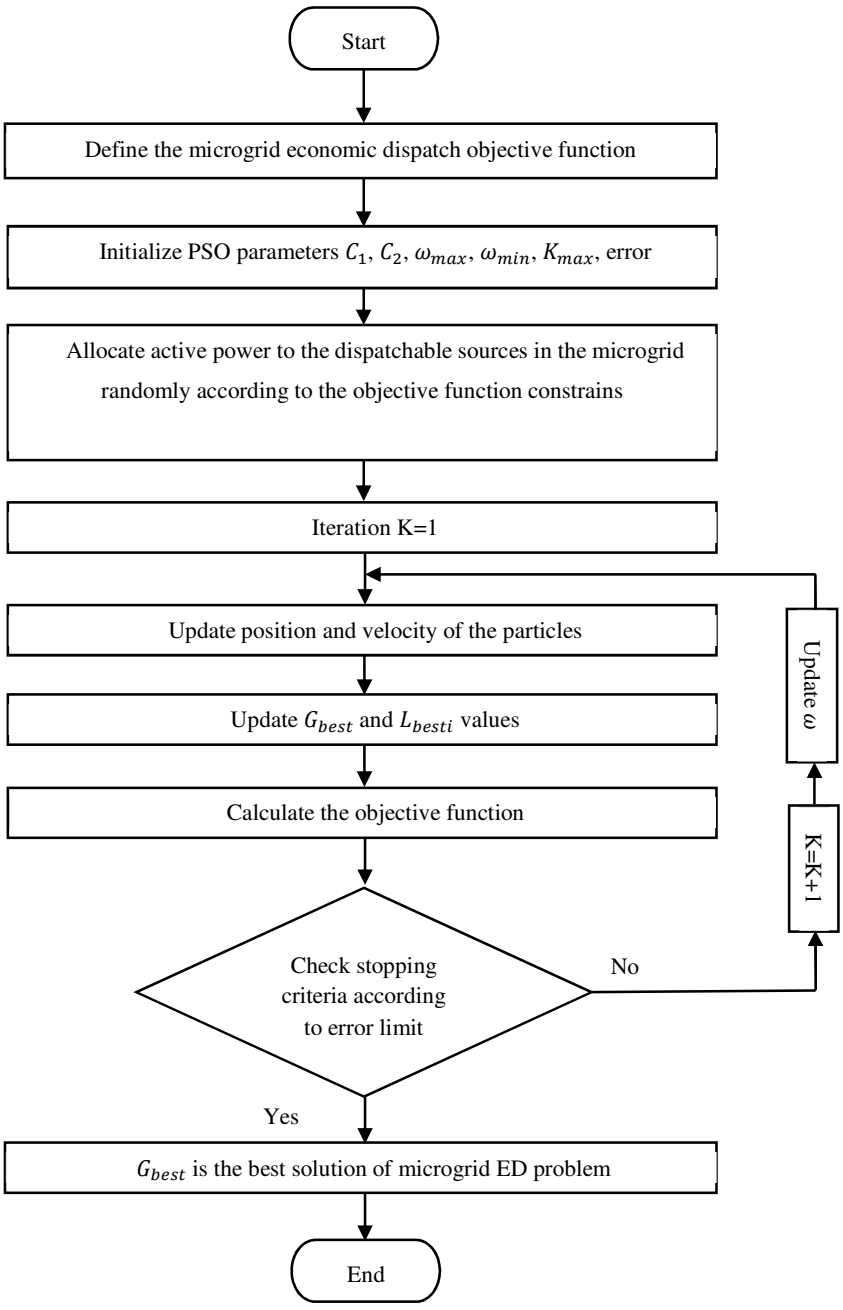

Figure 3.13: PSO Algorithm

Genetic Algorithm

GA is one of the most famous algorithms used for optimization. It was inspired by the process of natural selection to produce high-quality generation. It belongs to the evolutionary algorithms family and used to produce high quality solution for the optimization problem. The algorithm consists of several procedures that can be summarized in several steps. At the beginning, it initiates the population, then evaluate this generation according to the fitness function. After that, genetic operations as selection, crossover and mutation process taken place to produce a better generation. The process repeated according to the number of iterations until best solution obtained.

The algorithm generates the initial population in N-dimensional strings. These strings contain the parameters of the optimization problem and they are coded in the form of binary digits. Binary strings are the basic structure that GA algorithm can deals with. in fact, they represent the chromosomes where each binary digit represents a gene. Second, the algorithm evaluates the individuals of the population according to the fitness function as:

$$f(X) = \frac{1}{1 + F(x)} \tag{49}$$

where $f(X)$ is the fitness function and F(x) is the objective function of the optimization problem. In the next stage, three genetic operators produce the new generation; reproduction, crossover and mutation. In reproduction, copies of the old chromosomes are placed in matting pole according to the fitness value. The chromosome that has higher value, higher number of copies will be placed.

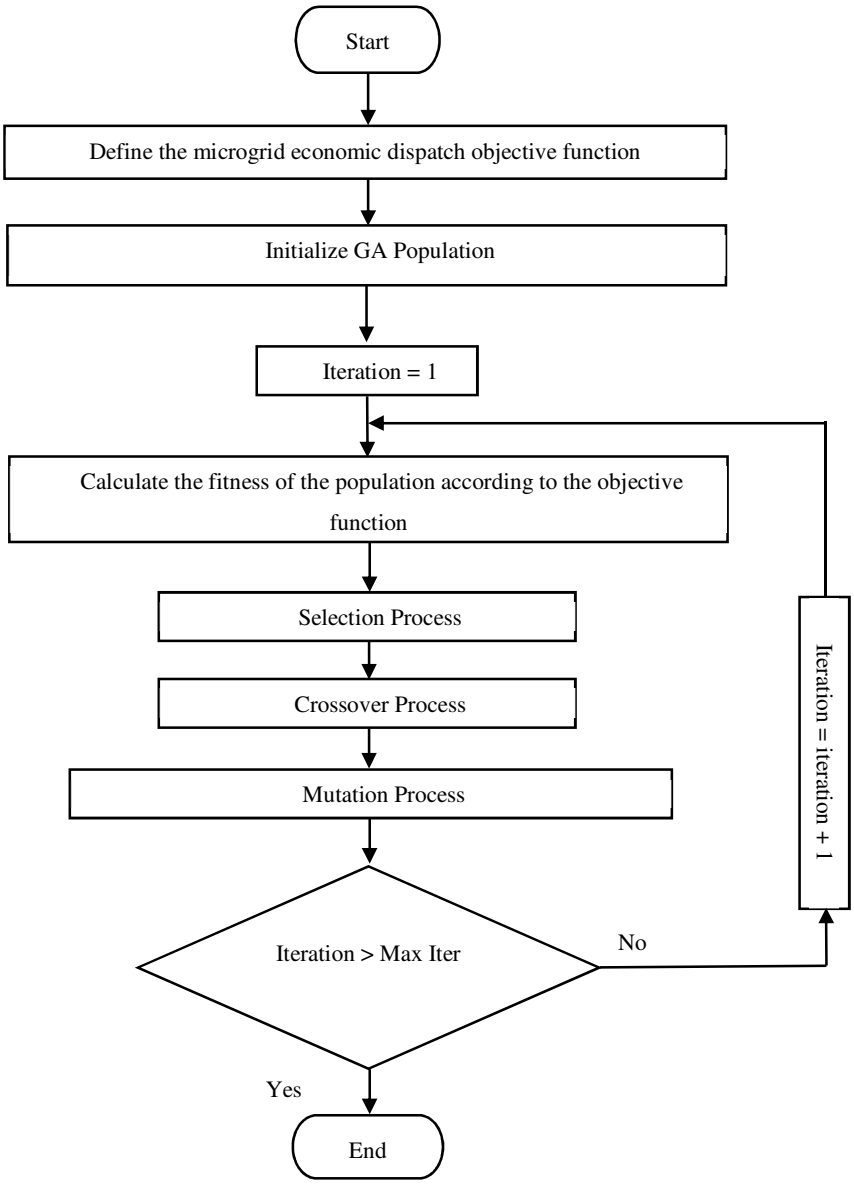

Figure 3.14: GA Algorithm

Then, chromosomes from the matting pole is selected depending on a common mechanism called roulette-wheel according to the fitness probability as:

$$P_f = \frac{f_i}{\sum_{j=i}^{N} f_i} \tag{50}$$

where f_i is the fitness value of the string and N is the number of individuals in the population. The second operator in the second stage is crossover that exchanges information of the strings in the matting pool to generate new stings. The third operator is mutation where the genes (binaries) inside the chromosomes (strings) are replaced by other ones to create a new structure [73], [74]. Figure 3.14 illustrates the flowchart for GA used for solving ED problem.

3.5.3 Optimized FLEMS with Economic Dispatch

The aim of economic dispatch problem for any power system that contains several dispatchable sources is solved to minimize the generation cost. The economic dispatch gives the optimal amount of power that each generator must produce in specific time to operate the system economically. It is considered as a controlling approach that depends on scheduling procedure. However, in this work, a new approach is proposed to control the dispatchable sources in the microgrid using economic dispatch within the optimized FLEMS.

The idea behind this approach is to set a limit value of power generation for each dispatchable source in the microgrid system that controlled by the optimized FLEMS in each hour of the day. Figure 3.15 illustrates the proposed controlling process. The economic dispatch problem for the proposed microgrid in this stage of is developed in 3.5.1 and simulation is conducted in MATLAB/Simulink. The obtained limits of power

generation for each hour of the day for each dispatchable source in the microgrid is embedded within the optimized FLEMS. The simulation results of the proposed method are compared with other methods results in previous sections and presented in next chapter. the comparison in energy savings are conducted among microgrid with FLEMS, microgrid with optimized FLEMS, and microgrid with optimized FLEMS considering economic dispatch.

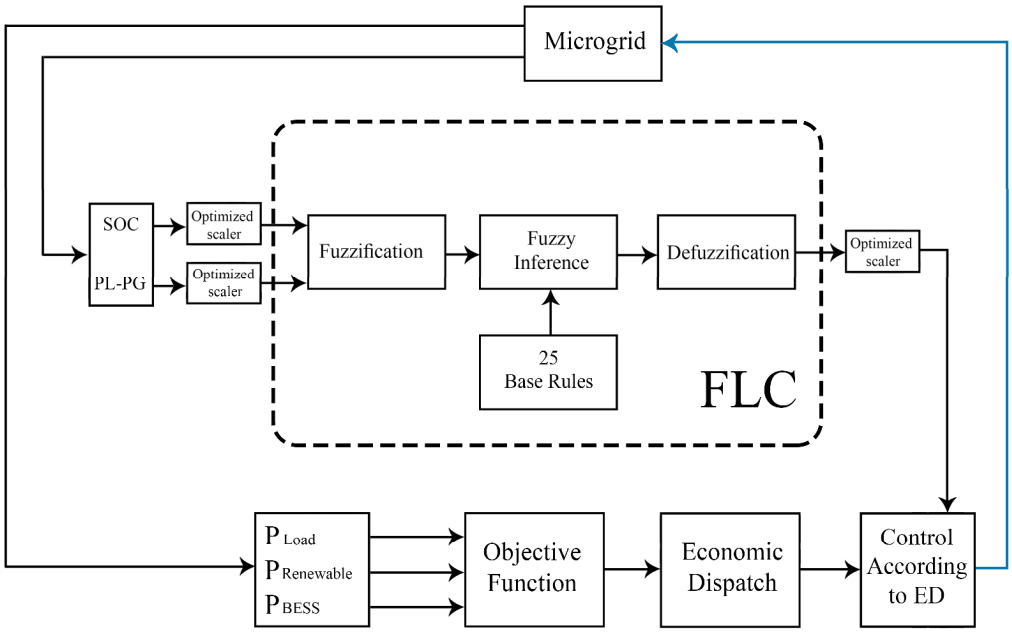

Figure 3.15: Proposed Microgrid FLEMS with Economic Dispatch

CHAPTER 4

SIMULATION RESULTS and DISCUSSIONS

The simulation of this work is divided into four main stages as explained earlier in Chapter 3. All microgrid components and power electronics used for integrating these components to form the microgrid is done using MATLAB/Simulink environment while the intelligent techniques used for optimization purpose is done by MATLAB coding and connected to the microgrid in the Simulink.

The first section in this chapter presents the simulation results and discusses for studying the effect of ambient temperature on the modeled PV solar system of the microgrid depending on real data of Dhahran city that in Saudi Arabia as a case study. The second section presents the results of simulation that conducted for investigating the potential for installing small-scale hybrid renewable energy system to supply residential house depending on real data collected from the area of the study. Energy analyzing is also conducted in this study for the purpose of investigation.

The third section exhibits the simulation results of the microgrid controlled by fuzzy logic energy management system of low complexity. Furthermore, the results are optimized using artificial optimization technique while maintaining the minimum possible number of fuzzy rules. Real data of two hot summer days in Dhahran city used in simulation as case of study. A comparison in the system efficiency before and after optimization is also presented.

The last section presents the simulation results of solved economic dispatch problem using three intelligent optimization techniques for lowering operation cost and enhancing the microgrid efficiency. In addition, the simulation results the microgrid controlled by optimized FLEMS considering the economic dispatch presented using real data for 24 hours of summer day as a case of study. A comparison in terms of efficiency and cost with conventional methods is also presented.

4.1 The Effect of Ambient Temperature on the Solar System

As explained earlier in Section 3.2.1, three models of 5kW photovoltaic solar power systems were built and tested to investigate the effect of different values of ambient temperature on the output power with fixed irradiation. The results of the test are presented in Table 4.1. It is noticeable that third way of connection of the PV arrays that illustrated in Figure 3.4 is the best one among others when exposed to high temperatures and fixed irradiation. Hence, this model is used in obtaining the best-operating temperature for PV systems during different seasons months in Dhahran. The same configuration also used in the microgrid in this work.

Table 4.1 Comparison of Power Output Three Different PV Configurations with Varing Temprature

Radiation [1000 w/ m^2]			
Temperature (Celsius)	Series (kW)	Parallel (kW)	Parallel & Series (kW)
10°	5.671	5.281	5.727
15°	5.688	5.297	5.744
20°	5.701	5.307	5.757
25°	5.708	5.316	5.764
30°	5.703	5.313	5.759
35°	5.682	5.294	5.738
40°	5.634	5.252	5.689
45°	5.547	5.174	5.600
50°	5.402	5.045	5.453
55°	5.180	4.845	5.228
60°	4.858	4.554	4.902

To obtain the best-operating temperature in different weather conditions, five months from different seasons in Dhahran were selected to be tested in the designed PV system. Solar irradiation and ambient temperature for January, February, April, July and October in 2016 are applied to the system.

Figure 4.1 illustrates the solar irradiation, ambient temperature for 23 days in January applied to 5kw PV model in addition to the power output for the same days. The temperature in this month is considered as perfect for the model since it is winter season. However, the solar irradiation plays a key role in the output power. Winter season in

Dhahran usually be rainy and cloudy which means low irradiation, hence low power generated from PV system.

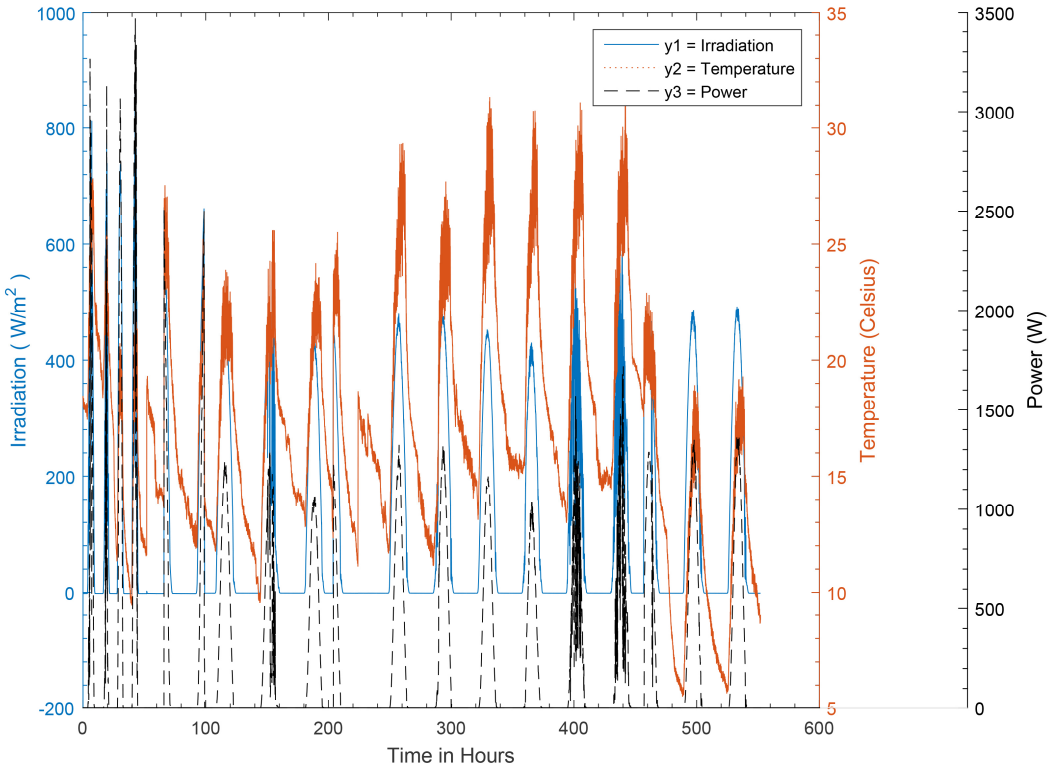

Figure 4.1: Irradiation and Ambient Temperature of January with Power Output From 5kw PV System

The input environmental data for the PV system and the power output of second month which is February are illustrated in Figure 4.2. For more clarification, the month days separated into two halves. In first half, the power output still low except for the first two days. This is due to the low irradiation in winter season in Dhahran although the temperature still in lower values during the day hours. The second half shows increasing in the power output while the sun irradiation getting to increase by the end of winter season.

On the other hand, the temperature is also increasing, and this affects passively on the power output as will be seen in the next months results.

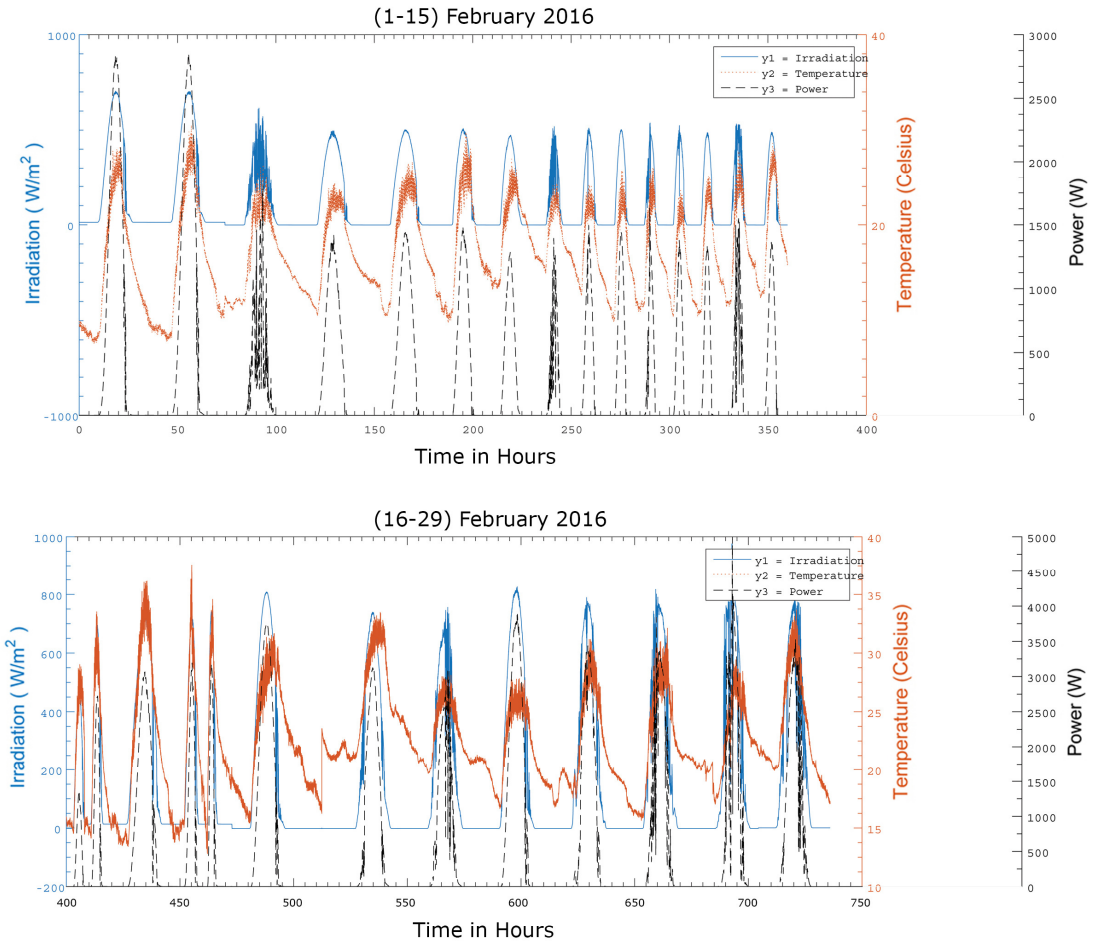

Figure 4.2: Irradiation and Ambient Temperature of February with Power Output From 5kw PV System

April is the third month chosen for simulation. Figure 4.3 shows the power output generated based on the applied solar irradiation and ambient temperature for 12 days of this month in the PV system. Irradiation amount reaches its optimum levels in April at Dhahran. The ambient temperature is still in acceptable range with an average of 30°C.

Hence, the power output generated from 5kw PV system reaches its highest level in spring season. Some days in the figure show low generation due to the clouds and rains.

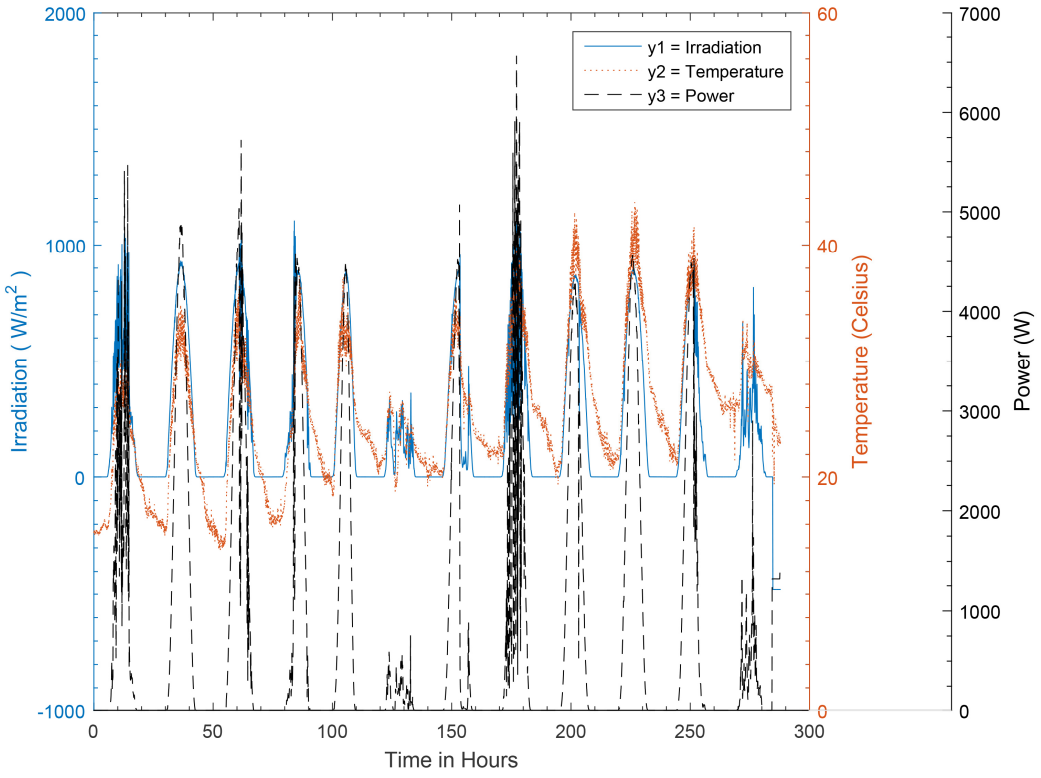

Figure 4.3: Irradiation and Ambient Temperature of April with Power Output From 5kw PV System

Moving to the hottest month in the summer season in Dhahran which is July as shown in Figure 4.4, the power output is decreased by 23% when compared with April as shown in Figure 4.3. This is due to the high increase in temperature in summer months that reaches up to 50°C in midday hours, hence, this affects the power output of the PV system passively although that solar irradiation is high and most of July days is shiny and no clouds shade the PV panels. However, the temperature here is playing the key role in this situation.

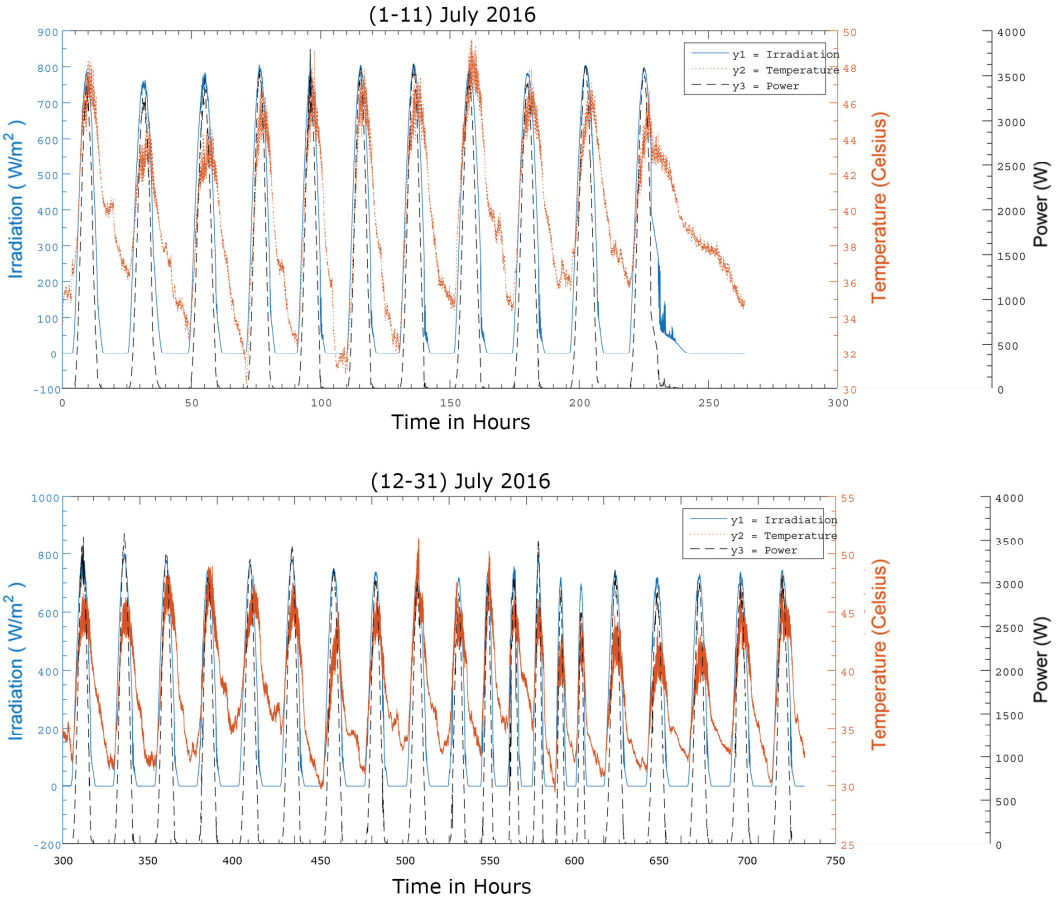

Figure 4.4: Irradiation and Ambient Temperature of July with Power Output From 5kw PV System

Figure 4.5 exhibits the input environmental data and simulation results for the designed PV system in October; the last month of simulation in this stage. The results show a stable power generation during the whole month days. However, the efficiency still not as high as spring season; around 76% of that in April, although the ambient temperature decreases during this month. One explanation for this is that the change of incident angel of sunrays in autumn season is differentiated from that in spring season due to the change in earth position around the sun which changes its rotation axis position consequently.

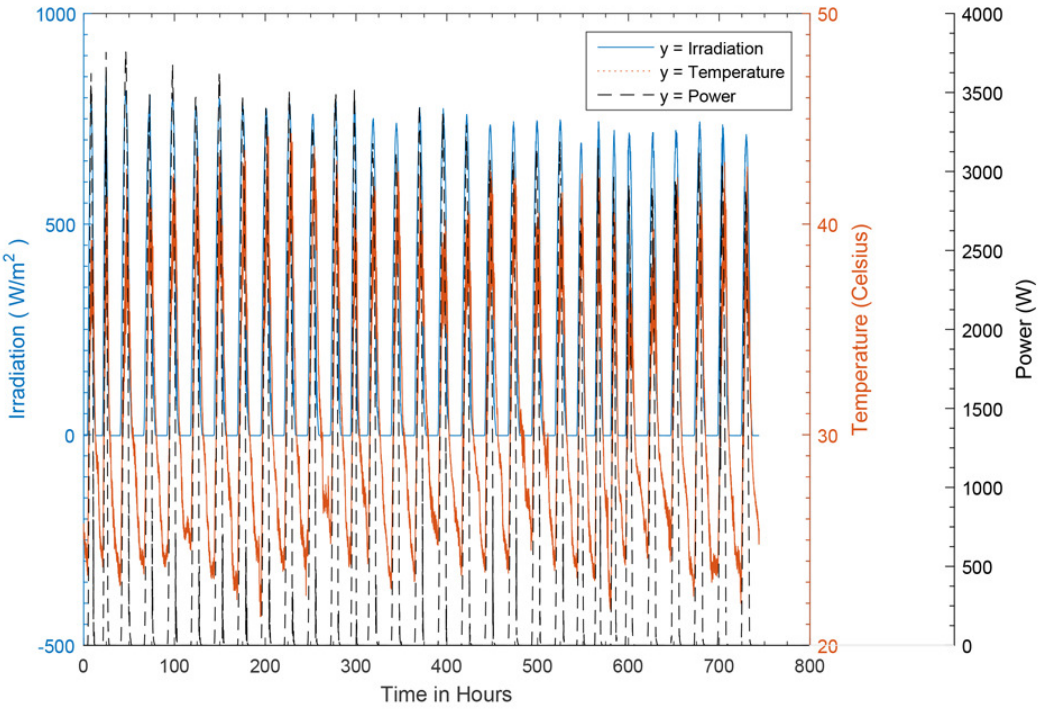

Figure 4.5: Irradiation and Ambient Temperature of October with Power Output From 5kw PV System

From simulation results of this stage, its noticeable that the ambient temperature plays a major role in PV system efficiency even if the solar irradiation is high. The ideal temperature of any PV system is 25°C. However, existed cooling technologies for PV systems cannot decrease the temperature to this value in hot weather conditions such as in summer in Dhahran city. Therefore, a set point for ambient temperature called best-operating temperature is obtained depending on the generated power from high generation days of each month as exhibited in Table 4.2. Taking these set points of ambient temperature in consideration during cooling process, PV system can operate properly and generate acceptable amount of power in hot areas like Dhahran city in Saudi Arabia.

Table 4.2 Best-Operating Temperature for Five Months in Dhahran

Month	Best Operating Temperature
January	22.50° C
February	28.74° C
April	33.76° C
July	44.80° C
October	37.85° C

4.2 Results of Renewable Energy Potential in Dhahran

This section allocated for presenting the results of investigating the feasibility for installing small-scale HRES and energy analysis generated from it under weather conditions of Dhahran. The simulation of this section divided into two parts: the first part obtains the annual average energy generated from both PV and WT systems depending on annual average environmental data collected in 2016. The second part analyzes the energy generated from the HRES for three different days from different seasons in the same location and compared with real residential load demand.

4.2.1 Obtaining Annual Average Energy of Small-Scale HRES

The average solar irradiation, ambient temperature and wind speed for 365 day in 2016 are illustrated in Figures (4.6 - 4.8) respectively. These data applied to the HRES model to obtain the annual average energy.

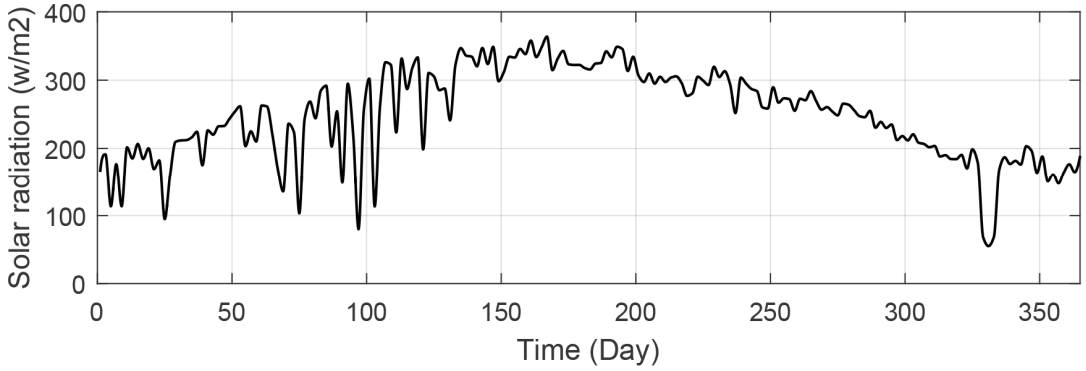

Figure 4.6: Average Solar Irradiation for 365 days in 2016 Applied to the PV System

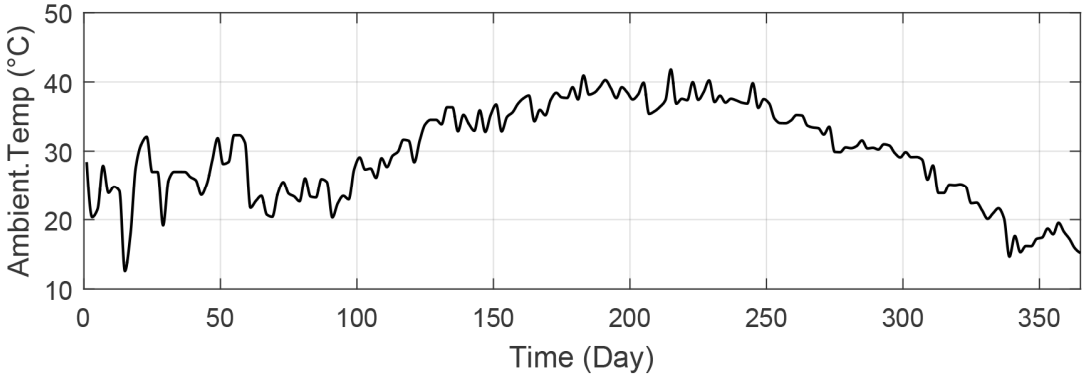

Figure 4.7: Average Ambient Temperature for 365 days in 2016 Applied to the PV System

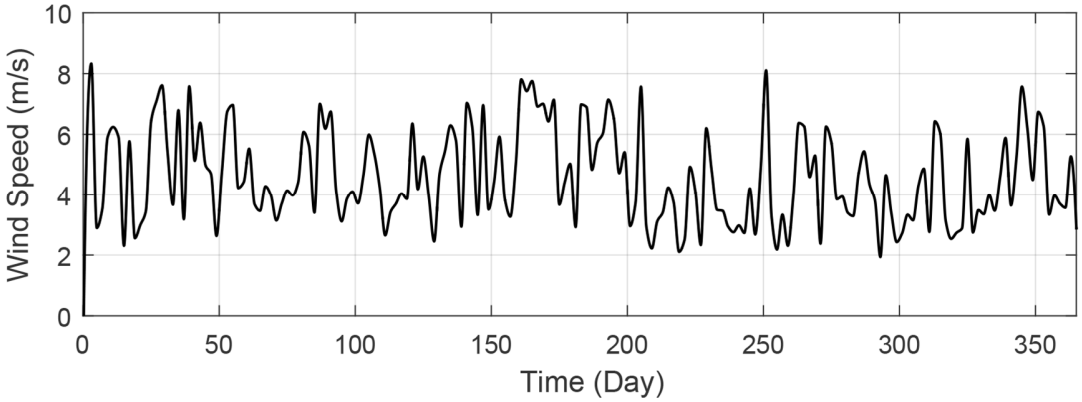

Figure 4.8: Average Wind Speed for 365 days in 2016 Applied to the WT System

Figure 4.9 illustrated the average annual generation of 5kw PV solar system. The figure shows that the power generated from PV system is influenced by irradiation amount that falls on the PV modules and influenced by the increase of ambient temperature passively. Dhahran experiences the highest solar irradiation during summer and spring seasons. On the other hand, the ambient temperature also gets increased in these seasons to its highest level of the year.

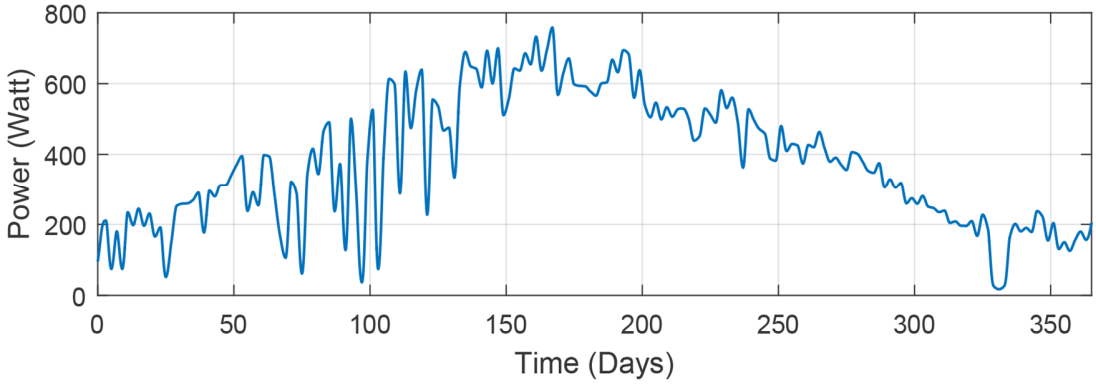

Figure 4.9: Average Output Power for 365 days in 2016 from 5kw PV System

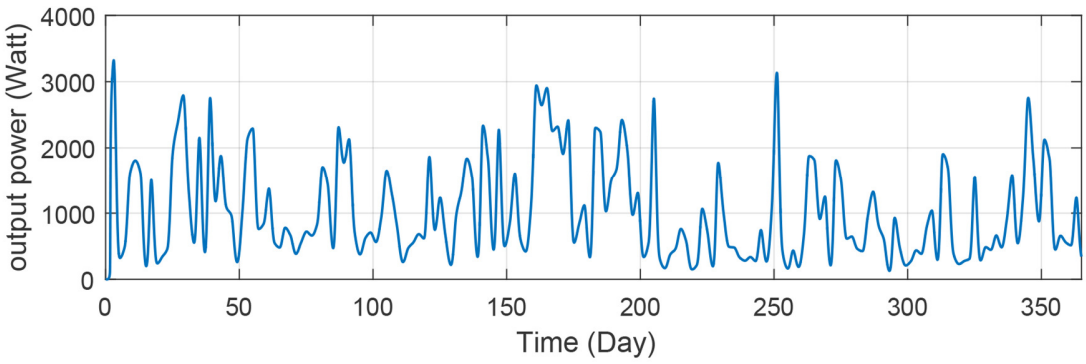

Figure 4.10: Average Output Power for 365 days in 2016 from 5kw WT System

According to the data recorded, Dhahran experiences moderate wind speed during afternoon period in normal weather condition. The average wind speed in Dhahran is around 5.5 m/s as shown in figure 4.8. Thus, small-scale WT that has low cut-in speed ranging between 3.5 to 4.5 m/s would be an appropriate option for HRES in such region. Figure 4.10 shows the annual average from WT system in 2016. The annual load demand of residential house during the same year is 9006.15 kWh that means HRES generation can meet the residential demand. Table 4.3 exhibits the average energy generated annually from each source of the HRES in 2016.

Table 4.3 Average Energy Generated from Hybrid (RES) in 2016

HRES Component	Annual Average Energy
Solar Photovoltaic System	3334.98 kwh
Wind Turbine System	2693.71 kwh
Total	8113.67 kwh
Residential Load Demand	9006.15 kWh

4.2.2 Analysis of Three Different Seasonal Days Compared with Residential Load Demand

Solar irradiation, ambient temperature and wind speed real data for 24 hours from different seasonal days in 2016 applied to the HRES. Figure 4.11 exhibits real environmental data of 26th of March. In this day, the solar irradiation is high, and ambient temperature is moderate as is the case in most of spring days. Thus, the solar generation is in its best at this month of the year. The system generation compared with house load demand as exhibited in Figure 4.12.

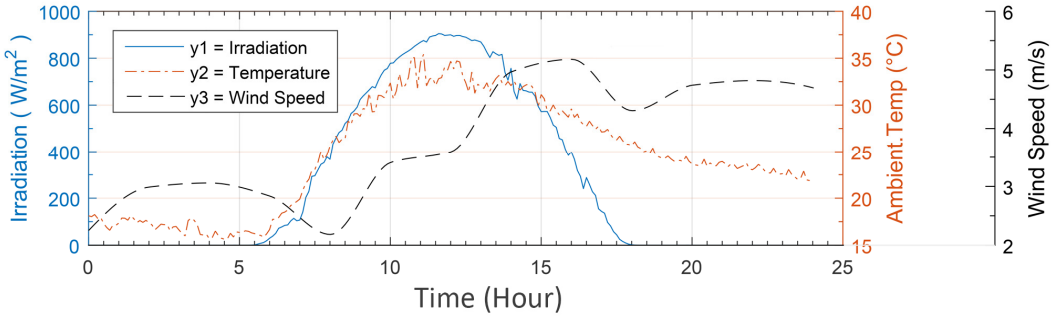

Figure 4.11: Solar Irradiation, Ambient Temperature and Wind Speed of 26th of March

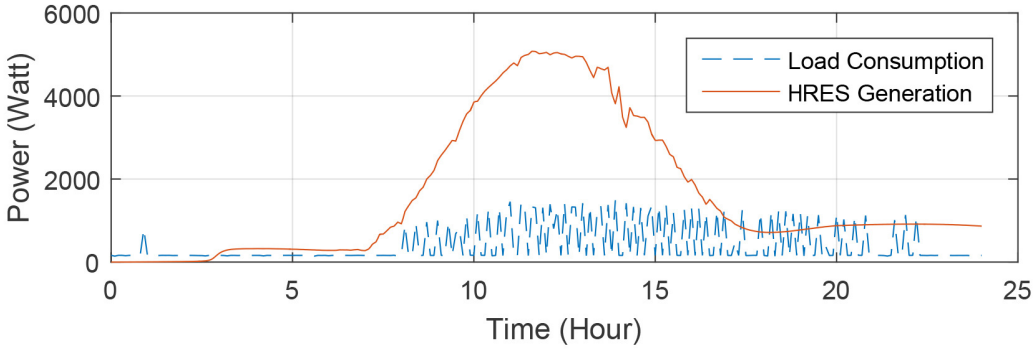

Figure 4.12: HRES Generation Compared with Residential Load Demand in 26th of March

The system generation starts to meet the load demand from early morning hours up to sunset. It meets the load demand most of the day hours. The house load demand in this day is 10.2268 kWh and there is an excess of energy of 28.5kWh. Table 4.4 exhibits energy analysis calculation from simulation results of this day.

Table 4.4 Energy Generated from HRES and Surplus Energy in 26th of March 2016

HRES Component	Energy
Wind Turbine System	13.182 kWh
Solar Photovoltaic System	25.62 kWh
Total generation	38.8 kWh
Load consumption	10.2268 kWh
Surplus	28.573 kWh

The second day chosen for testing the system is 27th of July in summer season. Figure 4.13 illustrates the recorded environmental data for this day. It is noticeable that solar irradiation is at its best near the optimum value for PV panels which is 1000w/m^2, however, the ambient temperature increased by 10 degrees than it was in spring season.

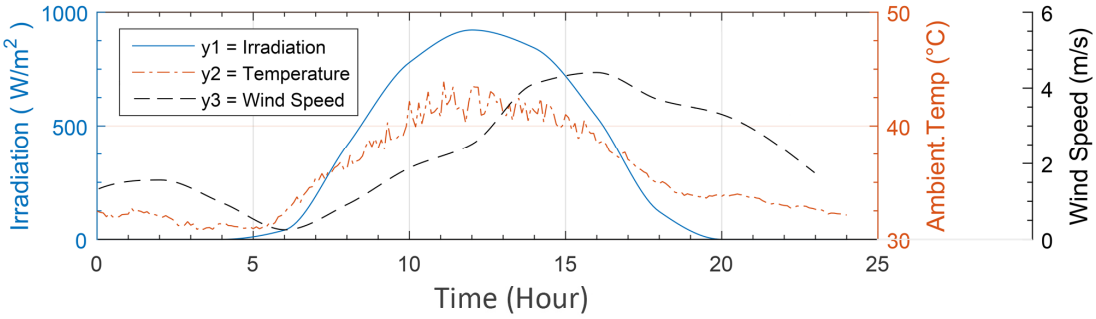

Figure 4.13: Solar Irradiation, Ambient Temperature and Wind Speed of 27th of July

Figure 4.14 illustrates HRES generation along with load demand in this day. In this day, the system starts power generation from early morning hours up to midnight, however it meets the load demand only from 9 AM to 4 PM. Although the system does not meet the total demand of the day, it generated an excess energy in midday hours as shown in the same figure. An existence of backup system to store the surplus energy in midday hours and compensate low energy production at night is a necessary need.

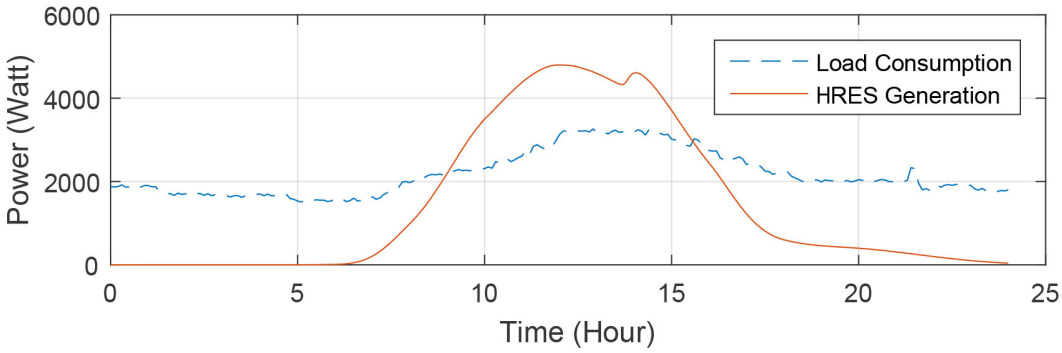

Figure 4.14: HRES Generation Compared with Residential Load Demand on 27th of July

Energy consumption of the house in this day is 52.36 kWh while the total energy generation is 34.6 kWh. Therefore, another sources of energy other than batteries are needed in summer season. This is due to the increase of ambient temperature to high degrees during summer in eastern region of Saudi Arabia. Hence, residential load demand increases drastically due to use of air conditioners all day. Table 4.5 presents energy analysis of the HRES in this day and exhibits the difference between generation and load consumption by the amount of needed energy to be compensated.

Table 4.5 Energy Generated from HRES and Surplus Energy in 27th of July 2016

HRES Source	Energy
Wind Turbine System	4.56 kWh
Solar Photovoltaic System	30.0571 kWh
Total generation	34.6179 kWh
Load consumption	52.3577 kWh
Surplus	17.7398 kWh

The last day chosen for testing in the system was 27th of October in autumn season. Figure 4.15 shows environmental recorded data of this day. A noticeable drop in temperature than in summer is offset by a decrease in irradiation due to the change of incidence angle of sun in autumn season which consequently leads to decrease in solar efficiency in this season months.

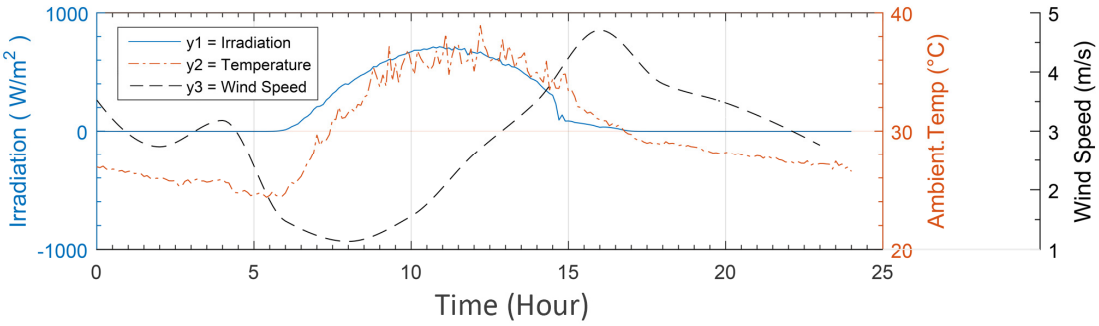

Figure 4.15: Solar Irradiation, Ambient Temperature and Wind Speed of 27th of October

Figure 4.16 shows the system generation in this day compared with load demand of the house for 24 hours. HRES generation meets the load demand during midday hours (from 9 AM to 1 PM) with an excess energy that can be stored in energy storage system for later usage. The total energy generation in this day is 21 kWh while the house load demand is

18.3 kWh. The total load demand of the day is almost near the generation with an excess of 2.8 kWh. This means that the use of storage system will make the system supply the residential house completely from renewable energy during this season days. Table 4.6 presents energy analysis of HRES during the third day of simulation. Dhahran in winter season experiences cold weather with a moderate winds and moderate amount of irradiation offset by very low energy consumption in residential houses which makes the proposed system works efficiently in this season without need for other backup systems.

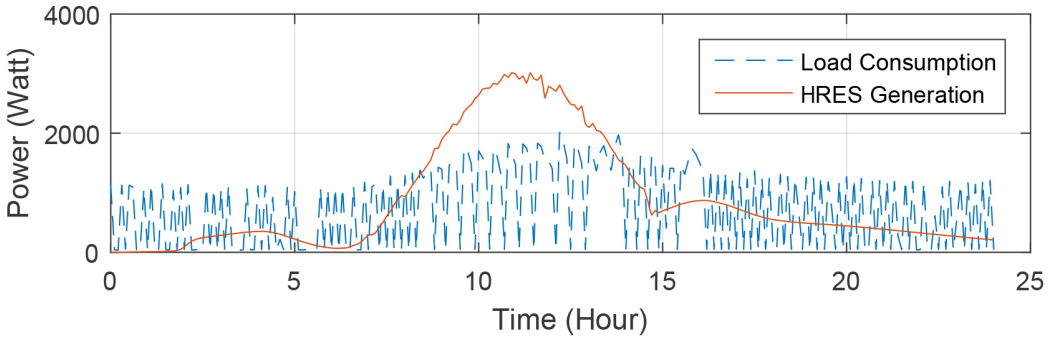

Figure 4.16: HRES Generation Compared with Residential Load Demand in 26th of October

Table 4.6: Energy Generated from HRES and Surplus Energy in 27th of October 2016

HRES Source	Energy
Wind Turbine System	7.040 kWh
Solar Photovoltaic System	13.97 kWh
Total generation	21.01 kWh
Load consumption	18.2385 kWh
Surplus	2.772 kWh

4.3 Results of Microgrid FLEMS Optimization Using ABC Technique

In this stage of simulation, all microgrid components are integrated together using power electronics devices controlled by FLEMS. Optimization using ABC algorithm is conducted to enhance the performance of the FLC that controls the operation of the fuel cell as a backup source. The optimization process is conducted for both; the membership function and the scaling factors of inputs and output of the FLC of the microgrid. The system tested using real data of two summer days in Dhahran city; 27 and 29 July 2016, using solar irradiation, ambient temperature, wind speed and residential load demand recorded inside KFUPM campus. Comparison in system efficiency with / without optimization is presented.

4.3.1 Optimizing FLC of Microgrid EMS Using ABC Algorithm

The proposed microgrid with the initial scaling factors for inputs and output of FLC and basic membership functions were simulated within ABC optimization algorithm. The algorithm is run with different number iteration; 20, 50 and 100, for 86400 seconds (24 hours) in MATLAB/Simulink. The more iteration, the better optimization results. Figures 4.17, 4.18, and 4.19 illustrate the optimization convergence during simulation process for different number of iterations. Optimal membership functions and scaling factors for FLC after optimization are exhibited in Tables 4.7 and 4.8. Figures (4.20 - 4.22) illustrate the optimized FLC membership functions.

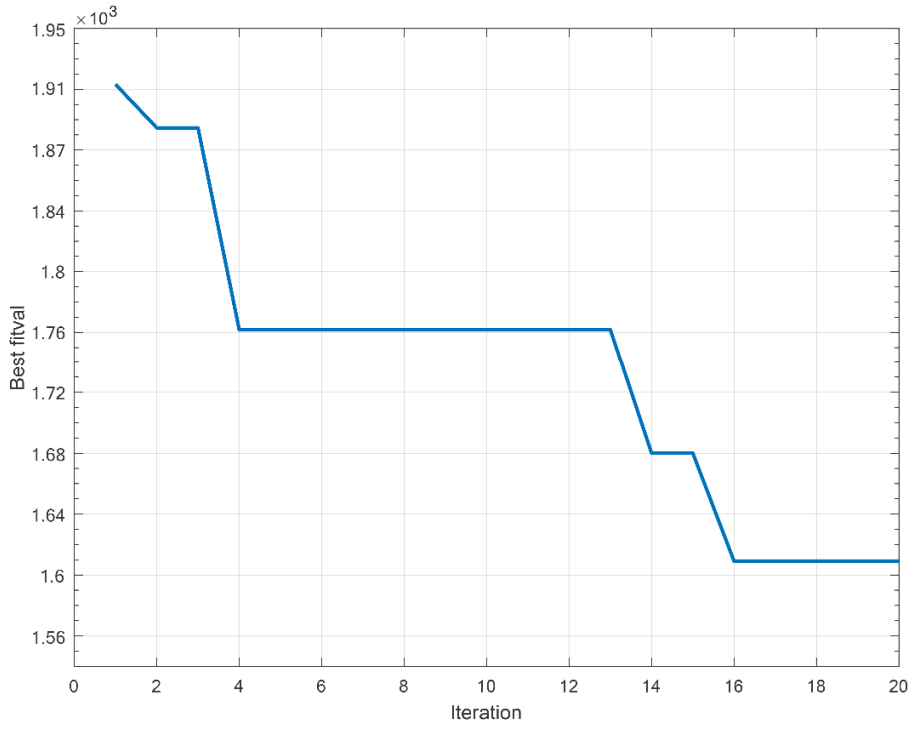

Figure 4.17: Conversion of FLC Optimization Using ABC by 20 Iterations

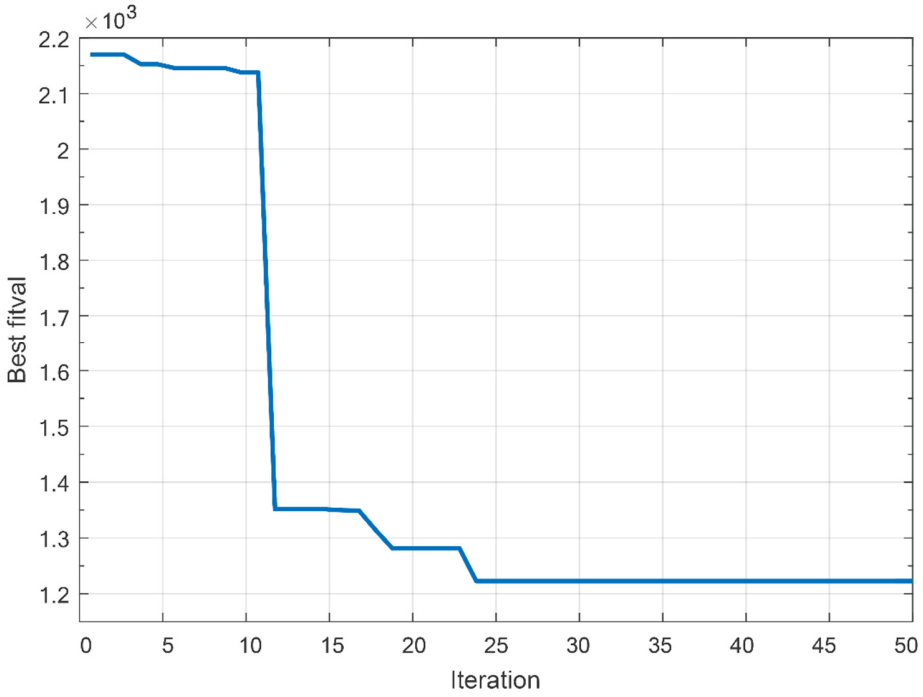

Figure 4.18: Conversion of FLC Optimization Using ABC by 50 Iterations

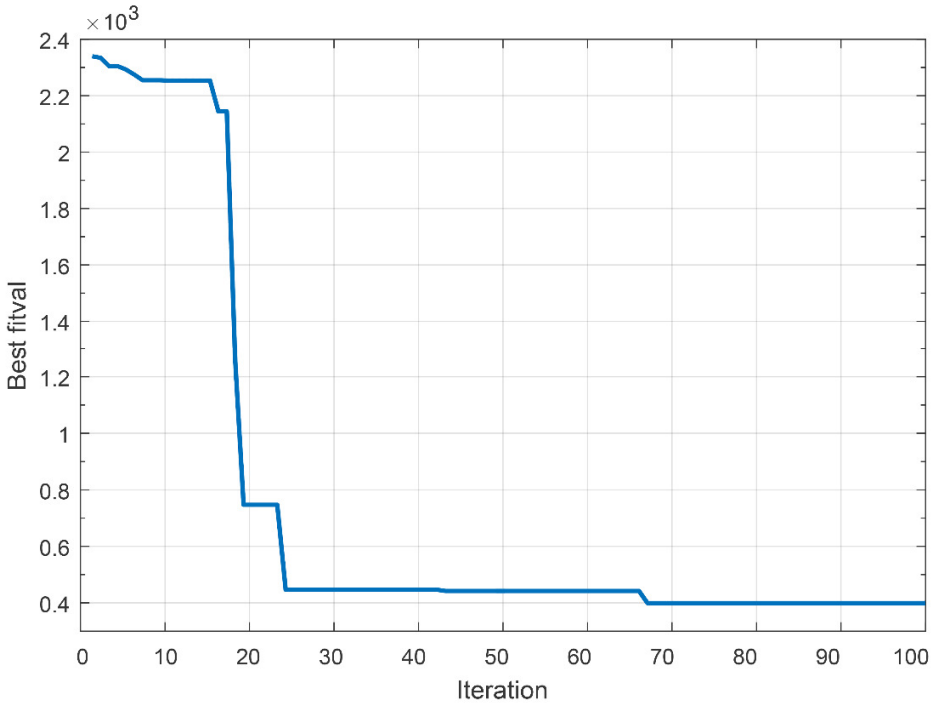

Figure 4.19: Conversion of FLC Optimization Using ABC by 100 Iterations

Table 4.7: Optimal Scaling Factors for FLC Obtained from ABC Optimization Algorithm

Factor	Optimal Value
K_{SOC}	1.293
$K_{NetPower}$	0.706
$K_{FCPower}$	0.9012

Table 4.8: Optimal Base Values of FLC Membership Functions Obtained from ABC Optimization

Membership Function	Left base point	Top point	Right base point
First FLC input membership functions optimized values (Battery SOC)			
VL_{soc}	0	0	0.15
L_{soc}	-0.0425	0.158	0.3373
M_{soc}	0.1762	0.4762	0.7762
H_{soc}	0.6034	0.8102	1
VH_{soc}	0.843	1	1
Second FLC input membership functions optimized values (Net Power)			
BN	-1	-1	-0.507
SN	-1.042	-0.5476	-0.04232
ZE	-0.5265	-0.02646	0.4232
SP	-0.07407	0.5741	1.074
BP	0,5	1	1
FLC output membership functions optimized values (Backup Power)			
VL_{fc}	-0.2876	-0.04662	0.0863
L_{fc}	-0.03	0.2276	0.485
M_{fc}	-0.2276	0.485	0.7426
H_{fc}	0.485	0.7462	1
VH_{fc}	0.7462	1	1

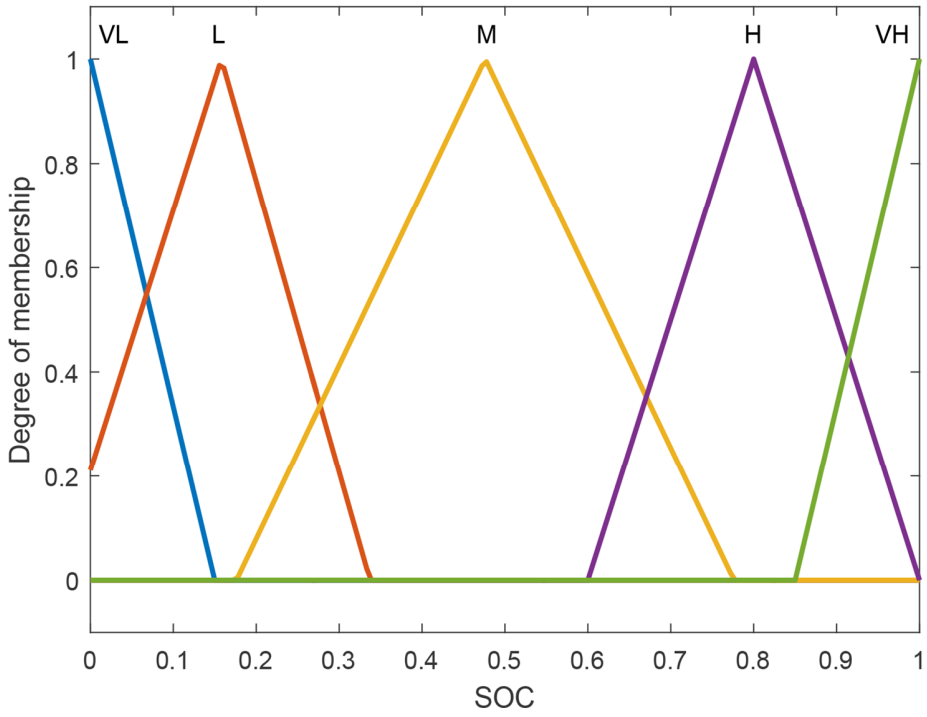

Figure 4.20: Optimized Membership Functions of First Input of FLC

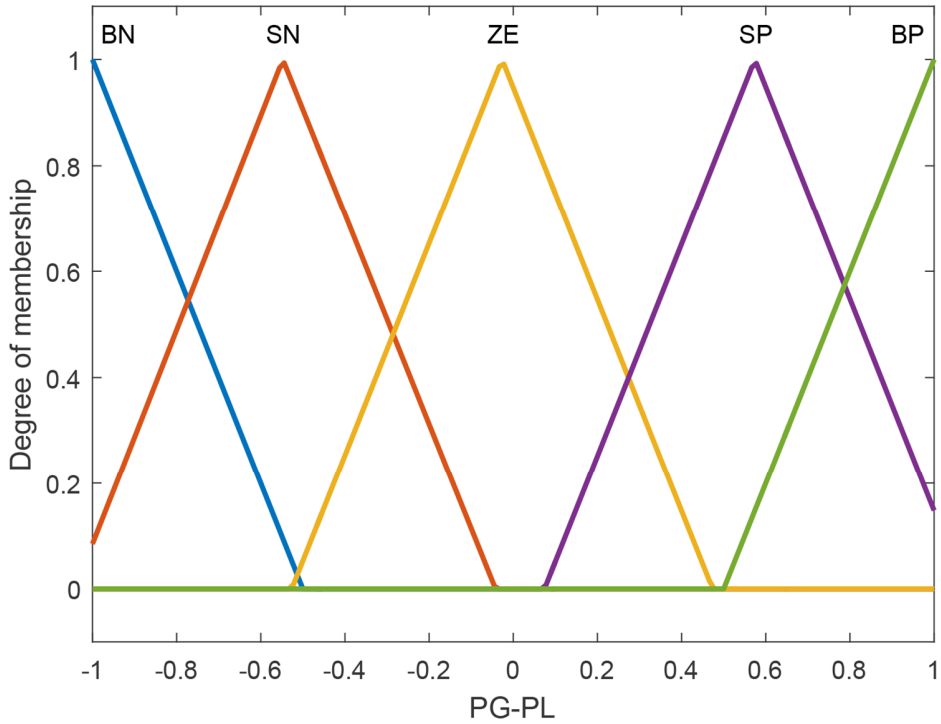

Figure 4.21: Optimized Membership Functions of Second Input of FLC

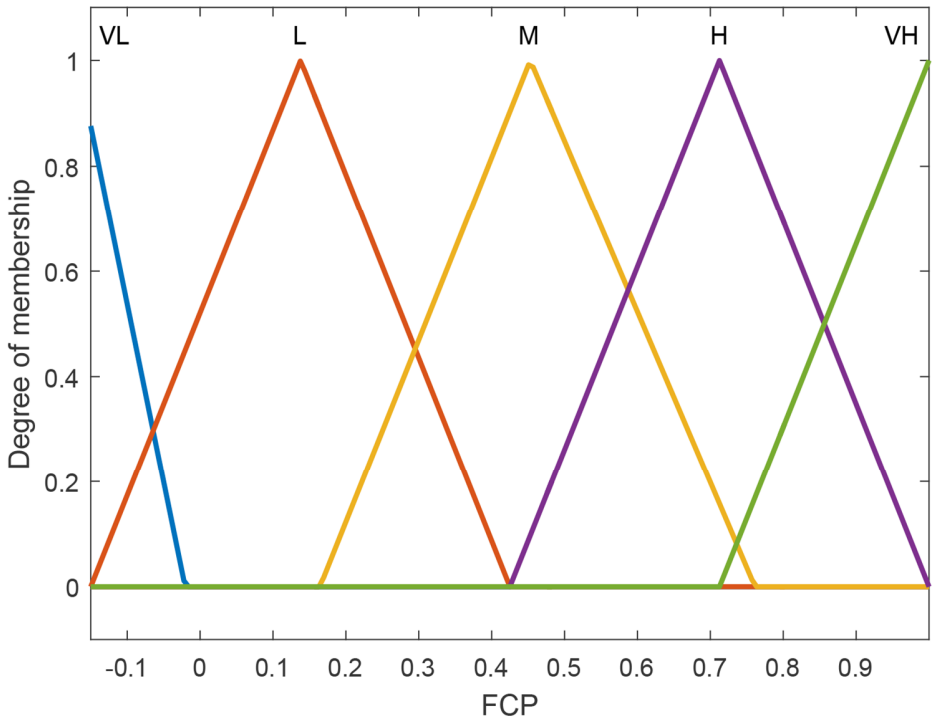

Figure 4.22: Optimized Membership Functions of The Output of FLC

4.3.2 Simulation Results of the Microgrid System with Optimized FLEMS

As mentioned previously, the simulation of the optimized FLEMS is carried out for two summer days that considered as the hottest days of the year according to the collected data to test the proper operation and efficiency of the proposed microgrid with / without optimization.

Microgrid Simulation Results of 27th of July

Figures (4.23 – 4.26) illustrate the real data applied to the microgrid in the first day of simulation. The SOC of the BESS is set initially to 100%.

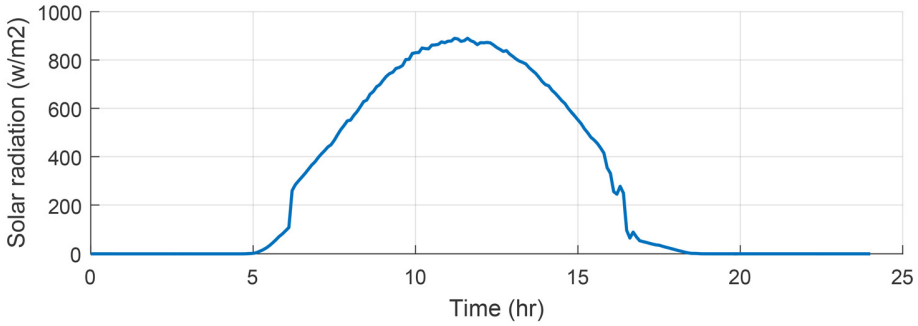

Figure 4.23: Solar Irradiation of 27th of July 2016 in Dhahran

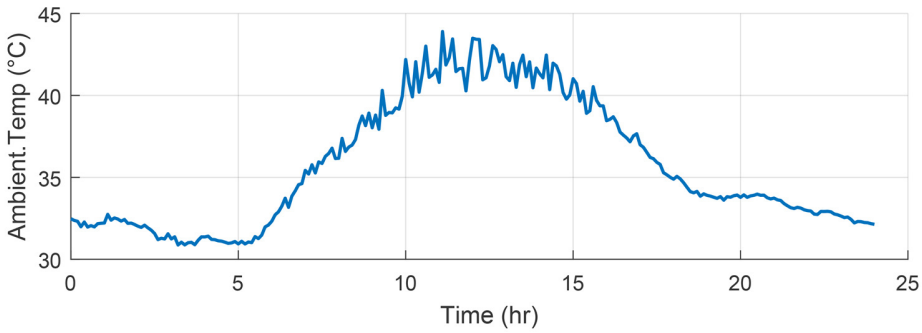

Figure 4.24: Ambient Temperature of 27th of July 2016 in Dhahran

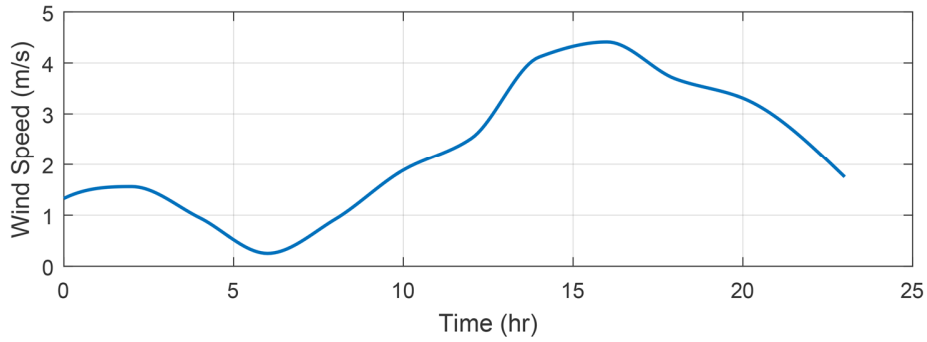

Figure 4.25: Wind Speed of 27th of July 2016 in Dhahran

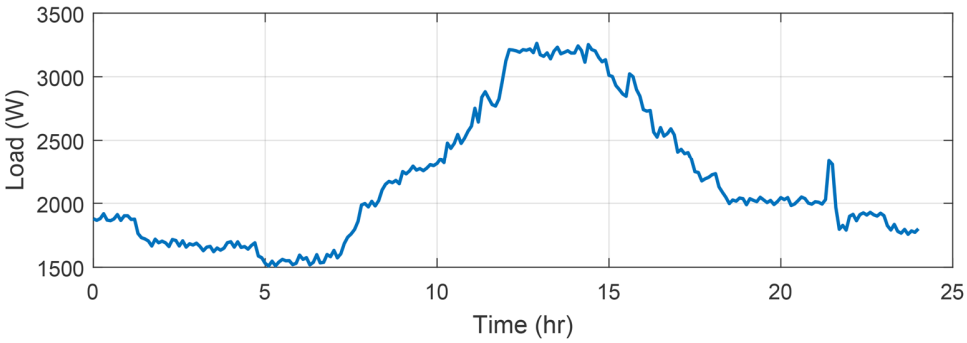

Figure 4.26: Residential Load of 27th of July 2016 in Dhahran

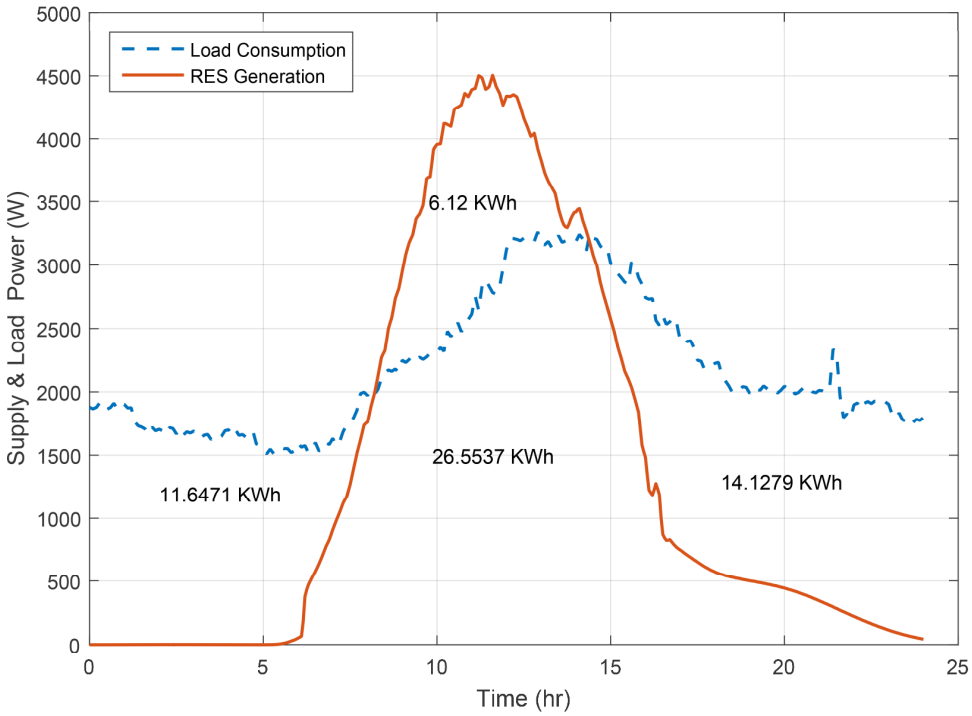

Figure 4.27: RE Generation VS Load Consumption with AUC Calculations on 27th of July 2016

Figure 4.27 illustrates the renewable energy generated from microgrid on 27th of July. Four areas of energy were calculated using AUC method. In first area during morning hours, residential load energy is (11.6571 kWh) and this amount of energy should be supplied by backup sources since the renewable generation cannot does. The upper energy area in the figure that has (6.12 kWh) during midday hours is the surplus energy from renewable sources after meeting all load demand and should be stored in the BESS. The middle area that has (26.5537 kWh) is the total load that met by renewable generation during day hours. The last area (14.1297kWh) is the residential load demand during evening and night hours that renewables cannot supply it with energy, hence, backup sources (BESS and fuel cell) should compensate it. Figures (4.28 – 4.30) exhibits the SOC, current and voltage of the BESS for 24 hours on 27th of July respectively.

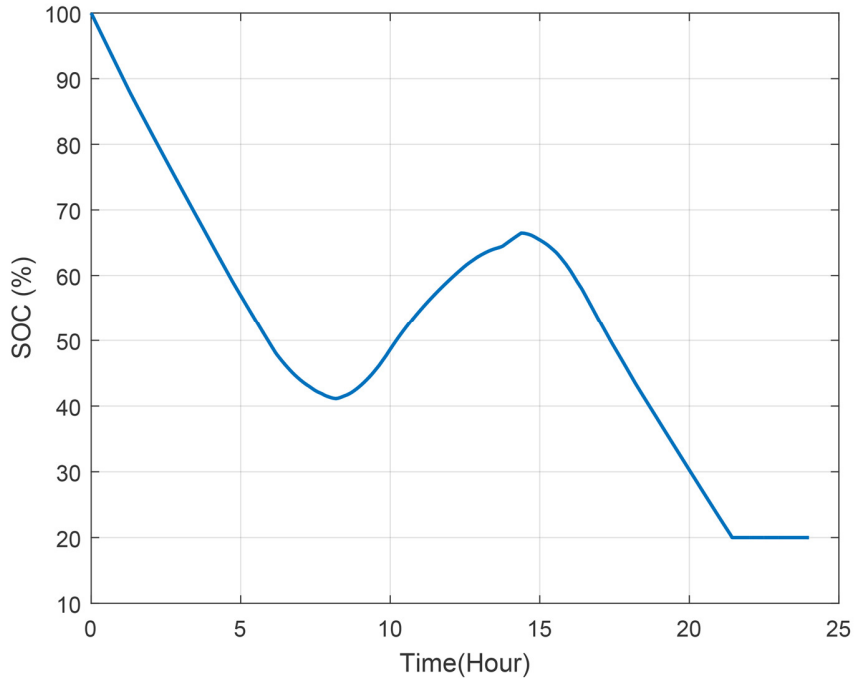

Figure 4.28: BESS SOC for 24 Hours on 27th of July 2016

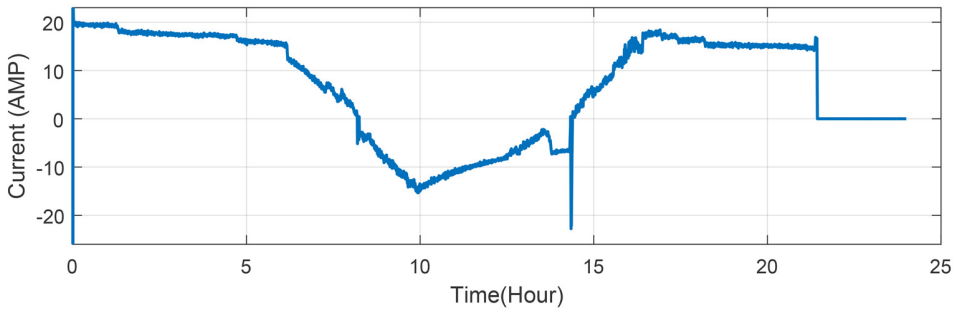

Figure 4.29: BESS Charging/Discharging Currents During 24 Hours on 27th of July 2016

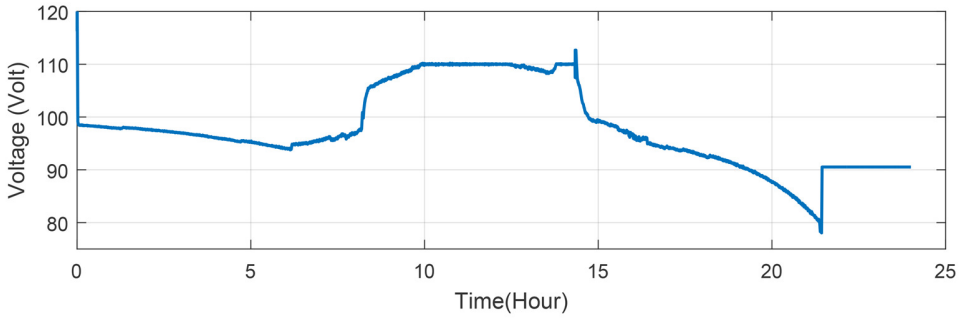

Figure 4.30: BESS Voltage During 24 Hours on 27th of July 2016

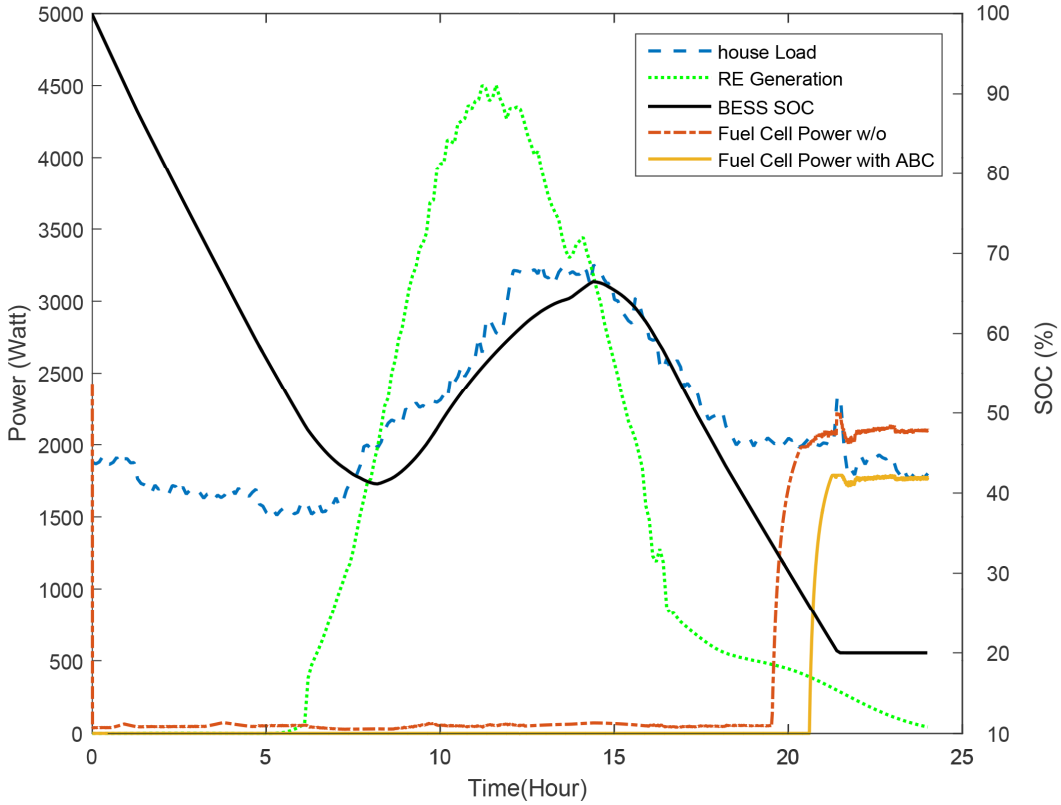

Figure 4.31: The Operation of the Fuel Cell for 24 Hours on 27th of July 2016 with / without ABC Optimization for FLEMS

Figure 4.31 exhibits the operation of the fuel cell with / without FLEMS optimization compared with the RES generation, load demand of the house and SOC of the BESS. More details of the operation are explained in the following analysis

Energy Dispatch Analysis for Microgrid on of 27th of July 2016

Table 4.9 exhibits the energy generated from each RES, load demand for the residential house, and the fuel cell generation that controlled by FLEMS with / without optimization.

Table 4.9: Generation and Consumption Energy Analysis of Microgrid on 27th of July 2016

Residential Load Consumption	52.3287 kWh
PV System Generation	27.5961 kWh
WT system Generation	5.0776 kWh
Total RE generation	32.6737 kWh
Fuel Cell (controlled by basic FLEMS)	9.8047 kWh
Fuel Cell (controlled by optimized FLEMS)	5.719 kWh

The energy dispatch for BESS in this day is divided into three periods as follows:

- First period (12:00 AM – 8:10 AM):

The BESS discharged from 100% to 41.14%; 58.86% was dispatched to house load. 58.86% (discharged amount) × 20 kWh (BESS Capacity) = 11.772 kWh which almost the same amount required to meet the first area demand as showed in Figure 4.27.

- Second period (8:10 AM – 2:20 PM):

The BESS charged from 41.14% to 66.5%; 25.36% was charged in BESS.

25.36% (charged amount) × 20kWh = 5.072 kWh.

- Third period (2:20 PM – 7.24 PM):

The BESS discharged from 66.5% to 20%; 46.5 % was dispatched to house load.

46.5% × 20 kWh = 9.3 kWh. The remaining period of the day (7:24PM – 11:59PM) compensated from fuel cell that controlled by FLEMS. Table 4.10 summarizes the energy dispatch of the BESS.

Table 4.10: BESS Operation Analysis on 27th of July 2016

Period	First Period (Discharging) 00:00AM-8:00AM	Second Period (Charging) 8:00AM – 2:20PM	Third Period (Discharging) 2:20PM – 7:24PM
Δ SOC	100% to 41.14%	41.14% to 66.5%	66.5% to 20%
Energy	11.772 kWh	5.072 kWh	9.3 kWh

The system efficiency is obtained to compare the difference between the microgrid FLEMS with / without optimization. Table 4.11 shows both efficiencies. For the purpose of comparison, efficiency of the system is calculated according to the given formula:

$$System\ \eta = \frac{(Load\ Consumption)}{BESS\ Energy\ Disch. + Total\ RE\ used\ by\ the\ load + Fuel\ Cell\ Energy} \quad (51)$$

Table 4.11: Comparison in System Efficiency with / without Optimization on 27th of July 2016

FLEMS	Efficiency
Without optimization	91.12%
With ABC optimization	98.09%

Microgrid Simulation Results of 28th of July 2016

Figures (4.32 – 4.35) illustrate the real data applied to the microgrid in the second day of simulation. The SOC of the BESS is the same from last day of simulation which is 20%.

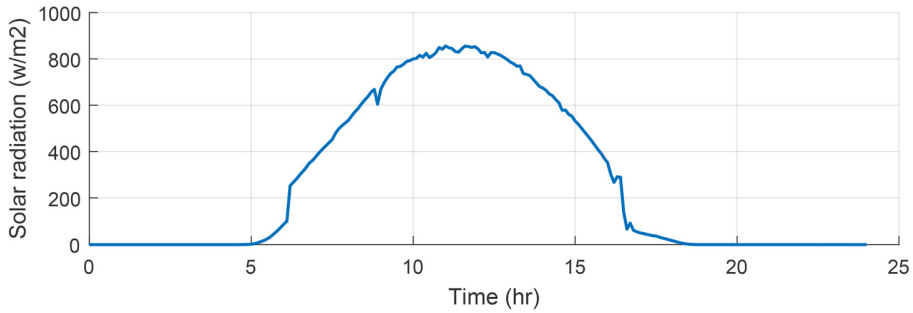

Figure 4.32: Solar Irradiation of 28th of July 2016 in Dhahran

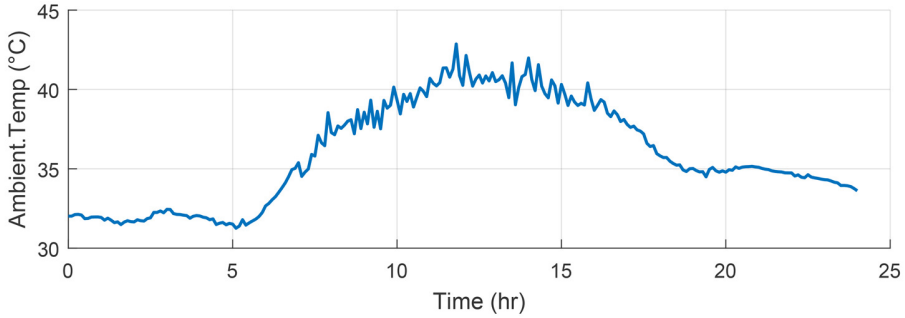

Figure 4.33: Ambient Temperature of 28th of July 2016 in Dhahran

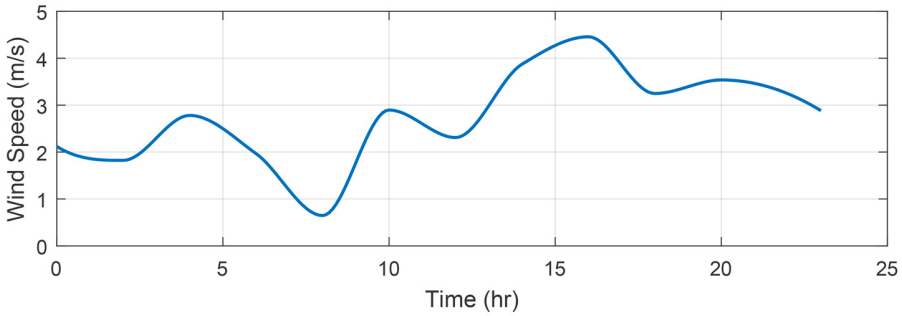

Figure 4.34: Wind Speed of 28th of July 2016 in Dhahran

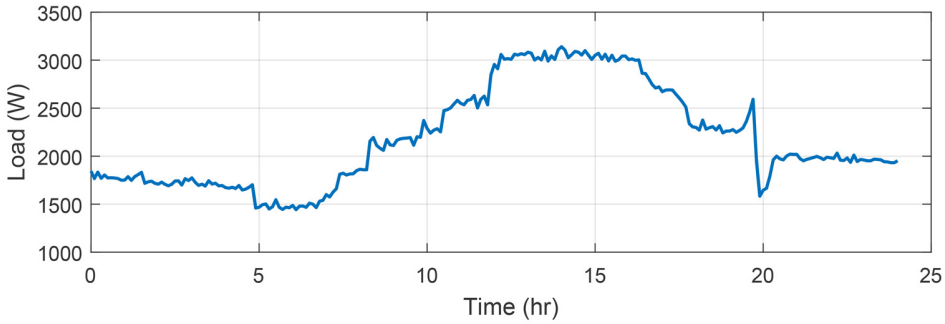

Figure 4.35: Residential Load of 28th of July 2016 in Dhahran

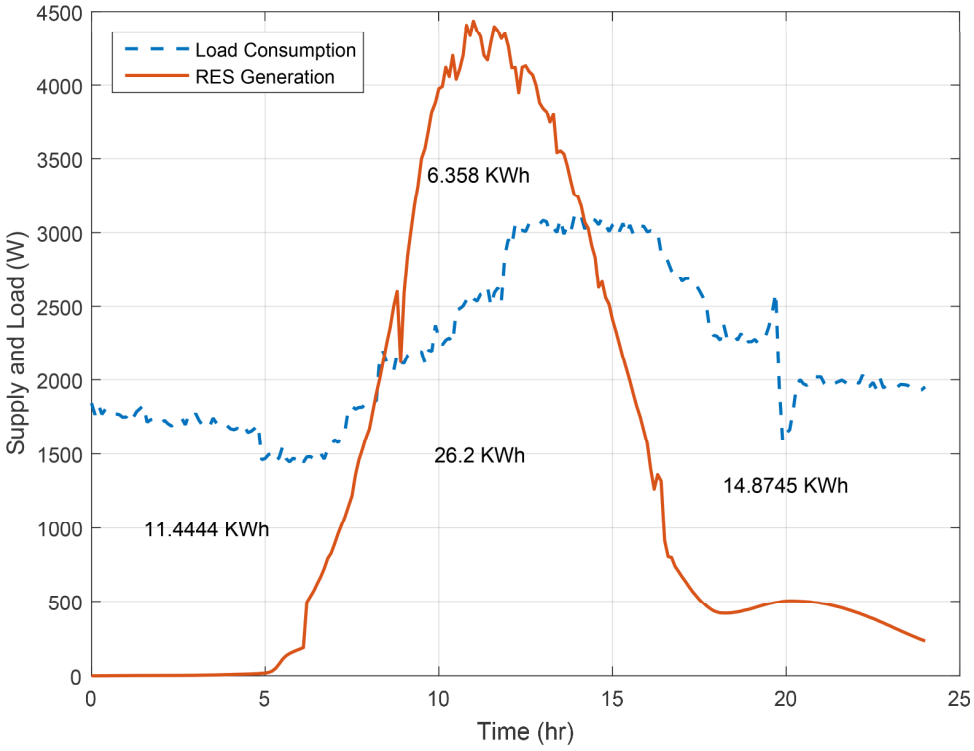

Figure 4.36: RE Generation VS Load Consumption with AUC Calculations on 28th of July 2016

Figure 4.36 illustrates the renewable energy generated from microgrid on 28th of July. Four areas of energy were calculated using AUC method. During morning hours in first area at the left of the figure, residential load energy is (11.4444 kWh) and this amount of energy should be supplied by backup sources since the renewable generation cannot does. The upper energy area of the figure that has (6.358 kWh) during midday hours is the surplus energy from renewable sources after meeting all load demand and should be stored in the BESS. The middle area that has (26.2 kWh) is the total load that met by renewable generation during day hours. The last area (14.8745 kWh) is the residential load demand during night hours that cannot be supplied from renewables generation. Therefore, backup

sources (BESS and fuel cell) should compensate it. Figures (4.37 – 4.39) exhibits the SOC, current and voltage of the BESS for 24 hours on 28th of July respectively.

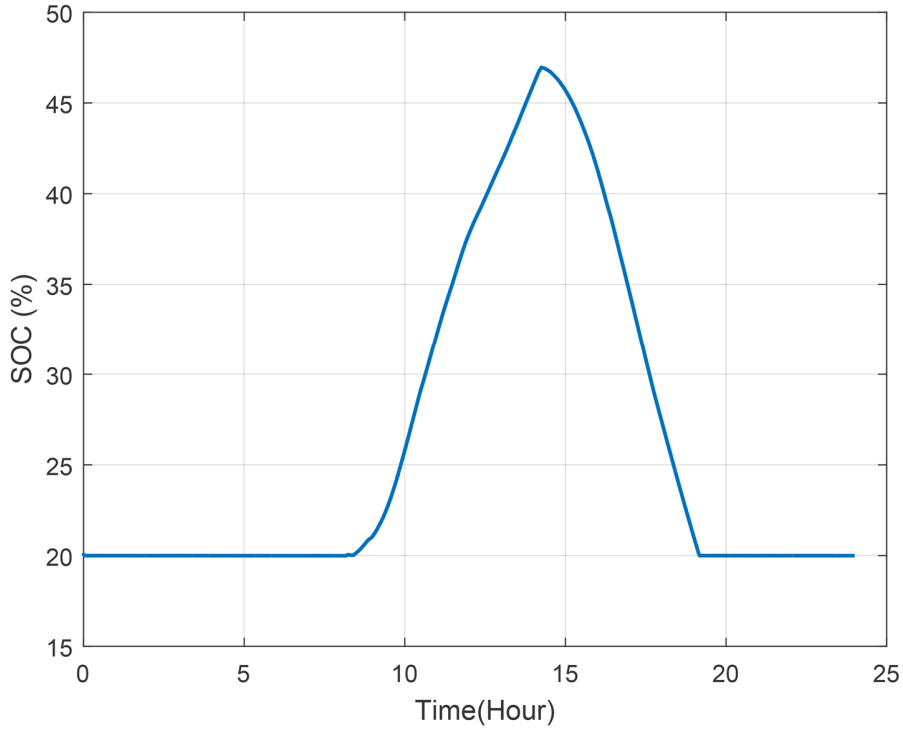

Figure 4.37: BESS SOC for 24 Hours on 28th of July 2016

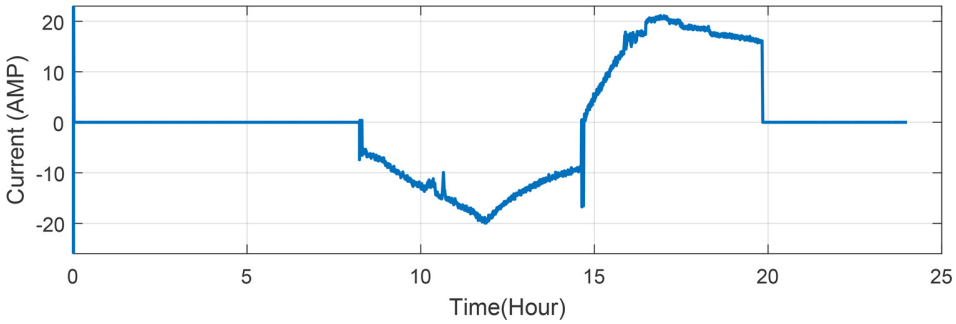

Figure 4.38: BESS Charging/Discharging Currents During 24 Hours on 28th of July 2016

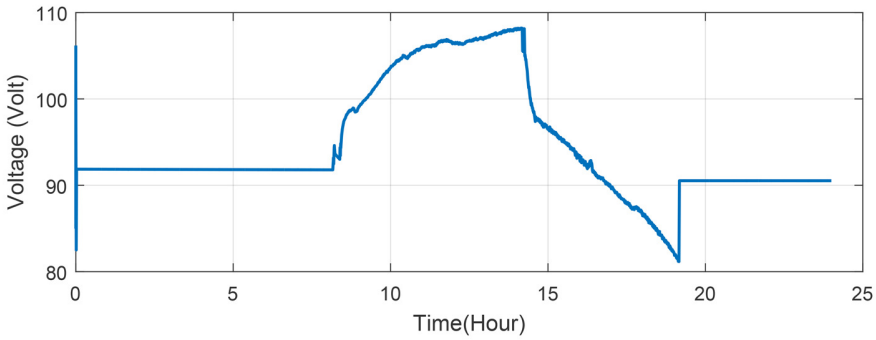

Figure 4.39: BESS Voltage During 24 hours on 28th of July 2016

Figure 4.40 shows the operation of the fuel cell with / without FLEMS optimization compared with the RES generation and load demand of the house. The following analysis gives more understanding about the microgrid operation.

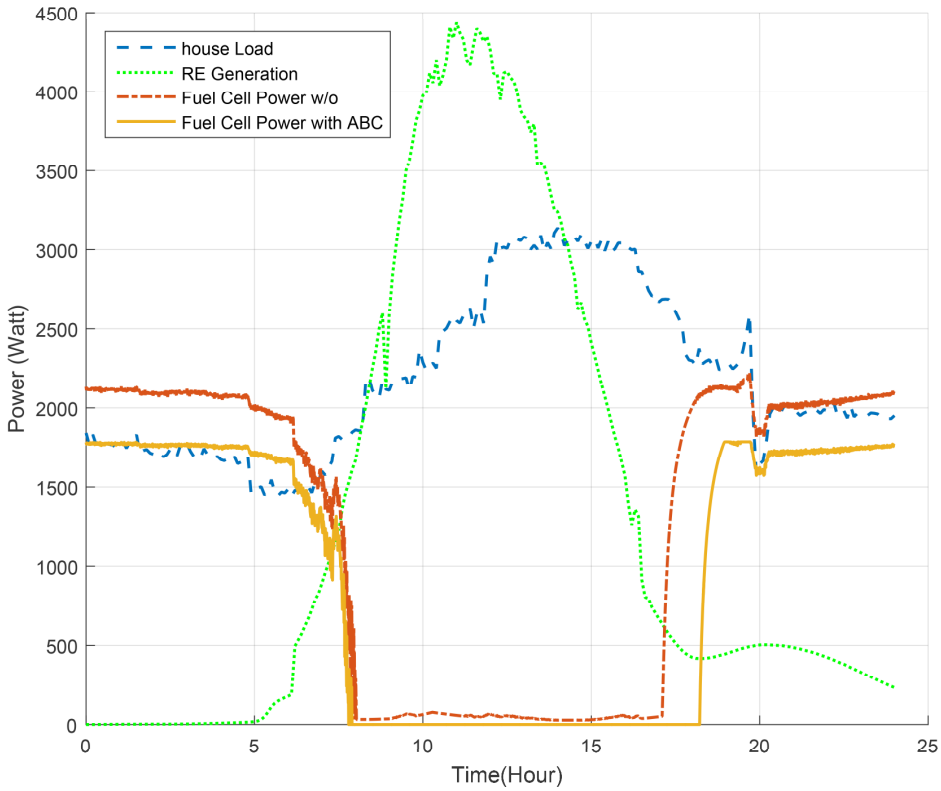

Figure 4.40: The Operation of the Fuel Cell for 24 Hours on 28th of July 2016 with / without ABC Optimization for FLEMS

Energy Dispatch Analysis for Microgrid on of 28th of July 2016

Table 4.12 exhibits the energy generated from each renewable source, energy load demand of the residential house and the fuel cell energy that controlled by FLEMS with / without optimization on the second day of simulation.

Table 4.12: Generation and Consumption Energy Analysis of Microgrid on 28th of July 2016

Residential Load Consumption	52.5189 kWh
PV System Generation	28.7939 kWh
WT system Generation	3.7641 kWh
Total RE generation	32.558 kWh
Fuel Cell (controlled by basic FLEMS)	29.3366 kWh
Fuel Cell (controlled by optimized FLEMS)	22.4899 kWh

The energy dispatch for BESS in this day is divided into three periods as follows:

- First period (12:00 AM – 8:10 AM):

The BESS has no energy to be discharged because all of its energy was discharged to the house load in previous night, hence the left period in the Figure 4.36 should be supplied from the other backup source; fuel cell.

- Second period (8:10 AM – 2:15 PM):

The BESS started to charge from 20% to 47%; 27% was charged in BESS.

27% (charged amount) × 20kWh = 5.4 kWh.

- Third period (2:15 PM – 5:00 PM):

The BESS discharged from 47% to 20%, hence 27 % of BESS energy was dispatched to house load.

The remaining period of the day (5:00PM – 11:59PM) compensated from fuel cell that controlled by FLEMS. Table 4.13 summarizes the energy dispatch of the BESS.

Table 4.13: BESS Energy Operation Analysis on 28th of July 2016

Period	**First Period (Discharging) 00:00AM-8:10AM**	**Second Period (Charging) 8:10AM – 2:15PM**	**Third Period (Discharging) 2:15PM – 5:00PM**
Δ SOC	20%	20% to 47%	47% to 20%
Energy	0	5.4 kWh	5.4 kWh

The system efficiency is calculated according to the formula in (51) to compare the difference between the microgrid FLEMS with / without optimization. Table 4.14 shows both efficiencies.

Table 4.14: Comparison in System Efficiency with and without Optimization on 28th of July 2016

FLEMS	**Efficiency**
Without optimization	86.18%
With ABC optimization	97.07%

4.4 Results of Optimized Microgrid FLEMS Considering Economic Dispatch

This is the final stage of simulation and the results of the proposed method to enhance the performance of the optimized FLEMS depending on economic dispatch is presented in this section. Since diesel generator in this part replaces the wind turbine system, the economic dispatch problem is solved depending on real data for 24 hours of a summer day in Dhahran using three different intelligent techniques which are: artificial bee colony, particle swarm optimization and genetic algorithm. Then, the microgrid simulated using the best technique that minimizes the operation cost of the backup sources in the proposed microgrid. Cost and efficiencies are calculated to prove the effectiveness of the proposed method.

4.4.1 Simulation Results of Economic Dispatch Using Three Intelligent Techniques

Real data of 28th of July 2016 was used in simulation for solving the economic dispatch problem using the three-optimization technique. Tables (4.15 – 4.17) exhibit the economic dispatch results of artificial bee colony, particle swarm optimization and genetic algorithm respectively with total cost of generation for each technique.

Table 4.15: Economic Dispatch Solution Using ABC Technique

Time (h)	FC (W)	DG (W)	RE Gen. (W)	House Load (W)	BESS Supply (W)
1	1545.403	298.2779	0	1843.681	0
2	1467.416	283.1387	0	1750.555	0
3	1431.891	277.172	0	1709.063	0
4	1485.572	286.6482	0	1772.22	0
5	1403.547	270.7464	0	1674.293	0
6	1229.208	236.9774	0	1466.185	0
7	1211.029	233.2711	43.63771	1487.862	0
8	636.6834	122.2966	838.1992	1597.172	0
9	167.7575	31.5025	1662.303	1861.561	0
10	0	0	2572.191	2115.248	0
11	0	0	3688.539	2286.499	0
12	0	0	4171.665	2553.053	0
13	0	0	4071.112	2959.199	0
14	0	0	3540.936	3095.96	0
15	0	0	2660.951	3139.717	478.766
16	826.4287	159.0213	1650.371	3035.966	402.9997
17	908.5584	174.9316	720.9348	3002.192	1197.774
18	1152.026	222.0738	14.19419	2668.332	1280.088
19	2187.312	422.4882	0	2609.77	0
20	1911.005	368.995	0	2279.933	0
21	1388.388	267.8123	0	1656.186	0
22	1685.124	325.2758	0	2010.446	0
23	1667.578	321.8222	0	1989.327	0
24	1639.153	316.3475	0	1955.419	0
Total Cost of Conventional Backup Generation				**704.5295792**	

Table 4.16: Economic Dispatch Solution Using PSO Technique

Time (h)	FC (W)	DG (W)	RE Gen. (W)	House Load (W)	BESS Supply (W)
1	1545.38815	298.211847	0	1843.681	0
2	1467.38882	283.111176	0	1750.555	0
3	1432.70384	276.396163	0	1709.063	0
4	1485.58588	286.634125	0	1772.22	0
5	1403.46456	270.735439	0	1674.293	0
6	1229.20183	236.998174	0	1466.185	0
7	1210.77019	233.429809	43.63771	1487.862	0
8	636.683395	122.286605	838.1992	1597.172	0
9	167.757456	31.5025436	1662.303	1861.561	0
10	0	0	2572.191	2115.248	0
11	0	0	3688.539	2286.499	0
12	0	0	4171.665	2553.053	0
13	0	0	4071.112	2959.199	0
14	0	0	3540.936	3095.96	0
15	0	0	2660.951	3139.717	478.766
16	826.428703	159.021297	1650.371	3035.966	402.9997
17	908.558395	174.921605	720.9348	3002.192	1197.774
18	1152.0403	222.059702	14.19419	2668.332	1280.088
19	2187.3	422.5	0	2609.77	0
20	1910.921	368.979005	0	2279.933	0
21	1388.30035	267.799648	0	1656.186	0
22	1685.13346	325.266538	0	2010.446	0
23	1667.37207	321.827932	0	1989.327	0
24	1638.97897	316.331029	0	1955.419	0
Total Cost of Conventional Backup Generation				**704.5253399**	

Table 4.17: Economic Dispatch Solution Using GA Technique

Time (h)	FC (W)	DG (W)	RE Gen. (W)	House Load (W)	BESS Supply (W)
1	1566.2	277.5	0	1843.681	0
2	1555.6	195	0	1750.555	0
3	1563.1	146	0	1709.063	0
4	1487.76	285.3	0	1772.22	0
5	1402.3	272	0	1674.293	0
6	1201.6	264.6	0	1466.185	0
7	1214	230.3	43.63771	1487.862	0
8	673	85.9935	838.1992	1597.172	0
9	108.3	91.0033	1662.303	1861.561	0
10	0	0	2572.191	2115.248	0
11	0	0	3688.539	2286.499	0
12	0	0	4171.665	2553.053	0
13	0	0	4071.112	2959.199	0
14	0	0	3540.936	3095.96	0
15	0	0	2660.951	3139.717	478.766
16	804.1974	181.2525	1650.371	3035.966	402.9997
17	943.3537	140.1363	720.9348	3002.192	1197.774
18	1182.3	191.8	14.19419	2668.332	1280.088
19	2171.8	438	0	2609.77	0
20	2011.7	268.3	0	2279.933	0
21	1409.3	246.9	0	1656.186	0
22	1363.7	646.8	0	2010.446	0
23	1684.4	305	0	1989.327	0
24	1626	329.6	0	1955.419	0
Total Cost of Conventional Backup Generation				**704.8097585**	

When comparing the total cost for 24 hours using different optimization techniques, it is obvious that ABC and PSO techniques reduces the cost more than GA. However, PSO optimization technique is the best among the tree techniques with little difference when compared with ABC. Hence, PSO is used in the economic dispatch scheduling within FLEMS of the microgrid. Figure 4.41 illustrates the best cost value during optimization process using PSO.

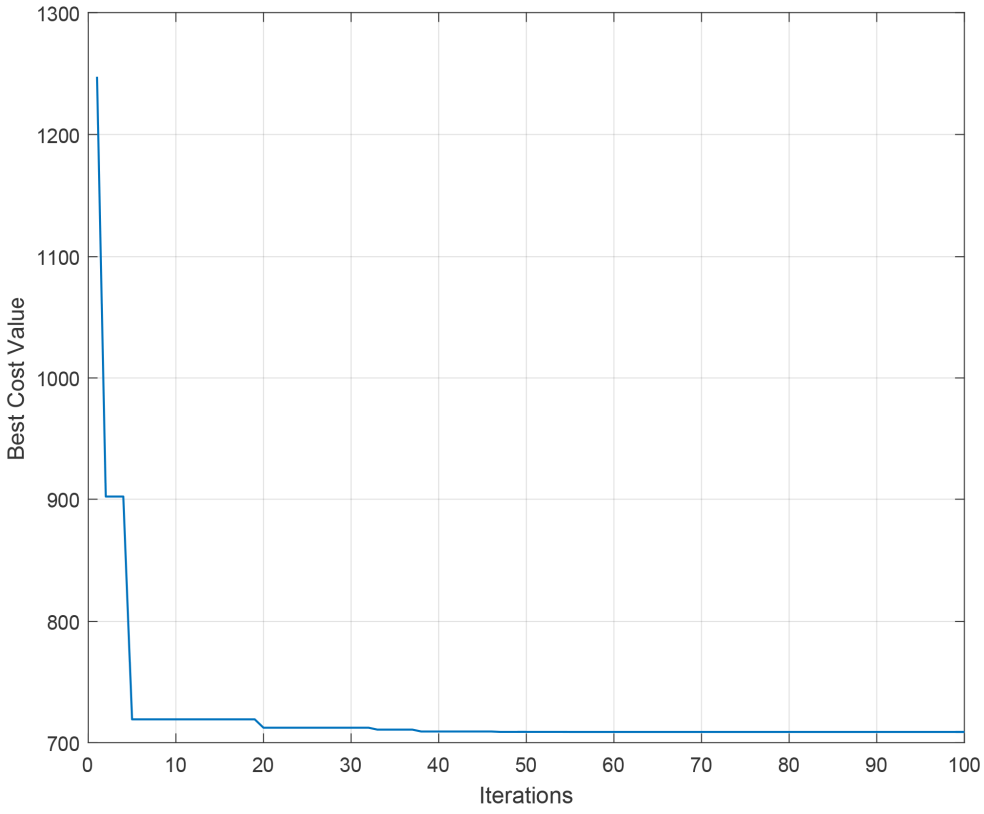

Figure 4.41: Convergence of Best Value of the Cost Function Using PSO

4.4.2 Simulation Results of the Microgrid with Optimized FLEMS Considering Economic Dispatch in 28th of July

To test the effectiveness of the proposed method for using economic dispatch scheduling within the optimized FLEMS of the microgrid, solar irradiation, ambient temperature and house load profile of 28th of July 2016 as illustrated in Figures 4.32 and 4.33 are applied to the microgrid model in this stage. The operation of the fuel cell and the diesel generator during this day controlled by the proposed method is shown in Figure 4.42.

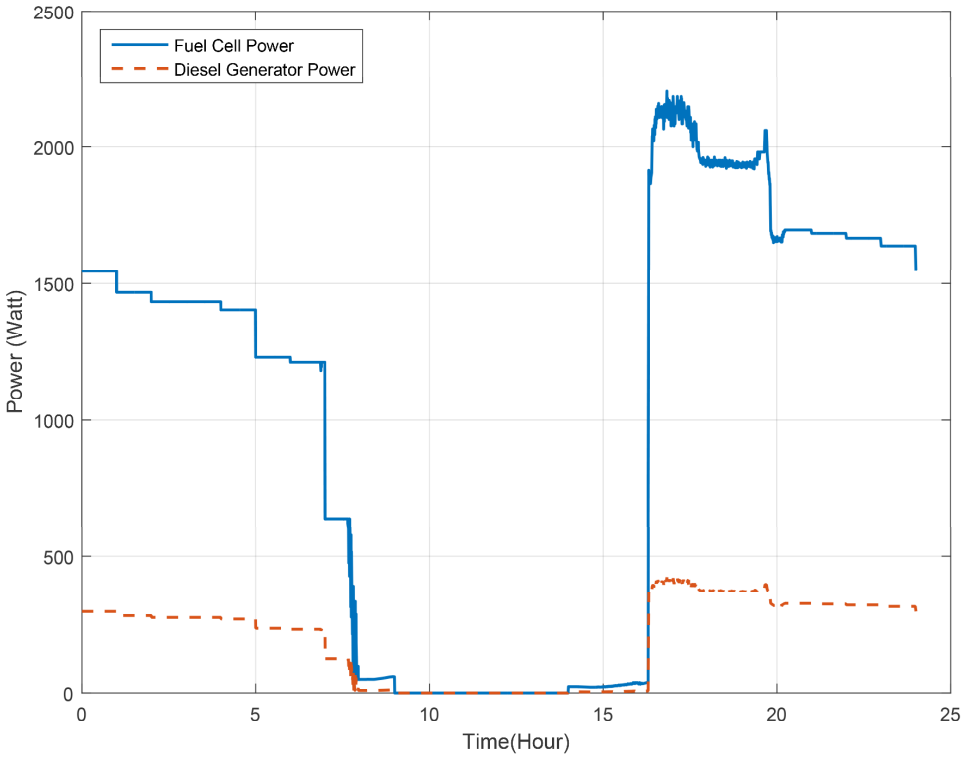

Figure 4.42: Operation of Fuel Cell and Diesel Generator in the Microgrid on 28th of July Controlled by Optimized FLEMS Considering Economic Dispatch Using PSO

To investigate the effectiveness of the proposed method using economic dispatch within the microgrid FLEMS, three different scenarios are simulated:

- Microgrid that has PV and WT as RES operating with FC and BESS as a backup system controlled by FLEMS without optimization.
- Microgrid that has PV and WT as RES operating with FC and BESS as a backup system controlled by optimized FLEMS using ABC.
- Microgrid that has only PV as RES operating with FC, DG and BESS as a backup system controlled by optimized FLEMS and considering Economic Dispatch.

Figure 4.43 illustrates a comprehensive view of the microgrid operation for 24 hours with three different scenarios.

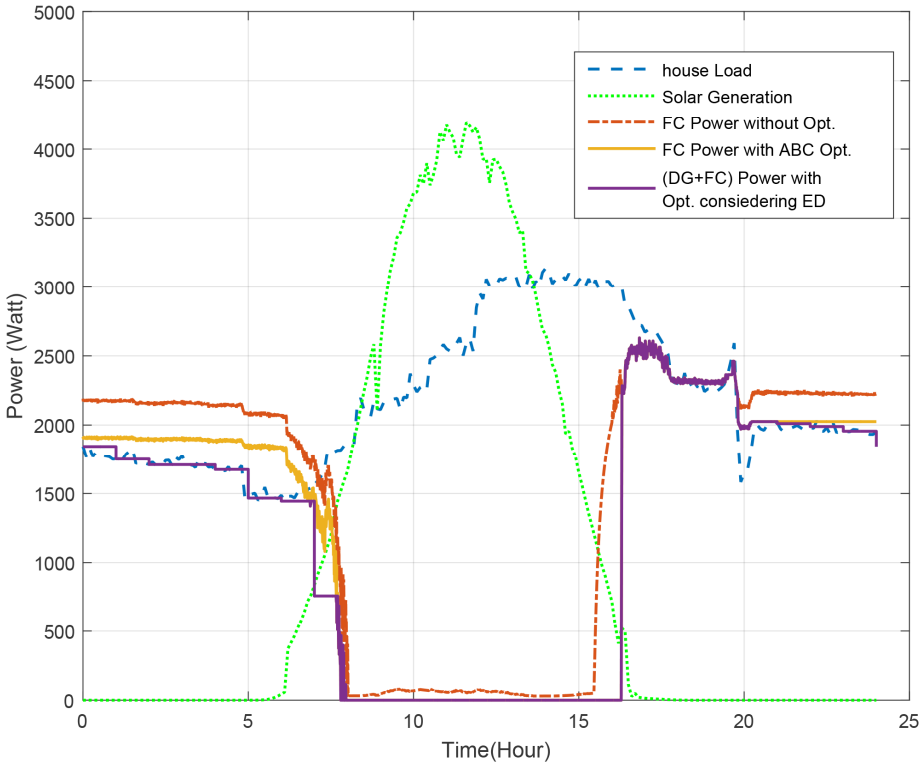

Figure 4.43: Operation of the Microgrid Backup System in Three Different Scenarios

Efficiency and Cost:

Table 4.18 exhibits the efficiency of the system in the three scenarios. The results show that the proposed method has the most efficient operation during 24 hours of the day.

Table 4.18: System Efficiency in Three Different Methods

Method	Efficiency
MG controlled by FLC without optimization	86.97 %
MG controlled by FLC with ABC optimization	94.5 %
MG controlled by FLC with ABC optimization depending on ED	97.67 %

Cost calculation is done to compare the proposed method in this work with conventional economic dispatch scheduling. The exhibited results in Table 4.19 show that the proposed method reduces the cost by 11.19%

Table 4.19: Cost Comparison between Optimized FLC using ED and Conventional ED operation

Method	Cost / day
operation using ED only	704.53
operation by opt. FLC considering ED	625.65

CHAPTER 5

CONCLUSION and RECOMMENDATION

5.1 Conclusions

In conclusion, optimizing FLC using intelligent techniques such as ABC can enhance the efficiency of FLEMS of a microgrid and give high level of reliable and precise control. However, optimizing FLEMS considering economic dispatch can give a higher level of efficiency and minimize the cost of generation as well. In this work, a standalone DC microgrid consists of photovoltaic solar system, wind turbine system, battery energy storage system, fuel cell and diesel generator supplying residential load demand controlled by FLEMS of low complexity that consists of only 25 base rules. The FLEMS is optimized using one of the recent and effective optimization techniques which is artificial bee colony and it gives better results in terms of control efficiency. Further optimization for the FLEMS of the microgrid depending on economic dispatch is proposed in this work and the results show enhancement in control efficiency and reduction in generation cost when compared with conventional economic dispatch methods. All simulations done in this work based on real data of solar irradiation, ambient temperature, wind speed collected in 2016 in Dhahran city that lies in the eastern region in Saudi Arabia. The residential load profile data is also recorded in 2016 inside KFUPM campus, house NO. 3307 based HVAC VFD system. particularly, two analysis and investigation studies are conducted in this work. The first one for studying the effect of ambient temperature on the solar photovoltaic system

and best-operating temperature is obtained for five months in Dhahran. The other one for investigating the potential of installing small-scale hybrid renewable energy system for residential usage in Dhahran. Analysis of the second study that depends on simulation results conducted in different seasonal days show that it is possible to install renewables at the study location with the help of backup systems such as battery storage system and fuel cell.

5.2 Recommendation

Further extension and improvement of this work can be summarized as follows:

- Optimizing the FLEMS by tuning other parameters of the FLC such as the fuzzy rules using the same intelligent technique in this work; artificial bee colony.
- Using other optimization techniques for solving the economic dispatch problem to minimize the generation cost of the proposed microgrid FLEMS.
- Changing the microgrid mode to grid-connected and include other components of the microgrid into the economic dispatch problem such as the battery energy storage system and solar photovoltaic system.

References

[1] M. V. Kok, “Renewable energy sources: current perspectıves and future prospects in Turkey,” *Energy Sources, Part A Recover. Util. Environ. Eff.*, vol. 37, no. 1, pp. 1–10, 2015.

[2] Iea, “Transport energy efficiency,” 2010.

[3] A. Hirsch, Y. Parag, and J. Guerrero, “Microgrids: A review of technologies, key drivers, and outstanding issues,” *Renew. Sustain. Energy Rev.*, vol. 90, no. September 2017, pp. 402–411, 2018.

[4] M. Rouse, “Microgrid,” *whatis*, 2013. [Online]. Available: https://whatis.techtarget.com/definition/microgrid.

[5] Z. Cheng, J. I. E. Duan, and M. Chow, “To centralize or to distribute: That is the question,” no. MARCH, pp. 6–24, 2018.

[6] M. Krarti, K. Dubey, and N. Howarth, “Evaluation of building energy efficiency investment options for the Kingdom of Saudi Arabia,” *Energy*, vol. 134, pp. 595–610, 2017.

[7] Z. Abdmouleh, R. A. M. Alammari, and A. Gastli, “Recommendations on renewable energy policies for the GCC countries,” *Renew. Sustain. Energy Rev.*, vol. 50, pp. 1181–1191, 2015.

[8] M. Groissböck and M. J. Pickl, “An analysis of the power market in Saudi Arabia: Retrospective cost and environmental optimization,” *Appl. Energy*, vol. 165, pp. 548–558, 2016.

[9] I. Mezghani and H. Ben Haddad, “Energy consumption and economic growth: An empirical study of the electricity consumption in Saudi Arabia,” *Renew. Sustain. Energy Rev.*, vol. 75, no. June 2015, pp. 145–156, 2017.

[10] J. Eto, V. Budhraja, C. Martinez, J. Dyer, and M. Kondragunta, “Research, development, and demonstration needs for large-scale, reliability-enhancing, integration of distributed energy resources,” in *Hawaii International Conference on system Sciences*, 2000, pp. 1–7.

[11] C. Marnay, R. Blanco, K. S. Hamachi, C. P. Kawann, J. G. Osborn, and F. J. Rubio, “Integrated assessment of dispersed energy resources deployment,” *Consort. Electr. Reliab. Technol. Solut.*, no. June 2000, pp. 5–54, 2000.

[12] P. Piagi and R. H. Lasseter, “Distributed energy resources integration,” *Power Syst. Eng. Res. Center, Univ. Wisconsin-Madison*, 2001.

[13] J. D. Kueck, R. H. Staunton, S. D. Labinov, and B. J. Kirby, “microgrid energy management system,” *CERTS Progr. Off. Lawrence Berkeley Natl. Lab.*, 2003.

[14] M. S. Jiménez and N. Hatziargyriou, “Research activities in Europe on integration of distributed energy resources in the electricity networks of the future,” in *2006 IEEE Power Engineering Society General Meeting*, 2006, pp. 1–4.

[15] M. R. Vallem, J. Mitra, and S. B. Patra, “Distributed generation placement for optimal microgrid architecture,” in *Proceedings of the IEEE Power Engineering Society Transmission and Distribution Conference*, 2006, pp. 1191–1195.

[16] T. Ma, P. Li, Y. Wang, and Y. Tan, “Architecture-oriented assurance technology in microgrid,” in *Proceedings - Symposia and Workshops on Ubiquitous, Autonomic and Trusted Computing in Conjunction with the UIC 2010 and ATC 2010 Conferences, UIC-ATC 2010*, 2010, pp. 346–351.

[17] J. Jimeno, J. Anduaga, J. Oyarzabal, and A. G. de Muro, “Architecture of a microgrid energy management system,” *Eur. Trans. Electr. POWER*, vol. 21, no. 2, pp. 1142–1158, 2011.

[18] W. Su and J. Wang, “Energy management systems in microgrid operations,” *Electr. J.*, vol. 25, no. 8, pp. 45–60, 2012.

[19] E. Barklund, N. Pogaku, M. Prodanovi, C. Hernandez-Aramburo, nd T. C. Green, “Energy management system with stability constraints for stand-alone autonomous microgrid,” in *2007 IEEE International Conference on System of Systems Engineering, SOSE*, 2007.

[20] Q. Jiang, M. Xue, and G. Geng, “Energy management of microgrid in grid-connected and stand-alone modes,” *IEEE Trans. Power Syst.*, vol. 28, no. 3, pp. 3380–3389, 2013.

[21] L. Zhang, N. Gari, and L. V. Hmurcik, “Energy management in a microgrid with distributed energy resources,” *Energy Convers. Manag.*, vol. 78, pp. 297–305, 2014.

[22] H. Kanchev, D. Lu, F. Colas, V. Lazarov, and B. Francois, “Energy management and operational planning of a microgrid with a PV based active generator for smart grid applications,” *IEEE Trans. Ind. Electron.*, vol. 58, no. 10, pp. 4583–4592, 2011.

[23] Y. H. Chen, S. Y. Lu, Y. R. Chang, T. T. Lee, and M. C. Hu, “Economic analysis and optimal energy management models for microgrid systems: A case study in Taiwan,” *Appl. Energy*, vol. 103, pp. 145–154, 2013.

[24] K. Rangarajan and J. Guggenberger, “Cost analysis of renewable energy-based microgrids for rural energy management,” in *IIE Annual Conference. …*, 2011, p. 9.

[25] Q. Shafiee, J. M. Guerrero, and J. C. Vasquez, “Distributed secondary control for islanded microgrids-a novel approach,” *IEEE Trans. Power Electron.*, vol. 29, no. 2, pp. 1018–1031, 2014.

[26] W. Shi, X. Xie, C. C. Chu, and R. Gadh, “Distributed optimal energy management in microgrids,” *IEEE Trans. Smart Grid*, vol. 6, no. 3, pp. 1137–1146, 2015.

[27] C. Chen, J. Wang, F. Qiu, and D. Zhao, “Resilient distribution system by microgrids formation after natural disasters,” *IEEE Trans. Smart Grid*, vol. 7, no. 2, pp. 958–966, 2016.

[28] A. Merabet, K. T. Ahmed, H. Ibrahim, R. Beguenane, and A. M. Y. M. Ghias, "Laboratory scale microgrid based wind-PV-battery," *IEEE Trans. Sustain. Energy*, vol. 8, no. 1, pp. 145–154, 2017.

[29] M. Hosenuzzaman, N. A. Rahim, J. Selvaraj, M. Hasanuzzaman, A. B. M. A. Malek, and A. Nahar, "Global prospects, progress, policies, and environmental impact of solar photovoltaic power generation," *Renew. Sustain. Energy Rev.*, vol. 41, pp. 284–297, 2015.

[30] N. L. Panwar, S. C. Kaushik, and S. Kothari, "Role of renewable energy sources in environmental protection: A review," *Renew. Sustain. Energy Rev.*, vol. 15, no. 3, pp. 1513–1524, 2011.

[31] M. D. Archer and A. G. Martin, *Clean Electricity from Photovoltaics*, 4th ed. Imperial College Press, 2015.

[32] M. Villalva, J. Gazoli, and E. Filho, "Comprehensive approach to modeling and simulation of photovoltaic arrays," *IEEE Trans. Power Electron.*, vol. 24, no. 5, pp. 1198–1208, 2009.

[33] D. Revati and E. Natarajan, "Enhancing the efficiency of solar cell by air cooling," *Indian J. Sci. Technol.*, vol. 9, no. 5, pp. 1–6, 2016.

[34] A. J. Veldhuis, A. Nobre, T. Reindl, R. Ruther, and A. H. M. E. Reinders, "The influence of wind on the temperature of PV modules in tropical environments, evaluated on an hourly basis," in *Conference Record of the IEEE Photovoltaic Specialists Conference*, 2013, vol. 31, no. 0, pp. 824–829.

[35] B. Wang, Z. Wang, Y. Sun, F. Wang, Z. Zhen, M. Zengqiang, and H. Ren, "Research on influence between photovoltaic power and module temperature and ambient temperature," in *2016 IEEE International Conference on Power System Technology (POWERCON)*, 2016, pp. 1–5.

[36] S. Zahurul, N. Mariun, M. L. Othman, H. Hizam, I. Zainal, and A. Arash, “Ambient temperature effect on amorphous silicon (A-Si) photovoltaic module using sensing technology,” in *2015 Ninth International Conference on Sensing Technology Ambient*, 2015, no. April 2014, pp. 235–241.

[37] N. H. Zaini, M. Z. Ab Kadir, M. Izadi, N. I. Ahmad, M. A. M. Radzi, and N. Azis, “The effect of temperature on a mono-crystalline solar PV panel,” in *2015 IEEE Conference on Energy Conversion, CENCON 2015*, 2016, pp. 249–253.

[38] A. Pradhan and S. M. Ali, “Analysis of solar PV performance with change in temperature,” *Int. J. Appl. Eng. Res.*, vol. 11, no. 7, pp. 5225–5227, 2016.

[39] C. U. Ike, “The effect of temperature on the performance of a photovoltaic solar system in eastern Nigeria,” *Int. J. Eng. Sci.*, vol. 3, no. 12p, pp. 10–14, 2013.

[40] R. R. Yager and L. A. Zadeh, An introduction to fuzzy logic applications in intelligent systems, 165th ed. Springer, 2012.

[41] Y.-K. Chen, Y.-C. Wu, C.-C. Song, and Y.-S. Chen, “Design and implementation of energy management system with fuzzy control for DC microgrid systems,” *IEEE Trans. Power Electron.*, vol. 28, no. 4, pp. 1563–1570, 2013.

[42] G. Kyriakarakos, A. I. Dounis, K. G. Arvanitis, and G. Papadakis, “A fuzzy logic energy management system for polygeneration microgrids,” *Renew. Energy*, vol. 41, pp. 315–327, 2012.

[43] M. H. Moradi, M. Hajinazari, S. Jamasb, and M. Paripour, “An energy management system (EMS) strategy for combined heat and power (CHP) systems based on a hybrid optimization method employing fuzzy programming,” *Energy*, vol. 49, no. 1, pp. 86–101, 2013.

[44] O. Erdinc, O. Elma, M. Uzunoglu, U. S. Selamogullari, B. Vural, E. Ugur, A. R. Boynuegri, and S. Dusmez, “Experimental performance assessment of an online energy management strategy for varying renewable power production suppression,” *Int. J. Hydrogen Energy*, vol. 37, no. 6, pp. 4737–4748, 2012.

[45] H. Zhang, A. Davigny, F. Colas, Y. Poste, and B. Robyns, “Fuzzy logic based energy management strategy for commercial buildings integrating photovoltaic and storage systems,” *Energy Build.*, vol. 54, pp. 196–206, 2012.

[46] P. García, J. P. Torreglosa, L. M. Fernández, and F. Jurado, “Optimal energy management system for stand-alone wind turbine/photovoltaic/ hydrogen/battery hybrid system with supervisory control based on fuzzy logic,” *Int. J. Hydrogen Energy*, vol. 38, no. 33, pp. 14146–14158, 2013.

[47] S. Berrazouane and K. Mohammedi, “Parameter optimization via cuckoo optimization algorithm of fuzzy controller for energy management of a hybrid power system,” *Energy Convers. Manag.*, vol. 78, pp. 652–660, 2014.

[48] F. R. Salmasi and M. Hosseinzadeh, “Power management of an isolated hybrid AC/DC micro-grid with fuzzy control of battery banks,” *IET Renew. Power Gener.*, vol. 9, no. 5, pp. 484–493, 2015.

[49] I. Abadlia, T. Bahi, and H. Bouzeria, “Energy management strategy based on fuzzy logic for compound RES/ESS used in stand-alone application,” *Int. J. Hydrogen Energy*, vol. 41, no. 38, pp. 16705–16717, 2016.

[50] D. Arcos-Aviles, J. Pascual, L. Marroyo, P. Sanchis, and F. Guinjoan, “Fuzzy logic-based energy management system design for residential grid-connected microgrids,” *IEEE Trans. Smart Grid*, vol. 9, no. 2, pp. 1–1, 2016.

[51] S. Angalaeswari, O. V. G. Swathika, V. Ananthakrishnan, J. L. F. Daya, and K. Jamuna, “Efficient power management of grid operated microgrid using fuzzy Logic controller (FLC),” *Energy Procedia*, vol. 117, pp. 268–274, 2017.

[52] D. Arcos-Aviles, D. Sotomayor, J. L. Proano, F. Guinjoan, M. P. Marietta, J. Pascual, L. Marroyo, and P. Sanchis, “Fuzzy energy management strategy based on microgrid energy rate-of-change applied to an electro-thermal residential microgrid,” *IEEE Int. Symp. Ind. Electron.*, pp. 99–105, 2017.

[53] T. Chaiyatham, I. Ngamroo, S. Pothiya, and S. Vachirasricirikul, “Design of optimal fuzzy logic-PID controller using bee colony optimization for frequency control in an isolated wind-diesel system,” 2009, vol. 1, pp. 1–4.

[54] T. Chaiyatham and I. Ngamroo, “A bee colony optimization based-fuzzy logic-pid control design of electrolyzer for microgrid stabilization,” *Int. J. Innov. Comput. Inf. Control*, vol. 8, no. 9, pp. 6049–6066, 2012.

[55] and E. R. F. Villalva, Marcelo Gradella, Jonas Rafael Gazoli, “Modeling and circuit-based simulation of photovoltaic arrays,” in *Power Electronics Conference COBEP’09*, 2009, pp. 1244–1254.

[56] D. Miao and J. Shen, “Comparative study on permanent magnet synchronous generator systems with various power conversion topologies,” in *4th International Conference on Power Engineering, Energy and Electrical Drives*, 2013, no. May, pp. 13–17.

[57] C. N. Bhende, S. Mishra, and S. G. Malla, “Permanent magnet synchronous generator-based standalone wind energy supply system,” *IEEE Trans. Sustain. Energy*, vol. 2, no. 4, pp. 361–373, 2011.

[58] G. Ofualagba and E. U. Ubeku, “Wind energy conversion system- wind turbine modeling,” in *2008 IEEE Power and Energy Society General Meeting - Conversion and Delivery of Electrical Energy in the 21st Century*, 2008, pp. 1–8.

[59] P. Swain and D. Jena, “Modeling , simulation & optimal control of non- linear PEM fuel cell with disturbance input,” in *IEEE Sponsored 2nd International Conference on Innovations in Information Embedded and Communication Systems, ICIIECS’15*, 2015, pp. 1–7.

[60] U. Akram, M. Khalid, and S. Shafiq, “Optimal sizing of a wind/solar/battery hybrid grid-connected microgrid system,” *IET Renew. Power Gener.*, vol. 12, no. 1, pp. 72–80, 2018.

[61] K. Kusakana and H. J. Vermaak, “Hybrid diesel generator/renewable energy system performance modeling,” *Renew. Energy*, vol. 67, pp. 97–102, 2014.

[62] “KC200GT high efficiency multicrystal photovoltaic module datasheet.”

[63] S. Al-Sakkaf, M. Kassas, and M. Khalid, “The effect of ambient temperature on the power output of 5kW hotovoltaic olar power system,” in *Sustainability in Energy and Buildings: Research Advances*, 2017, vol. 6, no. 1, pp. 1–13.

[64] D. Karaboga, “An idea based on honey bee swarm for numerical optimization,” *Tech. Rep. TR06, Erciyes Univ.*, no. TR06, p. 10, 2005.

[65] D. Karaboga and B. Basturk, “Artificial bee colony (ABC) optimization algorithm for solving constrained optimization problems,” in *International fuzzy systems association world congress*, 2007, pp. 789–798.

[66] N. Augustine, S. Suresh, P. Moghe, and K. Sheikh, “Economic dispatch for a microgrid considering renewable energy cost functions,” in *nnovative Smart Grid Technologies (ISGT)*, 2012, pp. 1–7.

[67] G. W. Chang, H. J. Lu, and H. J. Su, “Short-term distributed energy resource scheduling for a DC microgrid,” *Energy Power Eng.*, vol. 5, no. 4B, pp. 15–21, 2013.

[68] M. A. Abido, “Multiobjective evolutionary algorithms for electric power dispatch problem,” *IEEE Trans. Evol. Comput.*, vol. 10, no. 3, pp. 315–329, 2006.

[69] R. Eberhart and J. Kennedy, “A new optimizer using particle swarm theory,” in *Proceedings of the Sixth International Symposium on Micro Machine and Human Science, 1995. MHS’95*, 1995, pp. 39–43.

[70] Y. Shi and R. Eberhart, “A modified particle swarm optimizer,” in *Evolutionary Computation Proceedings, 1998. IEEE World Congress on Computational Intelligence., The 1998 IEEE International Conference on*, 1998, pp. 69–73.

[71] A. Mahor, V. Prasad, and S. Rangnekar, “Economic dispatch using particle swarm optimization : A review,” vol. 13, pp. 2134–2141, 2009.

[72] M. A. Abido, “Multiobjective particle swarm optimization for environmental / economic dispatch problem,” vol. 79, pp. 1105–1113, 2009.

[73] A. Koridak, M. Rahli, and Y. Mimoun, “Hybrid optimization of the emission and economic dispatch by the genetic algorithm,” *Leonardo J. Sci.*, no. 14, 2008.

[74] S. P. Singh, R. Tyagi, and A. Goel, “Genetic algorithm for solving the economic load dispatch,” *Int. J. Electron. Electr. Eng.*, vol. 7, no. 5, pp. 523–528, 2014.

Vitae

Name : Shehab Ebrahim Mohammed Al-Sakkaf

Nationality : Yemeni

Date of Birth : 24/12/1987

Email : shihabsat@hotmail.com

Mobile : +967 734339937 / +966 508428033

Address : Yemen – Hadhramout – Mukalla – P.O. Box: 52014

Academic Background :

- B.Sc in Electronic and Telecommunication Engineering (August 2012), from Hadhramout University, Mukalla, Yemen
- M.Sc in Electrical Engineering, May 2018 King Fahd University of Petroleum and Minerals, Dhahran, Saudi Arabia.

Publications:

- S. Al-Sakkaf, M. Kassas, and M. Khalid, "The effect of ambient temperature on the power output of 5kW photovoltaic solar power system," in *Sustainability in Energy and Buildings: Research Advances*, 2017, vol. 6, no. 1, pp. 1–13.